STRUCTURE AND ACTIVITY STUDIES ON MUTANTS OF THE ENZYME DIHYDROFOLATE REDUCTASE

Thesis submitted for the degree of
Doctor of Philosophy
at the University of Leicester

by

Janette Ann Thomas BSc (CNAA)
Department of Biochemistry
University of Leicester

November 1990

ProQuest LLC
789 East Eisenhower Parkway
P.O. Box 1346
Ann Arbor, MI 48106-1346

To my family and friends

ABSTRACT

During the course of this thesis four mutants of *Lactobacillus casei* dihydrofolate reductase have been studied to determine the role of the individual amino acids in the structure and function of the enzyme.

The mutants tryptophan-21⇒histidine and threonine-63⇒alanine were successfully made by site specific mutagenesis. The mutant aspartate-26⇒glutamine was successfully expressed and purified but did not bind as tightly to the methotrexate affinity column as the wild type. This mutant had only 1% of the activity of the wild type enzyme.

The threonine-63⇒glutamine mutant was successfully expressed and purified. The equilibrium binding constants of substrates and inhibitors binding to binary and ternary enzyme complexes were the same as wild type except the binding of the oxidised coenzyme to the mutant apoenzyme, which was reduced three fold. k_{cat}, and K_M for NADPH were unaffected by the mutation, however the apparent pK_a of catalysis and the pK_a of the isotope effect were both reduced by 0.5 pH units. Nmr analysis revealed no structural changes at residues near the mutation or to the bound coenzyme, however there were small structural affects seen at the substrate binding site, at least 15Å away from the mutation. A movement along the backbone of helix-C, from glutamine-43 at the mutation site, to the substrate binding site is hypothesized to cause these affects.

Expression of threonine-63⇒alanine was only detected when the temperature was at 30°C rather than the usual 40°C. k_{cat} and the binding of substrate and inhibitors were the same as wild type. The binding of coenzyme was reduced by six hundred fold, the rate of association reduced by fifty fold and the rate of dissociation increased by twelve fold. Nmr analysis revealed the adenine and the 2' phosphate moieties of NADPH are affected by the mutation, the adenine ring being further away from residues in the protein. These affects were not simply due to the loss of the hydrogen bond between threonine and the protein but must also be caused by some conformational change in the protein.

ACKNOWLEDGMENTS

There are many friends and colleagues I would like to thank for their support, advice, and friendship at various stages in producing this thesis.

Firstly I owe much to my supervisor Professor Gordon Roberts for his valued advice, support, and patience. I am also greatly indebted to Dr's John Arnold and Julie Andrews, John for his friendship and help with the nmr work and Julie for her kindness in teaching me molecular biology, and allowing me to work in her laboratory for two weeks. Also, thanks to each for proof reading parts of this thesis.

I should like to convey my appreciation to colleagues in the Biological NMR Centre and the Biochemistry department at Leicester and at NIMR, Mill Hill, for their valued advice and encouragement provided during my research. These include Ramin Badii-Azandahi, Clive Bagshaw, Jaswir Basran, Andy Bates, Rachel Bellingham, Berry Birdsall, Jim Feeney, Julie Fisher, Ronnie Frederick, Derek Gamble, Alison Grimshaw, Paul Hallet, Andy Heath, Eva Hyde, Izabella Jasinska, Peter Kilby, Lu-Yun Lian, Tony Maxwell, Iain Murray, Jean Newby, Andrew Prescott, Bill Primrose, Vasudevan Ramesh, Charnjit Seehra, Bill Shaw, Pritpal Slaich, Mike Sutcliffe, Shabih Syed, Wendy Tomlinson, Jan White, and Ji Chun Yang.

Last but not least, I am very grateful for the support and encouragement provided by my parents Ann and Tony, brother Nick, sister Suzie, and grandmother Olive Balchin, and closest friends, Robbie Neilson, Liza and Melanie Dawson-Whisker, Terry Dawson, Paul McBride, Louise Clifford, Colin Orford and Iain Pitfield.

ABBREVIATIONS

AMINO ACIDS

Ala (A)	Alanine
Arg (R)	Arginine
Asn (N)	Asparagine
Asp (D)	Aspartic acid
Asx (B)	Aspartic acid or asparagine
Cys (C)	Cysteine
Gln (Q)	Glutamine
Glu (E)	Glutamic acid
Glx (Z)	Glutamic acid or Glutamine
Gly (G)	Glycine
His (H)	Histidine
Ile (I)	Isoleucine
Leu (L)	Leucine
Lys (K)	Lysine
Met (M)	Methionine
Phe (F)	Phenylalanine
Pro (P)	Proline
Ser (S)	Serine
Thr (T)	Threonine
Trp (W)	Tryptophan
Tyr (Y)	Tyrosine
Val (V)	Valine

COSY	Correlated spectroscopy
DEAE	Diethylaminoethyl
DHFR	Dihydrofolate Reductase
DNA	Deoxyribonucleic acid
dTMP	Deoxythymidylate
εNADP$^+$	Nicotinamide 1,N^6-ethenoadenine dinucleotide phosphate (oxidised form)
FH_2	Dihydrofolate
FH_4	Tetrahydrofolate
HOHAHA	Homonuclear Hartman Hahn
IPTG	Isopropylthio-β-D-galactoside
MES	4-morpholineethane sulphonic acid
MTX	Methotrexate

MUTANTS

D26N	DHFR with the mutation Aspartate 26⇒Asparagine
T63A	DHFR with the mutation Threonine 63⇒Alanine
T63Q	DHFR with the mutation Threonine 63⇒Glutamine
W21H	DHFR with the mutation Tryptophan 21⇒Histidine
WT	Wild type DHFR

NAD$^+$	Nicotinamide adenine dinucleotide (oxidised form)
NADH	Nicotinamide adenine dinucleotide (reduced form)
NADP$^+$	Nicotinamide adenine dinucleotide phosphate (oxidised form)
NADPH	Nicotinamide adenine dinucleotide phosphate (reduced form)
NMR	Nuclear magnetic resonance
NOE	Nuclear Overhauser effect
NOESY	Nuclear Overhauser Enhancement Spectroscopy

NUCLEOTIDES

A	Adenine
C	Cytosine
G	Guanine

T	Thymine

PAGE	Polyacrylamide gel electrophoresis
PEI	Polyethyleneimine
PTZ	Phenyltriazine
SDS	Sodium dodecyl chloride
TMP	Trimethoprim
UMP	Uridine monophosphate
UV	Ultraviolet
X-gal	5-bromo-4-chloro-3-indolyl-β-d-galactoside

CONTENTS

CHAPTER 4. NMR CHARACTERISATION OF MUTANT DHFR'S

CHAPTER 5. KINETIC CHARACTERISATION OF MUTANT DHFR'S

1. INTRODUCTION

1.1. INTRODUCTION

Dihydrofolate reductase (DHFR, tetrahydrofolate:$NADP^+$ oxoreductase, EC 1.5.1.3.) catalyses the reduction of 7,8-dihydrofolate (FH_2) to 5,6,7,8-tetrahydrofolate (FH_4) using NADPH as the coenzyme.

$$FH_2 + NADPH + H^+ \rightleftharpoons FH_4 + NADP^+$$

DHFR is highly specific for NADPH over NADH by a factor of 1000 fold (Feeney *et al.*, 1975) however the reasons for this specificity are as yet unknown. Folate can be enzymatically reduced at low pH but turnover is very slow, and almost non-existent at neutral pH for most mammalian DHFR (Freisheim and Matthews, 1984).

In vivo FH_4 is processed by the cell to carry a one-carbon group on N^5 and/or N^{10}, which can exist in a number of oxidation states including the methyl ($-CH_3$), methylene ($-CH_2-$), formyl (-CHO), formimino (-CHNH), and methenyl (-CH=) state. These one-carbon units are used in a wide variety of biosyntheses such as in the formation of purine nucleotides, glycine, methionine and thymine (Blakely, 1969). In the thymidylate biosynthetic pathway, DHFR reductively methylates dUMP, on the 5' position of the uracil ring, with N^5,N^{10}-methylene tetrahydrofolate to form dTMP. In the process, FH_4 is oxidised to FH_2 as well as donating a one-carbon unit. DHFR is therefore essential for the regeneration of FH_4 to maintain cellular levels, enabling biosyntheses including that of purines and thymidine required for nucleic acid synthesis (Figure 1.2).

Inhibitors of DHFR are often used as drugs for treating diseases such as cancer and bacterial infections. These drugs prevent regeneration of FH_4 and lead to inhibition of DNA synthesis and eventually to cell stasis or death. The structure of FH_4 and two such inhibitors are shown in figure 1.1.

There are a number of reviews regarding various aspects of research on DHFR including Schweitzer *et al.*, (1990), Roberts (1989), Blakley (1984) and Benkovic (1986).

Figure 1.1. Structure and atom numbering of folic acid (top), methotrexate (middle) and trimethoprim (bottom).

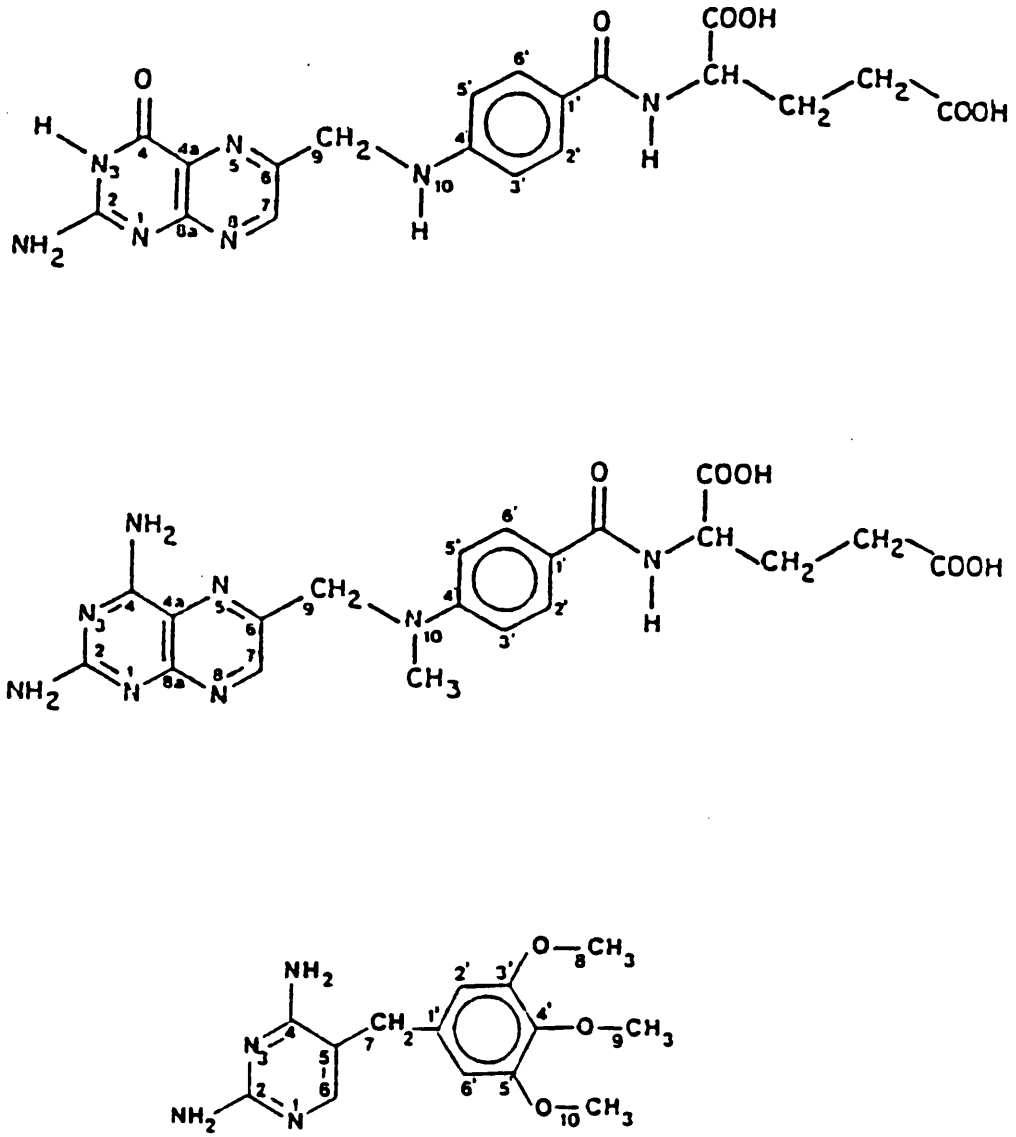

Figure 1.2. The biosynthesis of dTMP from dUMP and the regeneration of FH_4 by DHFR

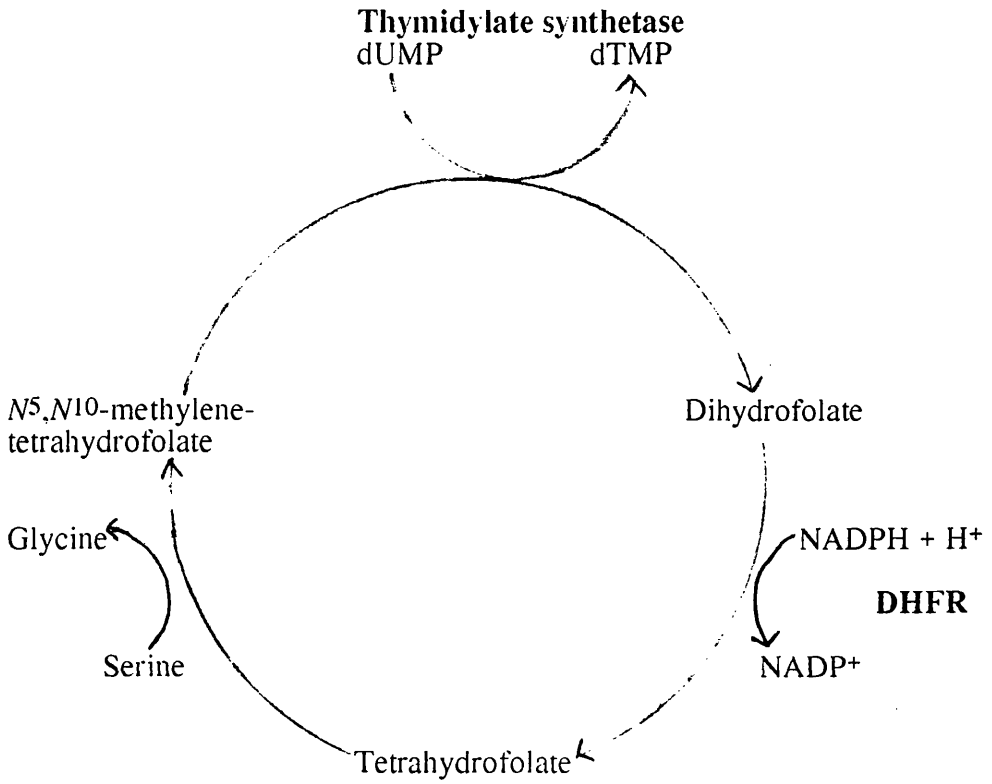

DHFR is widely studied for a variety of reasons, outlined below;

1. Because of its medical importance as a target for therapeutic drugs, DHFR is studied in an attempt to find improved, more species specific drugs. DHFR occurs in nearly all organisms (exceptions include the archaebacteria), therefore to treat bacterial disease it is essential to find compounds which specifically inhibit the enzyme of the infecting microbe rather than mammalian DHFR. An example of such a drug is trimethoprim (TMP). It is clear why DHFR inhibitors used for the treatment of cancer (e.g. methotrexate, MTX) are also highly toxic to normal growing cells since the DHFR's are identical.

2. The enzyme is also studied as a model system in the investigations of enzyme structure and function. The assay of the reaction is simple to follow using spectroscopic techniques, however DHFR is of particular value because of its small size (M_r ca. 18000-22000) and the fact that it exists as a monomer in

solution, thus it is amenable to structural studies by both nuclear magnetic resonance (nmr) and X-ray crystallography.

3. As a result of DHFR's medical significance there exists a broad range of inhibitors against DHFR which are useful aids in the study of the enzyme.

4. Purification of the enzyme is relatively easy,

5. Several DHFR enzymes have now been cloned and mutagenesis work is being carried out. As a model system, DHFR is an ideal tool for these relatively new mutagenesis investigations. There are crystal structures and a wealth of kinetic data available and the structure of the mutants can be compared using nmr.

1.2. DHFR STRUCTURE

The amino acid sequences of DHFR from several species have been determined including those from *S. faecium* (Gleisner *et al.*, 1974, Gleisner *et al.*, 1975, Peterson *et al.*, 1975), *L. casei* (Bitar *et al.*, 1977, Freisheim *et al.*, 1978), *E. coli* (Bennett *et al.*, 1974, Bennett *et al.*, 1978), Chicken liver (Kumar *et al.*, 1980), bovine liver (Lai *et al.*, 1982), mouse L1210 lymphoma (Barbehenn and Kaufman, 1980, Kumar *et al.*, 1980), porcine liver (Raccah, 1973) and recombinant human DHFR (Masters and Attardi, 1983).

The sequences of the vertebrate enzymes have greater homology to each other than those of the bacterial enzymes, as would be expected considering the greater evolutionary periods of the bacterial sources. The sequence homology between the *E. coli* and *L. casei* enzyme is only 25%. However, comparisons of the amino acid sequences in the light of the known crystal structures showed that most of the residues involved in ligand binding are highly conserved (Volz *et al.*, 1982).

Considerable effort has been dedicated by various groups to determine X-ray crystal structures of various DHFR complexes. The structures have been examined in order to determine the basis of specificity of inhibitor and coenzyme binding, and to provide hypotheses regarding the residues involved in binding and catalysis, ultimately to determine the details of the mechanism of the reaction.

Crystal structure coordinates of DHFR from a number of species in various complexes have been determined (table 1.1).

Table 1.1. The X-ray structures of DHFR complexes determined to date.

Species	Complex	Resolution,Å	Most Recent Reference
E. coli	MTX	1.7 refined	Bolin *et al.*, 1982
E. coli	TMP	2.3 refined	Baker *et al.*, 1981
			Matthews *et al.*, 1985a
E. coli	TMP analogues	2.3 refined	Kuyper *et al.*, 1985
E. coli	TMP/NADPH	3	Champness *et al.*, 1986
E. coli	$NADP^+$	2.4	Bystroff *et al.*, 1990
E. coli	$NADP^+$/folate	2.5	Bystroff *et al.*, 1990
L. casei	MTX/NADPH	1.7 refined	Bolin *et al.*, 1982
			Filman *et al.*, 1982
Chicken	PTZ/NADPH	2.9	Volz *et al.*, 1982
Chicken	TMP/NADPH	2.2 refined	Matthews *et al.*, 1985b
Chicken	NADPH	2 refined	Matthews *et al.*, 1985b
Chicken	various triazine and pyrimidine inhibitors with NADPH		
			Matthews *et al.*, 1985b
Mouse	TMP/NADPH	2 refined	Stammers *et al.*, 1987
Mouse	MTX/NADPH	2 refined	Stammers *et al.*, 1987
Human	Folate	2 refined	Oefner *et al.*, 1988
Human	MTX	3.5	Oefner *et al.*, 1988
Human	TMP	3.5	Oefner *et al.*, 1988

The first DHFR structures determined were those of the binary complex of *E. coli* DHFR with MTX (Matthews *et al.*, 1977) and the ternary complex of *L. casei* DHFR with MTX and NADPH (Matthews *et al.*, 1978, Matthews *et al.*, 1979). The structures were later refined to 1.7Å resolution (Bolin *et al.*, 1982, Filman *et al.*, 1982). The backbone structures (shown in figure 1.3) of the two enzymes are very similar despite there being comparatively little sequence homology; less than 25%. Some structural differences must be attributed to the use of different complexes for each enzyme, however the main differences lie in the loop regions which accommodate four of the five deletions or insertions between the two enzymes.

Figure 1.3. Ribbon diagrams of the backbone structures of E. coli DHFR in complex with MTX (A) and L. casei DHFR in complex with MTX and NADPH (B).

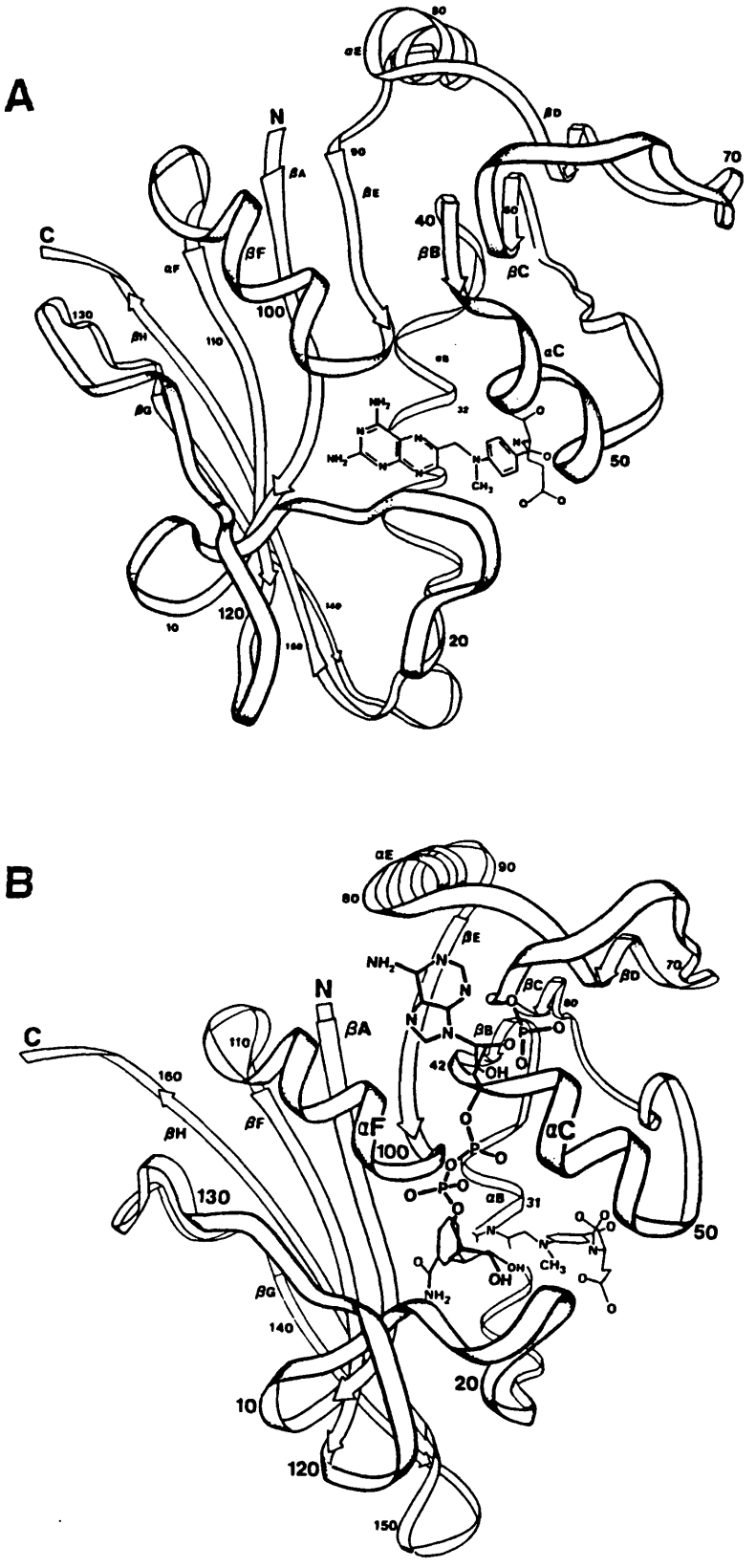

Since these first bacterial structures, DHFR from several other species has been crystalised and structures determined. Despite the diversity of the species and their amino acid sequences, they are all very similar in conformation. In general the molecule is folded into an 8 stranded β-sheet and 4 α-helices. NADPH binds in an extended conformation in a long shallow groove extending around one face of the enzyme and bound via a number of hydrophobic, ionic and hydrogen bond interactions. MTX (a close structural analogue of FH_2) binds to the other side of the enzyme with its pteridine ring nearly perpendicular to the *p*-aminobenzoyl aromatic ring. The positions of the two ligands allow the nicotinamide moiety of NADPH and the pyrazine ring of MTX to lie close to each other so the C4 of the nicotinamide lies close to the N5 to C6 bond of MTX, i.e. since MTX and the substrate bind to the same site, they are in reasonable proximity for the hydride ion to be donated from the nicotinamide ring of the coenzyme to the substrate during catalysis.

1.2.1. Coenzyme Binding

From the refined structure of the *L. casei* DHFR/MTX/NADPH complex (Filman *et al.*, 1982) the adenine moiety of NADPH binds in a shallow hydrophobic cleft sandwiched between the side chains of His64 and the conserved Leu62, with additional interactions from the side chain of Ile102, the backbone of Thr63 and the α, β, γ carbon atoms of Gln101. Thus there is a relative lack of specificity for the moiety. The adenine nitrogen atoms hydrogen bond with fixed water molecules which in turn make two hydrogen bonds with the backbone carbonyls of the protein. In the binding of the 2' phosphate the negatively charged oxygens are involved in an electrostatic interaction with the positively charged guanidinium group of Arg43 (conserved in all species except chicken which has lysine in this position, Volz *et al.*, 1982). ^{31}P nmr experiments have shown that the 2' phosphate is in the dianionic state when bound to DHFR (Feeney *et al.* 1975, Cayley *et al.*, 1980) and the charge interactions with Arg43 are thought to cause this unusual pK. Other interactions made by the 2'phosphate include hydrogen bonds with the side chain hydroxyl of Thr63, the N1 of His64 and the side chain of Gln65. The nicotinamide moiety interacts with a number of conserved residues in a loop between βA to αB and in βA and βE. The A side of the nicotinamide ring is in contact with the pteridine ring of the substrate, consistent with the premise that hydride ion transfer occurs with A side specificity. In addition, three oxygens (from the side chain of Thr45, and the backbone carbonyls of Ile13 and Ala97) lie coplanar with, and close to, the nicotinamide ring hydrogens at positions 2, 4 and 6 forming CH-O polar contacts. It is suggested by Filman *et al.* (1982) that these may help stabilise a positively charged nicotinamide ring in the transition state and will constrain the position of the nicotinamide to a limited geometry. However it should be noted that $NADP^+$ binds much more weakly than NADPH so this may not be the case unless $NADP^+$ in the transition state is in a different conformation. The pyrophosphate bridge is

extensively hydrogen bonded with the protein and these bonds cause a strain in one of the O-P-O bond angles as was shown by nmr experiments (Hyde *et al.*, 1980a,b).

The recently determined structure of *E. coli* DHFR/$NADP^+$/folate complex (Bystroff *et al.*, 1990) showed $NADP^+$ is bound in a very similar manner to NADPH in the *L. casei* DHFR/NADPH/MTX complex described above. In the *E. coli* structure, Arg98 plays a similar role to His64 of *L. casei* in closing over the bound Adenine ring. A difference was found at the nicotinamide moiety binding site where there were small differences in the distances with the carbonyl oxygens, possibly due to the presence of an additional oxygen from Tyr100 (Phe in *L. casei*). The structure of the *E. coli* DHFR binary complex with $NADP^+$ showed the nicotinamide ring was disordered, in agreement with nmr studies which suggested that this moiety of $NADP^+$ was weakly bound (Cayley *et al.*, 1980). The structure of avian DHFR bound with PTZ (Phenyltriazine) and NADPH again showed NADPH was bound in a similar conformation as the *L. casei* enzyme (Volz *et al.*, 1982) with only minor deviations attributable to amino acid differences.

1.2.2. Substrate and Inhibitor Binding

The conformations of MTX in binary complex with *E. coli* DHFR and in ternary complex with *L. casei* DHFR and NADPH (Matthews *et al.*, 1977, Matthews *et al.*, 1978, Matthews *et al* 1979, Bolin *et al*, 1982) have been determined and refined. The conformations of MTX in the two complexes are very similar. The main interactions in the binding of the glutamate carboxylates are two hydrogen bonds from the α-carboxylate to the guanidinium group of the strictly conserved Arg57. The binding of the γ-carboxylate of MTX generally appears weak and non specific and rather disordered and differs between the two enzymes. The *L. casei* enzyme has an hydrogen bond between His28 and one of the γ carboxylates whereas the *E. coli* enzyme only directly interacts with water molecules. The *p*-aminobenzoyl group lies in an hydrophobic pocket, its inner face interacting with residues Leu27 (*L. casei*) and Phe30, the latter residue being highly conserved, the other face is in contact with Phe49. Other hydrophobic residues near to the ring include, Pro50, and Leu54. The pteridine ring forms both hydrogen bonds and hydrophobic interactions with the protein. The 2-amino group and N1 form hydrogen bonds with Asp26 and the 2-amino group forms an hydrogen bond with a water molecule, which in turn forms an hydrogen bond with the strictly conserved Thr116 side chain, thus a network of interactions lie between Asp26, Thr116, the 2-amino group and N1 (see figure 1.4). The 4-amino group hydrogen bonds with the carbonyl of Leu4 and Ala97. The nitrogens of the pyrazine portion of the pteridine moiety form no hydrogen bonds directly with the protein. Nδ forms a weak hydrogen bond with a fixed water molecule which in turn bonds with Asp26, Trp21 and another fixed water which in its turn hydrogen bonds with the backbone

nitrogen of Leu23 (Leu23 and Trp21 are highly conserved). There are a number of hydrophobic residues in the binding site including Ala6, Phe30 (both strictly conserved), Leu19 and the nicotinamide ring.

Figure 1.4. The interactions between the pteridine moiety of MTX and DHFR as determined by X-ray crystallography. From Bolin et al., 1982.

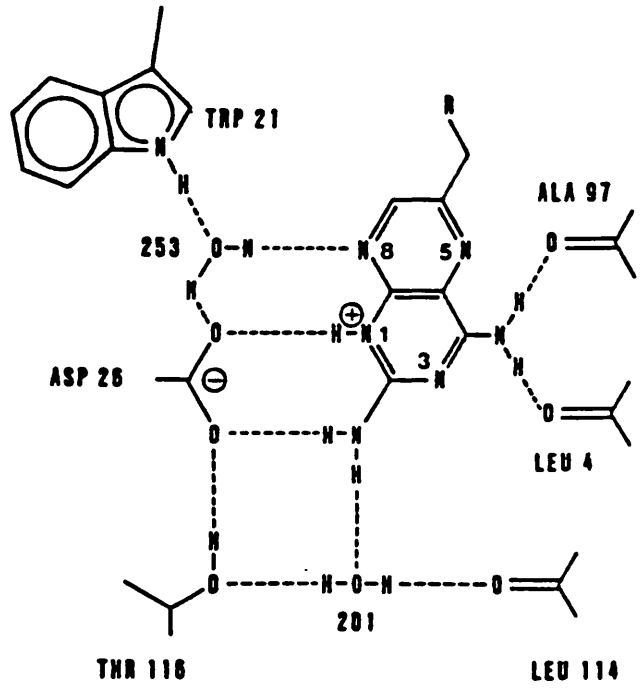

Until recently there were no crystal structures available for DHFR with the substrate bound instead of inhibitors and so there was no explanation for the very much tighter binding of the substrate analogue MTX. However experimental evidence produced by various groups suggested that the mode of binding of substrate was different to that of MTX (Erickson and Matthews, 1972, D'Souza and Freisheim, 1972, Greenfield *et al.*, 1972, Erickson and Matthews, 1973, Pastore *et al.*, 1974, Roberts *et al.*, 1974, Poe *et al.*, 1975). These results prompted Matthews *et al.* (1978) and Bolin *et al.* (1982) to examine the possible orientations of substrate based upon the bound structure of MTX. They suggested that the substrate binds in the same pocket as MTX but the pteridine ring is flipped over by 180° about the C6-C9 bond, with an additional smaller rotation about the C9-N10 bond. This would leave the *p*-aminobenzoylglutamate moiety in the same

orientation, correlating well with the results of Birdsall *et al.* (1977b) who showed by nmr studies that this *p*-aminobenzoylglutamate moiety was in the same environment for both substrate and MTX. In support of this hypothesis, studies by Charlton *et al.*, (1979) showed by nmr that the steriochemistry of reduction requires a "rotated" orientation of folate and FH_2 compared to that of MTX since both protons are added to the *si* face of the ring. The orientation of the pteridine ring of MTX allows an additional hydrogen bond between the MTX 4-amino group and the protein compared with the hypothesised orientation of FH_2. There is also favourable charge-charge interactions between Asp26 and the N1 of MTX, since it has been found by uv difference spectroscopy and nmr experiments that the N1 is protonated (Erickson *et al.*, 1974, Poe *et al.*, 1974, Gupta *et al.*, 1977, Hood *et al.*, 1978, Cocco *et al.*, 1981a, b,). This charge interaction and the additional hydrogen bond are presumed to effect the much tighter binding of MTX over the substrate. Figure 1.5 shows schematically the relative orientations of MTX and folate bound to the enzyme. Publication of the structure of human DHFR complexed with folate (Oefner *et al.*, 1988) proved the hypotheses that the pteridine ring of folate is in an inverse orientation to that of MTX. Oefner *et al.* (1988) suggest mechanisms for reduction based on their structure determinations. Asp26 is widely believed to be closely associated with the reduction of the C=N bond (where N5 becomes protonated) yet the structure shows N5 of FH_2 does not lie close to Asp26 or near to the conserved water molecule which is hydrogen bonded to Asp26. However, as was hypothesized by Gready (1985), rather than a direct protonation the structure could allow initial protonation of the oxo group (O4) of the pteridine ring followed by transfer of the proton to N5, either before or after hydride ion transfer. The proton transfer from O4 to N5 could be direct or through water molecules. Alternatively Asp26 could protonate N5 via a chain of bound water molecules. It is also suggested by Gready that the hydrogen atom on the reduced nicotinamide ring is in an ideal position to transfer to the C6 of bound FH_2 and that proton transfer to N5 before hydride transfer would be expected to lower the energy barrier of this hydride transfer.

Recent analyses of the crystal structure of *E. coli* DHFR complexed with $NADP^+$ and $NADP^+$ plus folate have also shown that folate binds in an inverse orientation to MTX (Bystroff *et al.*, 1990). These structures can be directly compared to previous studies on the *E. coli* DHFR/MTX complex and it was found that folate does not bind with a simple 180° rotation of the pteridine moiety but that the orientation of the ring is also somewhat twisted relative to the position of MTX. This "twist" results in some distortion of the hydrogen bonds with Asp27 (Asp-26 in *L. casei*) which the authors hypothesize could contribute to the weaker binding of substrate compared to MTX.

Figure 1.5. The relative orientations of folate (solid bonds) and methotrexate (open bonds) when bound to the E. coli DHFR/MTX binary complex or DHFR/folate/NADP+ ternary complex.

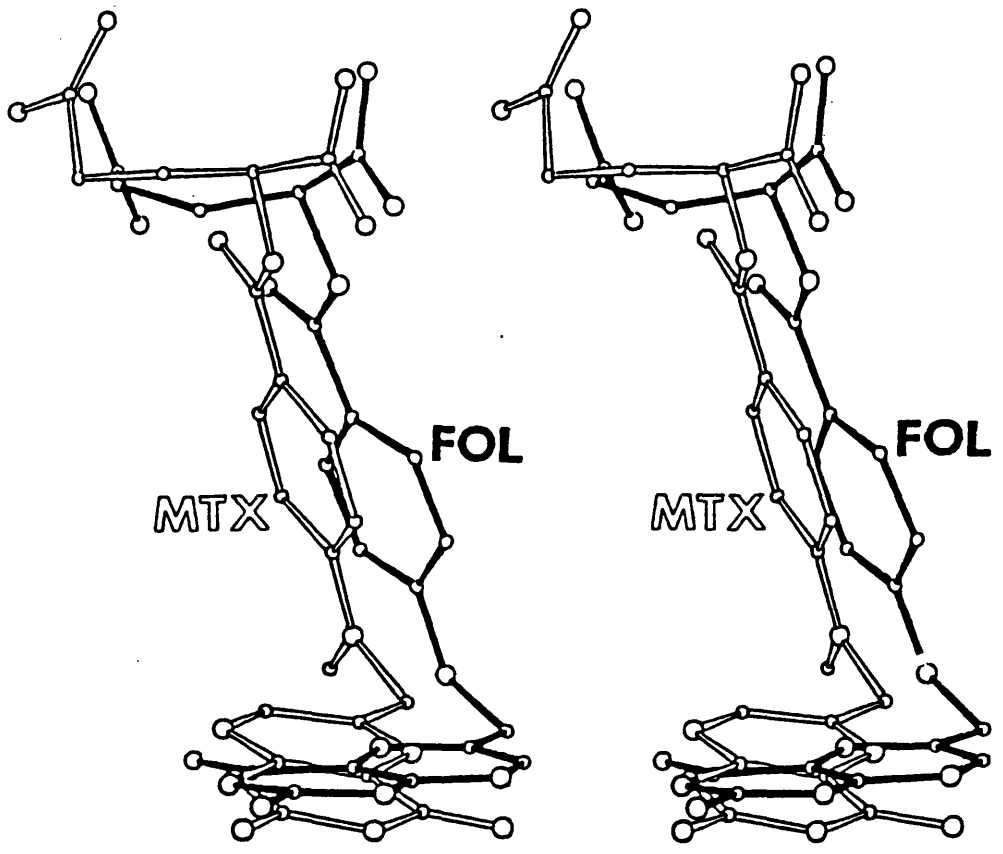

Crystal structures of DHFR from chicken liver complexed with TMP (Matthews *et al.*, 1985) were analysed and compared with the bacterial structures where TMP was bound and suggestions were made regarding the basis for inhibitor selectivity for bacterial rather than mammalian DHFR (Baccanari *et al.*, 1982). However Oefner *et al.* (1988) and Stammers *et al* (1987) have found distinct differences between the chicken and mammalian enzymes with the result that specific structural differences causing the differential binding are as yet undetermined.

Oefner *et al.*, (1988) have compared their initial refinements of the human DHFR/MTX complex with the structure of the mouse DHFR/MTX/NADPH complex

(Stammers *et al.*, 1987) and found considerable differences between the orientations of some of the side chains, the most noticeable difference being a different orientation of Phe31 at the active site. The two enzymes appear to have considerable conformational differences considering their extremely high sequence homology. It should be noted that the mouse enzyme is in ternary complex whereas the human is in binary complex, but this can probably be discounted as an explanation for the major differences since only comparatively minor variations have been found between the binary and ternary complexes of the bacterial enzymes. In addition, the human enzyme structures correlate well with the bacterial DHFR structures, implying that the mouse enzyme is unusual, or more likely, that the methodology in the mouse studies has locked the enzyme into a different, strained, conformational state.

1.3. CONFORMATIONAL EQUILIBRIA

DHFR from *Streptococcus faecium* has been shown by nmr to exist in two conformations (London *et al.*, 1979) and the broad lines seen in the nmr spectra of uncomplexed *L. casei* DHFR have been taken as suggesting that the free enzyme exists in more than one conformation (Kimber *et al.*, 1977). A number of experiments have shown that DHFR exists in more than one conformation when ligands are bound, the number and nature of the conformational differences depending on the particular ligand. For example *L. casei* DHFR in its ternary TMP/$NADP^+$ complex is a mixture of two slowly interconverting conformations (Gronenborn *et al.*, 1981a,b, Birdsall *et al.*, 1984, Cheung *et al.*, 1986, Searle *et al.*, 1988), the ternary pyrimethimine/$NADP^+$ exists in 2 conformations (Birdsall *et al.*, 1990b), the folate binary complex exists in at least two conformations (Birdsall *et al.*, 1987), and the folate/$NADP^+$ complex exists in three conformations (Birdsall *et al.*, 1981b, Birdsall *et al.*, 1982). In contrast, the $NADP^+$ complex exists in only one conformation (Hyde *et al.*, 1980a, Hyde *et al.*, 1980b). In these investigations the nmr experiments have revealed such information as the time-scales of interconversions, the likely locations of the ligands and their orientation in the conformers, and the regions of the protein where the conformers differ.

A recent publication by Birdsall *et al.*, (1989b) showed that in two of the three conformations of the folate/$NADP^+$ complex, folate is bound to the enzyme with its pteridine ring in the same orientation to that of MTX whereas in the third conformation folate binds with approximately a 180° rotation about the C2-NH_2 bond, this orientation being a suitable orientation for reduction. Folate can therefore bind in both a productive and non-productive mode which may have implications for catalysis, although it is not clear whether these two orientations also exist for the folate/NADPH complex.

The binding of the first ligand to the enzyme affects the affinity of the second ligand (Birdsall *et al.*, 1980a,b,). This cooperative effect has medical significance where species specificity of TMP binding is caused by the greater cooperativity of binding in the presence of coenzyme for the bacterial enzyme as compared to the mammalian enzyme (Baccanari *et al.*, 1982). Other examples of cooperativity include the binding of NADPH to the *L. casei* binary DHFR/MTX complex which binds 670 times better than to the enzyme alone, whereas $NADP^+$ only binds 12 times tighter. Some of the cooperativity of binding is thought to be caused by conformational changes occurring upon ligand binding, supporting evidence being provided by the fact that the *L. casei* DHFR nmr spectra shows numerous chemical shift differences between the binary and ternary MTX complexes (Feeney *et al.*, 1977, Kimber *et al.*, 1977). However this evidence is not conclusive and cooperativity of binding could arise solely from the interactions between the two substrates bound to the enzyme. Evidence in support of the hypothesis that the cooperative effects are not simply a result of ligand interactions, comes from Birdsall *et al.*, (1984). They found that coenzyme analogues such as thio-$NADP^+$ bind to the protein in such a way that the nicotinamide ring is not in contact with the protein (Feeney *et al.*, 1983), yet the enzyme still shows cooperativity of binding with TMP (Birdsall *et al.*, 1984). In this case the tighter binding must arise from conformational affects brought about by the binding of the remainder of the coenzyme distant from TMP. Other experimental evidence of conformational changes includes line shape analysis of ^{19}F resonances for 3'5'-difluoro MTX bound to *L. casei* DHFR which showed the rate of the *p*-aminobenzoyl ring flipping increases by 2.5 fold upon addition of $NADP^+$ (Clore *et al.*, 1984), thus there must be a conformational change allowing this to occur. Hammond *et al.*, (1986) provide strong nmr spectral evidence for conformational changes upon coenzyme binding. In addition to other assignments, they made assignments of resonances from four residues (Leu27, Phe49, Phe30, Leu54) that form part of the binding pocket around the *p*-aminobenzoyl ring. These residues are not in contact with the coenzyme but do show significant changes in chemical shift on coenzyme binding thus confirming the hypothesis that there is a conformational change around the benzoyl binding site.

Not all ligands have this "positive" cooperative affect with each other. The binding of folinic acid to *L. casei* DHFR was reduced 600 fold in the presence of NADPH compared to the free enzyme, this is called negative cooperativity (Birdsall *et al.*, 1981a). The simple observation of negative cooperativity argues for conformational changes occurring in the protein. The nmr spectra of these complexes show differences of chemical shift at the adenine binding site of NADPH which is distant from the folinic acid binding site, again suggesting that there are conformational changes in the protein causing this negative cooperativity (Birdsall *et al.*, 1981a, Feeney *et al.*, 1981).

1.4. KINETIC STUDIES

1.4.1. Kinetic Mechanism

The complete kinetic scheme of DHFR catalysis was not established until relatively recently, partly due to its complexity - the enzyme shows multiple phases of substrate binding (Cayley *et al.*, 1981) and hysteretic behaviour, although there is some doubt about the significance of this (Baccanari and Joyner, 1981, Penner and Frieden, 1985). In addition, both substrates have K_M's of less than 1μM and the rate of catalysis is very sensitive to salt concentration (Dann *et al.*, 1979, Stone and Morrison, 1982).

Complete kinetic schemes have been published for DHFR's from *E. coli* (Fierke *et al.*, 1987, Penner and Freiden, 1987), *L. casei* (Andrews *et al.*, 1989), and mouse (Thillet *et al.*, 1990) all of which are, in general, very similar to each other. The scheme for *L. casei* is shown in figure 1.6.

In the schemes there are two potentially rate limiting steps whose ratio varies with pH; at low pH the dissociation of FH_4 is rate limiting but as the pH is increased hydride ion transfer becomes increasingly rate limiting. From this scheme it can be seen that the effect of the negative cooperativity described under "conformational effects" above (where the binding of dihydrofolate is 80 times weaker in the ternary NADPH complex than the binary complex, Andrews *et al.*, 1989) is to facilitate the product release by the binding of the second ligand, NADPH. This effect is only seen between FH_4 and NADPH, not FH_2 and NADPH.

It is notable that despite the low amino acid sequence homology and evolutionary diversity, the three kinetic schemes are virtually identical, with only comparatively minor differences, which compares well with the structural similarity. The main differences between the schemes for the two bacterial enzymes are;

1. *L. casei* DHFR binds NADPH more tightly in both binary and ternary complexes
2. the internal equilibrium constant for hydride transfer (i.e. on the enzyme) is less favourable for *L. casei* DHFR because of both a decreased forward rate constant and an increased reverse rate constant.

The main difference between the bacterial and mouse DHFR kinetic schemes are;

1. the mouse DHFR is in solution as two conformers which both bind ligands with varying affinities but only one of which is catalytically active. Only one conformation of bacterial DHFR has been found to significantly bind ligands.
2. the hydride ion transfer rate is significantly faster for the mouse DHFR.

Figure 1.6. The kinetic scheme for L. casei DHFR in KMB buffer (see Chapter 5) pH 6.5, 25°C. The heavy arrows indicate the preferred pathway for steady state turnover.

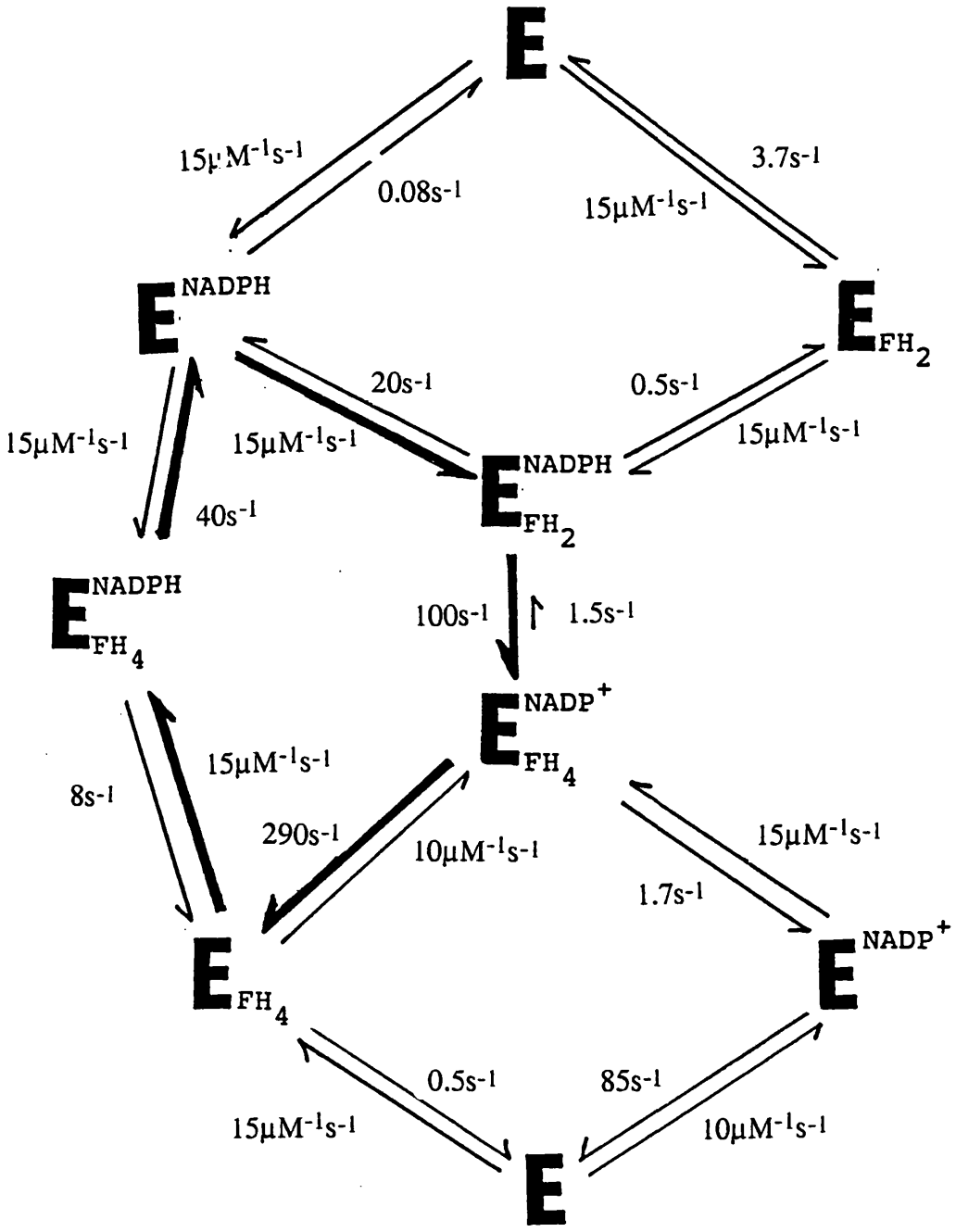

1.4.2. DHFR Catalytic Mechanism

It has been generally accepted that initial protonation of N5 would precede hydride transfer from C4 of NADPH to C6 of FH_2 (Huennekins and Scrimgeour, 1964, Lund, 1976) and kinetic isotope effect investigations have suggested that this is the case (Morrison and Stone, 1988). The rate of catalysis increases with decreasing pH, indicating that an ionising group at the active site must be protonated to obtain maximum velocity. In support of this the results of Stone and Morrison (1988) suggest that the ionising group is a neutral carboxylic acid and mutagenesis studies have shown that Asp27 (*E. coli* numbering) is important for substrate protonation (Howell *et al.*, 1986). As mentioned previously the only ionisable group in this region of the protein is Asp27 and so it is widely believed that this residue is the proton donor to FH_2. There is an anomaly in that Asp27 is not close to N5 of FH_2 (see the structure section), therefore the protonation of this nitrogen must occur indirectly, for example via protonation of O4 (Gready, 1985) or by transfer via a network of water molecules. There is also a possibility that the proton is transferred to N5 directly from the solvent with Asp27 stabilising this protonated transition state.

Two of the most recently proposed mechanisms are described below, both of which give the net reaction of transferring an hydride ion from NADPH and a proton from solution.

1. Stone and Morrison (Stone and Morrison, 1988, Morrison and Stone, 1988) propose a mechanism for catalysis based on a number of measured rate constants and isotope effects, where the proton comes from the Asp26 (*L. casei* numbering) residue. Figure 1.7 shows the proposed mechanism where the proton from Asp26 is transferred via a fixed water molecule at the active site with the result that Asp26 becomes negatively charged and the N3 of FH_2 is positively charged, FH_2 being in the enolic form. The lone pair electrons on N5 make a nucleophilic attack on the enolic hydrogen, facilitated by the positive charge on N3 which withdraws electrons. The result is N5 becomes positively charged and Asp26 negatively charged. The reaction then proceeds to form FH_4 by hydride ion transfer from NADPH. To support this mechanism the authors suggest that the complex hydrogen bonding network around the active site serves to decrease the basicity of Asp26 and increase the basicity of N5.

2. From the structure of human DHFR, Bystroff *et al.*, (1990) postulate another mechanism where essentially the proton is donated directly from the solvent (figure 1.8). In this mechanism Asp26 promotes enolisation of the pyrimidine ring such that O4 becomes protonated with the aid of the fixed water molecule, as above, but that Asp26 relays a proton from N3 to O4 rather than from the water to O4. The subsequent protonation of N5 occurs via a temporarily bound water molecule which hydrogen bonds to both O4 and N5,

and that the protonation is concerted with the return of the substrate to the keto form. The difficulty of accepting this mechanism is that the crystal structures of the enzyme with bound folate show the presence of an hydrophobic residue, usually leucine, near N5 rather than the proposed temporary water molecule. Comparison of 5 *E. coli* structures indicated that this hydrophobic residue lies in a very flexible segment of the protein making it feasible that a water molecule could temporarily bind. In this mechanism, Asp26 does not become ionised, which is still consistent with the results of Morrison and Stone (1988) who found that the carboxylic acid must be protonated for catalysis. However, theoretical studies have proposed that an ionised carboxylate hydrogen bonding to the pyrimidine ring could significantly raise the pK_a of N5, facilitating its protonation (Gready, 1985).

Bystroff *et al.* (1988) suggest how the transition state for hydride ion transfer can be stabilised by the proximity of the hydrophobic residue to N5. The hydrophobic residue is near the N5 end of the N5 to C6 bond and a carbonyl oxygen is near the C6 end, this geometry would favour the resonance form where C6 had carbonium ion character.

Figure 1.7. The proposed mechanism by Stone and Morrison (1988) for protonation of N5 of dihydrofolate.

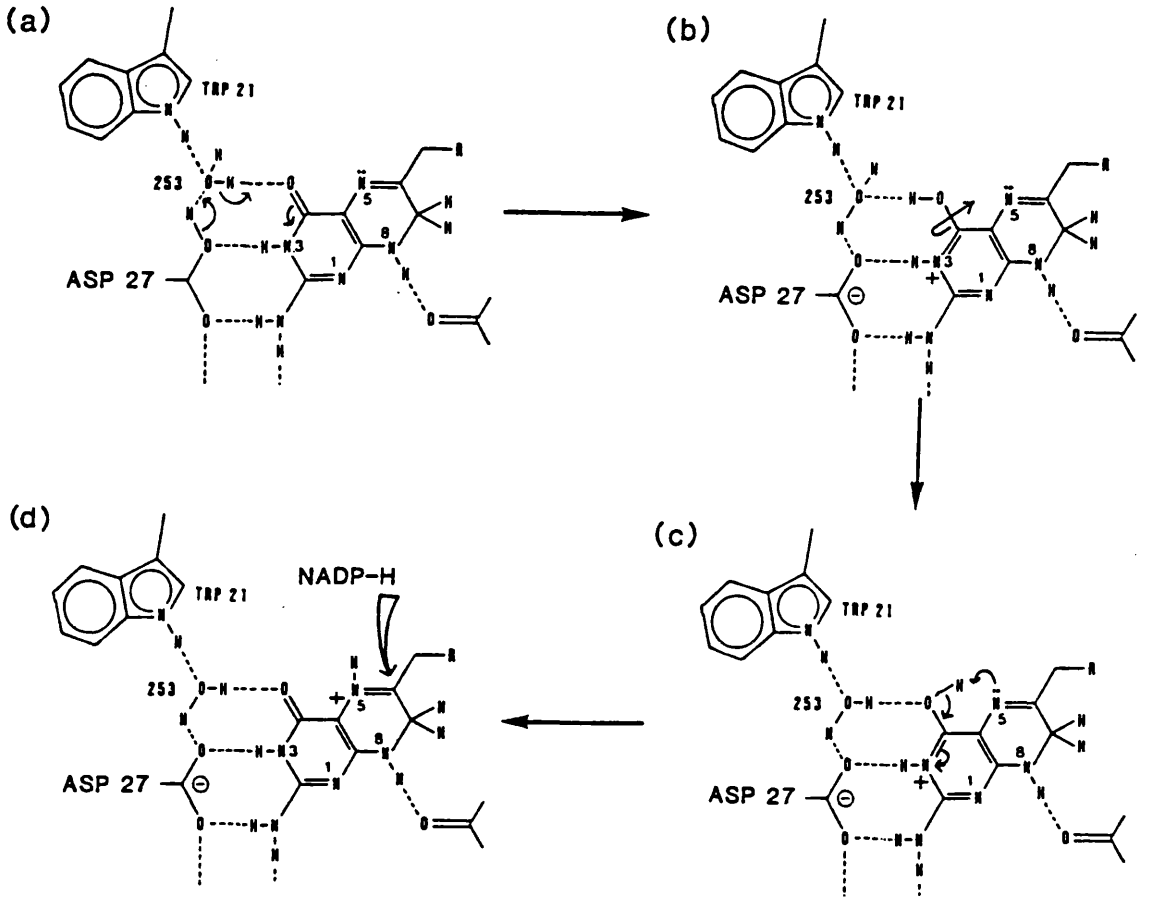

Figure 1.8. The proposed mechanism by Bystroff et al., (1990) for protonation of N5 of dihydrofolate and the proposed catalytic advantage of the proximity of an hydrophobic residue near the protonated N5.

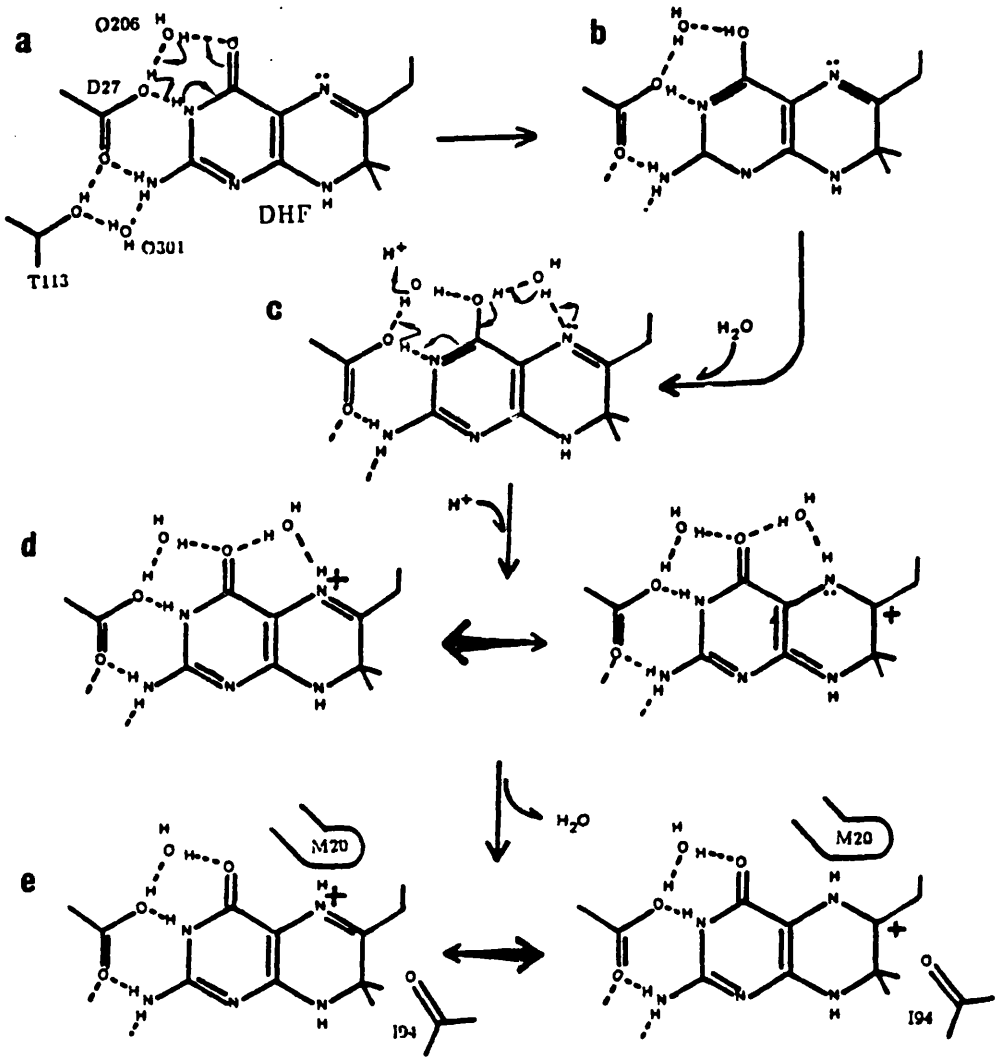

1.5. MUTAGENESIS STUDIES

A number of mutants of DHFR from various sources have been produced by site specific mutagenesis to probe the importance of specific amino acids in ligand binding and catalysis. Many groups are now using mutagenesis techniques, or "protein engineering", to study a wide variety of enzymes (reviewed by Shaw, 1987); however these studies are often hindered by the lack of structural information. DHFR is one of the few enzymes which has a refined X-ray structure and can be studied by nmr as well as having a fully characterised kinetic scheme. Those studying DHFR are in the enviable position of being able to examine the effects of a mutation upon DHFR structure and compare these with the change in function at the level of individual rate constants. Mutagenesis work on DHFR, beside answering questions specific to DHFR, is able to pioneer the investigations of the effects that mutations have upon enzyme structure and whether any general rules can be defined. Nmr is useful for mutagenesis studies, with the prior knowledge of the wild type crystal structure to assist in nmr assignments, for the comparison of mutant and wild type enzyme structures. It is particularly useful since both protein structure and conformational equilibria can be studied with the enzyme coupled with a variety of ligands. The reports to date of mutagenesis experiments on DHFR are summarised below.

Prendergast *et al.* (1989) employed mutagenesis to study human DHFR, examining the effects of mutating Phe31, a residue implicated in both the binding of dihydrofolate (Matthews *et al.*, 1985a,b) and in the species selectivity of TMP. The presence of an aromatic residue, in this case tyrosine, at position 31 in chicken liver enzyme was suggested to reduce the binding of TMP compared to bacterial DHFR's which have a leucine at this position. The mutant of human DHFR containing Leu31 does not have a different TMP inhibition constant with respect to wild type and so this residue appears not, in fact, to affect the species selectivity of TMP. The binding of coenzyme and catalytic properties were unaffected by the mutation in contrast to the binding of dihydrofolate which was significantly increased (by 43 fold), largely due to its slower off rate. The mutation implies that this residue is involved in the binding of substrate.

Prendergast *et al.* (1988) have also made a Cys6 to Ser mutation of the human enzyme to determine the role of Cys6, present in all vertebrate sources but absent in bacterial sources of DHFR. The Cys6 of vertebrate DHFR's specifically react with organic mercurials activating the enzyme, a phenomenon thought to be brought about by a conformational change (Freisham and Matthews, 1984, Duffy *et al.*, 1987). The results of the Cys6 to Ser mutant provides evidence that the mercurial activation does cause a conformational change and does so by breaking an hydrogen bond between the cysteine and another region of the protein. Perhaps surprisingly, the Ser6 mutant cannot make this

bond. As was expected, the cysteine residue is not required for substrate binding or catalysis (unless the serine is able to perform the same function).

Benkovic and coworkers have made mutants of *E. coli* DHFR at positions Phe31, Leu54, and Thr113. Phe31 lies in the hydrophobic pocket edge on to both the pteridine and *p*-aminobenzoyl rings and interacts with the pteroyl moiety of FH_2 through van der Waals contacts. The side chain of Leu54 is part of the hydrophobic region around the benzoyl glutamate portion of FH_2. The hydroxyl of Thr113 forms an hydrogen bond with the carboxylate of Asp27 and to a water molecule which in turn forms an hydrogen bond with the 2-amino group of the pteridine ring of FH_2.

Phe31 was mutated to a tyrosine and a valine (Taira and Benkovic 1987, Taira *et al.*, 1987, Chen *et al.*, 1987). The kinetic behaviour of the mutants in general was similar to the wild type enzyme and the dissociation of FH_4 remaining the rate limiting step. The main difference for each mutant was a two-fold increase in k_{cat} due to the faster dissociation of FH_4. The rate of hydride transfer was slightly decreased but not to the extent that it became rate limiting. The binding constants for both FH_2 and FH_4 were greatly decreased indicating the major role of Phe31 is in substrate binding.

Leu54 was mutated to a glycine, an isoleucine, and an asparagine (Mayer *et al.*, 1986, Murphy and Benkovic, 1989). The binding of $NADP^+$ and NADPH were virtually unaffected by any of the mutations except for a 15 fold decrease in NADPH dissociation from the Gly54 mutant. However, the dissociation constants FH_2 and MTX were affected and increased in the order Leu<Ile<Asn<Gly54. In contrast to the binding constants, the hydride ion transfer rate was affected by approximately the same amount by all three mutations and reduced by a factor of approximately 30, with the result that hydride transfer, rather than product release, is rate limiting. The pK_a of hydride ion transfer was altered by the mutations L54G and L54N suggesting some conformational change around the catalytic site (i.e. of Asp27) was caused by the mutations. The reasons for the affects of the mutations on the binding constants were discussed but it was clear that they could not be understood without structural data. The differential negative cooperativity (where the off rate of FH_4 is increased following the binding of NADPH, rather than $NADP^+$), is abolished by the mutant Ile54 with the result that products are released to leave a mixture of enzyme/$NADP^+$ and enzyme/FH_4 complexes rather than the enzyme NADPH complex as in the wild type enzyme. It is suggested by this group that the cause of the negative cooperativity is a result of repulsion between the two ligands which the mutant Ile54 somehow alleviates. However other studies provide evidence that a conformational affect is involved with some evidence that helix C contributes to this. It is notable that Phe49 (at the end of this helix) lies next to Leu54 (Hammond *et al.*, 1986, Birdsall *et al.*, 1981) and so the mutation effects may not be a simple reduction of the repulsion between the two

ligands but due to other conformational changes about helix-C. Overall no pattern could be seen in the results of these mutations and therefore Leu54 is probably involved in the precise positioning of FH_2 and no substitution can be easily tolerated without unpredictable alterations to the activity of the enzyme.

The strictly conserved threonine at position 113 in *E. coli* has been mutated to a valine (Chen *et al.*, 1985, Fierke and Benkovic, 1989). Extrapolating from the crystal structure with MTX and NADPH, it is believed that Thr113 is involved in the hydrogen bonding network with Asp27, a fixed water molecule and FH_2. The kinetic scheme of this mutant was identical in form to the wild type enzyme but there were changes in the values of individual rate constants. There was an increase in the intrinsic pK_a of Asp27, postulated to be because the mutation increases the stabilisation of the carboxylate form of this residue. The mutation reduces the binding of substrate and inhibitors, the binding of folate ligands were decreased by approximately 2.3 kcal/mol. The difference in binding energies between the mutant and wild type enzymes is believed to be too large to be accounted for simply by the loss of the hydrogen bond and so it is postulated that other factors such as conformational changes have occurred. The hydride-transfer rate constant was also decreased in both directions. It was noted by these authors that a decrease in hydride ion transfer rate has been seen in other mutants and so far has always been found to occur with a decrease in the binding of substrate (Benkovic *et al.*, 1988).

Adams *et al.* (1989) have studied mutations in the *E. coli* enzyme at Arg44 (changed to leucine) and His45 (changed to glutamine), of which the former forms an ionic contact with the 2' phosphate of NADPH and the latter forms an ionic contact with the pyrophosphate of NADPH. As expected, the binding of coenzyme is reduced by the mutations and the binding of FH_2 and FH_4 is not affected. However, although the binding of FH_2 and FH_4 is not affected, the transition state for hydride transfer is destabilised by both mutations, probably due to multiple conformations in the mutant-NADPH complexes. Interestingly the mutations have increased the pK_a of Asp27 by at least 1 pH unit despite the mutations being some distance away from this residue at the site of catalysis. This and other data indicate that the structure of the enzyme is different at a location some 20Å away from the mutations and apparently both ligand binding sites function together so that events which affect one site will have affects upon the other.

Huang *et al.*, (1989) have made a mutant of the human DHFR by changing the strictly conserved tryptophan at position 24, equivalent to Trp21 in the *L. casei* DHFR, to a phenylalanine. An attempt at examining the structure was made by antibody binding (ELISA) and protease susceptibility studies, which suggested the enzyme was in a more "open" or "flexible" conformation, possibly suggesting that Trp24 is important for maintaining the structural integrity of the native enzyme. The binding of coenzyme and

substrates are decreased by the mutation as a result of the structural changes. The k_{cat} of the mutant is increased five fold with respect to wild type at pH 7.5 however k_{cat} and k_{cat}/K_M ratio decrease more rapidly than wild type with increasing pH, i.e. the mutant is more susceptible to pH changes, probably due to the non-optimum hydrogen bonding with FH_2.

The *L. casei* enzyme has also been mutated at Trp21 to a Leu. This mutant has been studied both structurally (Birdsall *et al.*, 1989a) and kinetically (Andrews *et al.*, 1989). It is known from the crystal structure that in *L. casei* Trp21 forms an hydrogen bond to N8 of MTX, via a water molecule, and is in van der Waals contact with the nicotinamide ring of NADPH. The advantage of the *L. casei* work is that the structure and function of the mutant could be compared using nmr, whereas in all the work described above the authors have had to assume structural integrity or guess at the precise nature of the structural changes. The kinetic results showed that the hydride ion transfer rate was decreased by 100 fold making this the rate limiting step in the reaction, and the affinity for NADPH was decreased markedly, mainly due to an increased dissociation rate, with a lesser effect on $NADP^+$ and FH_2. The reason for the different affects the mutation has upon the binding of oxidised and reduced coenzyme can be explained by the much lower contribution the nicotinamide ring makes towards $NADP^+$ binding. Nmr was used to examine the structure of the mutant and it was found there were no substantial conformational changes in the protein and that the adenine end of the coenzyme and the folate binding site were essentially the same. The major change of structure compared to wild type was seen at the nicotinamide binding site, providing an explanation for the reduced hydride transfer rate.

DHFR has been modified by both the Kraut and Roberts groups to investigate the function of Asp27 *(E. coli)* (Asp26, *L. casei*), the residue widely believed to be the ionisable group involved in catalysis (see the kinetics section). Kraut and coworkers have made the mutations Asp27 to serine and asparagine (Howell *et al.*, 1986, 1987, London *et al.*, 1986, Villafranca *et al.*, 1987, Appleman *et al.*, 1988) which were examined by X-ray crystallography and kinetics. The Roberts group have made the mutation Asp26 to asparagine and glutamate (Jimenez *et al.*, 1989, Birdsall *et al.*, 1989a) studied by nmr. The Kraut group found that the crystal structures only showed significant structural perturbations at a site close to the mutation and involved two water molecules (figure 1.9). One of these is a fixed water (403) which hydrogen bonds with Asp27, and is replaced by the amido group of asparagine in the mutation. This results in an alteration of the hydrogen bonding network with residue 27 and affects the position of another water molecule, wat 567 (confirmed by the crystal structure). The movement also results in the wat403 molecule forming a strong hydrogen bond with a third fixed water molecule that is only weakly hydrogen bonded in the wild type. Other structural alterations in the protein were less than 0.2Å, thought to be insignificant, and the binding site of MTX is the same. The

Ser27 side chain is smaller than the aspartate and the space is filled with a new water molecule. Again no differences of greater than 0.2Å are seen in the protein or MTX binding site. UV difference spectroscopy of the wild type DHFR has revealed that the N1 of MTX is protonated and the basis of the strong binding is believed to be because of the ionic interaction between N1 the Asp27 side chain (Cocco *et al.*, 1981a,b, 1983, Hood and Roberts, 1978, Stone and Morrison, 1983).

Figure 1.9. Probable Hydrogen Bondings between MTX and wild type DHFR (A), Asn26 mutant (B), and Ser27 mutant (C).

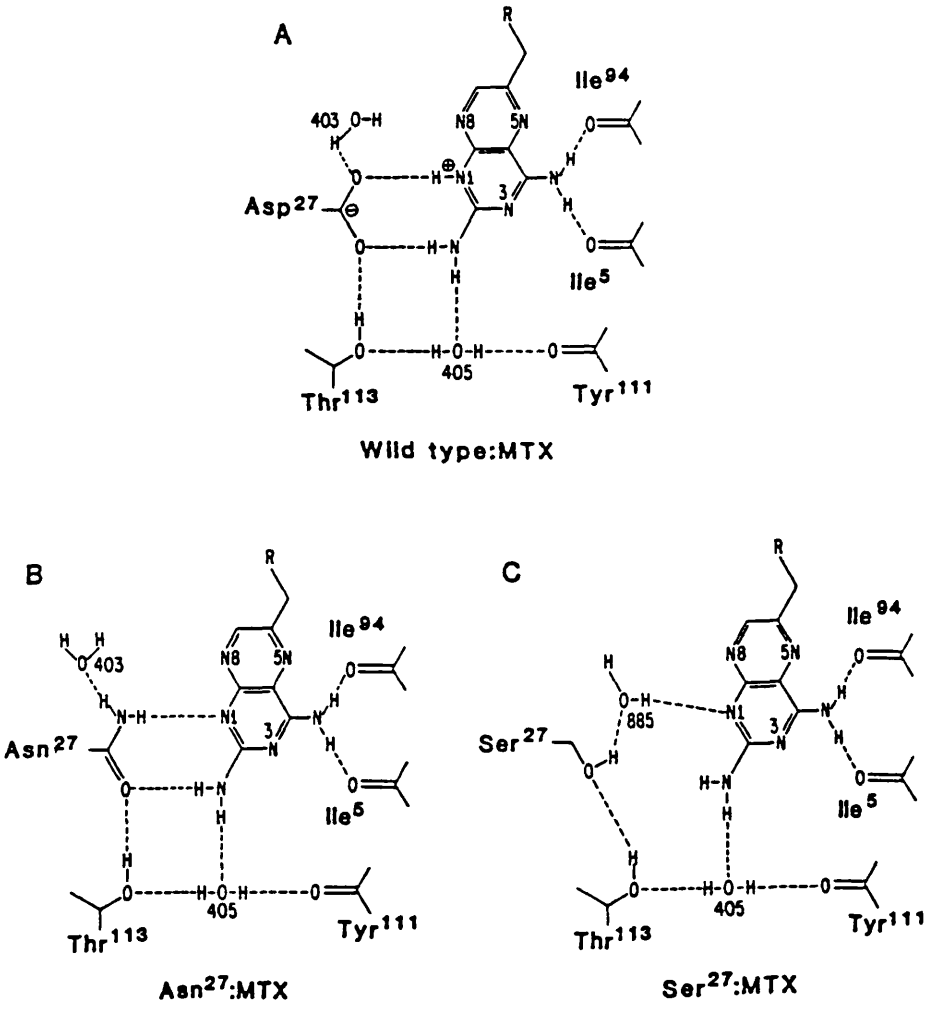

In contrast, the N1 of MTX was not protonated in either mutant yet only the Ser27 mutant had a significantly lower binding of MTX. This group found, from the Gln mutant results, that the ionic interaction only contributes 1.8 kcal/mol thus it appears it may not be merely the ionic interaction that forms the basis of the tight MTX binding and may rather be due to the interaction between the 4-amino group of MTX and the backbone carbonyls of Ile94 and Ile5 in the protein. The much reduced binding of the serine mutant can be explained by

the loss of an hydrogen bond, a van der Waals gap left between the 2-amino group and the enzyme aswell as the loss of the ionic interaction. The fact that the mutants were able to catalyse the reaction, albeit very slowly (k_{cat} is 68 and 300 times slower for Gln27 and Ser27 mutants respectively), is surprising since this residue was thought to be essential for catalysis. Measuring catalysis at a range of pH values showed the rate increased rapidly with decreasing pH (pK_a = 4 for the mutant and 8 for the wild type DHFR) whereas the K_M for FH_2 was independent of pH. The simplest explanation of this effect is that only protonated FH_2 is a substrate for the mutant DHFR's although both protonated and unprotonated bind with equal affinity, i.e. in the wild type Asp27 participates in protonation of the substrate allowing catalysis at an higher pH, the mutants will only catalyse the reaction provided the pH is low enough so that FH_2 is protonated.

The *L. casei* mutant Asp26 to glutamate (Birdsall *et al.*, 1989a) was found to have 90% of the activity of the wild type enzyme and the binding constant of the inhibitor TMP was very similar to wild type suggesting that Glu26 can make the same interactions as Asp26. The Glu26 mutant was studied by nmr when in binary complex with TMP and in ternary complex with folate and $NADP^+$. The structure of the complex with TMP was very similar to wild type, the only apparent difference being very small movement of TMP of less than 0.2Å, and some small dynamic differences in the rate of the benzyl ring flipping (which is very sensitive to conformational changes) and the rate of association and dissociation of TMP to the enzyme. These results indicate some small conformational changes, probably to allow the carboxylate of glutamate to bind effectively with N1 of TMP. These studies show that the sequence difference at this residue, conserved as an aspartate in bacterial enzymes and a glutamate in vertebrate enzymes (Matthews *et al.*, 1985a) does not in itself confer specificity of binding of TMP to bacterial over vertebrate enzymes. Studies on the wild type DHFR/folate/$NADP^+$ complex has been shown by nmr to exist in three conformations, I IIa and IIb, the relative ratios being pH dependant (Birdsall *et al.*, 1982, 1989b). The D26E mutant does not perturb these equilibria but at least one of the conformations has some structural differences, as characterised by chemical shift changes in the signals from bound folate and coenzyme. However, the main difference between the wild type conformations is the orientation of the pteridine ring which is rotated by 180° in the form IIb (the catalytically functional orientation) compared to forms I and IIa (which is a nonproductive orientation) (Charlton *et al.*, 1979) and this gross difference is retained by the mutation. Thus, if Asp26 is responsible for the pH dependence of this equilibrium, then Glu26 in this mutant must be acting in a similar way and a definitive conclusion cannot be reached.

A mutation in the *L. casei* DHFR where Asp26 has been changed to an asparagine was also made by the Roberts group (Jiminez *et al.*, 1989). In agreement with the same mutation in *E. coli*, the rate of catalysis was reduced by a factor of approximately 100. The

D26N mutant has abolished the pH dependent conformational equilibria suggesting that Asp26 is responsible for the pH dependence of this equilibrium. The mutant appears to exist in one conformation which does not change with pH. Comparison of the proton chemical shifts of assigned resonances with those of the various conformations of the wild type enzyme indicate that the protein is locked into form I which predominates at low pH in the wild type, where the ionisable group controlling the equilibria (apparently Asp26) is protonated (Birdsall *et al.*, 1982, 1989a). Thus it appears that the asparagine mimics the protonated state of aspartate leading to the adoption of conformation I. In this conformation folate binds in the MTX-like, non productive, orientation (Birdsall *et al.*, 1989b). Paradoxically this result does not confirm that Asp26 is the proton donor in the reaction since it suggests that the substrate binds in a non-productive manner when this residue is protonated. However the results were from the folate complex with oxidised coenzyme rather than the substrate dihydrofolate with reduced coenzyme. The structural changes caused by the mutation are small and local to the region around the mutation. This and the other results are in agreement with the crystal structure and kinetic results of the corresponding *E. coli* mutation described above.

A mutant of the *L. casei* DHFR has been made where a conserved tryptophan at position 21 was changed to a leucine (Birdsall *et al.*, 1989a, Andrews et al., 1989). This residue is close to both the coenzyme and substrate binding sites and forms an hydrogen bond, through a water molecule, to the N8 of MTX. The major effects of this substitution were to decrease the hydride transfer rate constant by 100 fold making it the rate limiting step, and to decrease the affinity for NADPH and $NADP^+$ by 3.5 and 0.5 kcal mol^{-1} respectively (mainly due to increased dissociation rates). The folate binding site and the adenosine region of the coenzyme form the same ionic interactions and adopt the same conformations and no large structural change in the protein are observed. The major structural change is at the nicotinamide moiety of the coenzyme, which binds with a different orientation due to the loss of an hydrophobic interaction with the carboxamide nitrogen of bound NADPH, offering an explanation of the reduced hydride transfer rate. The marked difference in the effect of the mutation on the oxidised and reduced coenzymes can be explained by the smaller contribution of the oxidised nicotinamide ring to the overall binding (Birdsall *et al.*, 1980a,b). In the ternary complex of wild type DHFR bound with TMP and $NADP^+$ there is an equilibrium between two conformations of the coenzyme, one where the nicotinamide moiety is bound in the normal binding pocket of the enzyme and the other where the nicotinamide is extended into solution. In the mutant there is only one conformation seen and this is the same as the wild type conformation where the nicotinamide moiety extends into solution. These results provide a clear indication of the importance of the interaction between Trp21 and the carboxamide nitrogen to the binding of coenzyme.

1.6. BACKGROUND TO THE THESIS

At the start of this thesis a great deal was known about DHFR from various sources. In summary of the above discussions the main points are listed below;

* the crystal structure from various bacterial and vertebrate sources, and more recently of the human enzyme are known
* a considerable amount of research involving nmr experiments on the *L. casei* DHFR has led to a substantial number of proton resonance assignments, recent developments have these assignments almost complete by the use of 3D nmr techniques (Birdsall, Carr, Feeney, personal communication)
* a complete kinetic scheme has been determined for bacterial, and very recently the mouse, enzymes
* DHFR from various sources have been cloned and mutagenesis techniques developed.

Despite this wealth of information regarding the enzyme, the mechanism of how the net reaction of transferring an hydride ion from NADPH and a proton from solution, is catalysed by DHFR is as yet unknown. In the past, the traditional methods of studying structure and function affects were by chemical modification of the protein or by using various substrates and analogues. The development of mutagenesis techniques now allows an alternative method of studying the structure/activity relationship. This project was to study the affects of mutations upon the structure of *L. casei* DHFR and correlate these affects with any kinetic differences, in order to ascertain the contribution of the altered amino acid to DHFR structure and function.

1.6.1. Summary of Mutants Studied in This Thesis

In the course of the studies detailed in this thesis, experiments on four mutants have been performed, these are;

1. tryptophan at position 21 changed to a histidine (W21H)
2. aspartic acid at position 26 changed to a glutamine (D26N)
3. threonine at position 63 changed to a glutamine (T63Q)
4. threonine at position 63 changed to an alanine (T63A).

The position of each mutant in the enzyme structure is shown in photograph 1.1. My participation in the research of these mutants differed for each, outlined in table 1.2. In

the research of the T63A mutant I did the work from inception to conclusion, i.e making the mutant by site specific mutagenesis. expressing and purifying the mutant, measuring various kinetic parameters and binding constants and examining the structure of various complexes by nmr. For T63Q the mutant was made by Dr J. Andrews, other than this my research on this mutant was the same as for T63A. My role in the D26N research was the expression and purification of this mutant and for W21H I accomplished the mutagenesis experiments.

Table 1.2. A summary of the experiments carried out for each mutant.

Experiment	T63Q	T63A	D26N	W21H
Mutagenesis		√		√
DHFR expression	√	√	√	
DHFR purification	√	√	√	
NMR	√	√		
Kinetics	√	√	some preliminary	

The rationale behind the D26N and W21H mutations is described in the following whereas that for the threonine mutations is detailed in the beginning of the nmr chapter.

1.6.2. D26N

The aspartic acid residue at position 26 in the *L. casei* enzyme was mutated for two main reasons. Firstly it is believed to be involved in the protonation of FH_2 (Stone and Morrison, 1984, Howell *et al.*, 1986) and secondly the ion pair interaction formed between the acid and the protonated N1 of MTX, TMP and other inhibitors is believed to form the basis of the tight binding of inhibitors compared to the substrate. The mutation D26N would be expected to have a similar geometry to wild type but it would not be able to act as a proton donor.

1.6.3. W21H

Tryptophan at position 21 is a strictly conserved residue in all DHFR's examined to date (Bolin *et al.*, 1982). The residue lies close to both the coenzyme and substrate and forms an hydrogen bond to the N8 of the MTX pteridine ring via a water molecule (Bolin *et al.*, 1982). It has been found that the mutation where Trp21 was mutated to a leucine led to dramatic changes in coenzyme binding at the nicotinamide moiety (Birdsall *et al.*, 1989a) with a concomitant loss of activity (Andrews *et al.*, 1989). The mutation W21H is therefore designed to be more conservative, where the imidazole ring of histidine replaces the 5 membered "pyrrole" part of tryptophan. The aim is that the contribution this residue makes to the binding of coenzyme and substrate can be probed by the mutation and the importance of its ionisation state can be probed by pH titrations.

Photograph 1.1. Ribbon drawing of L. casei crystal structure in ternary complex with NADPH (blue) and MTX (red), the positions of threonine-63, aspartate-26 and tryptophan-21 are shown.

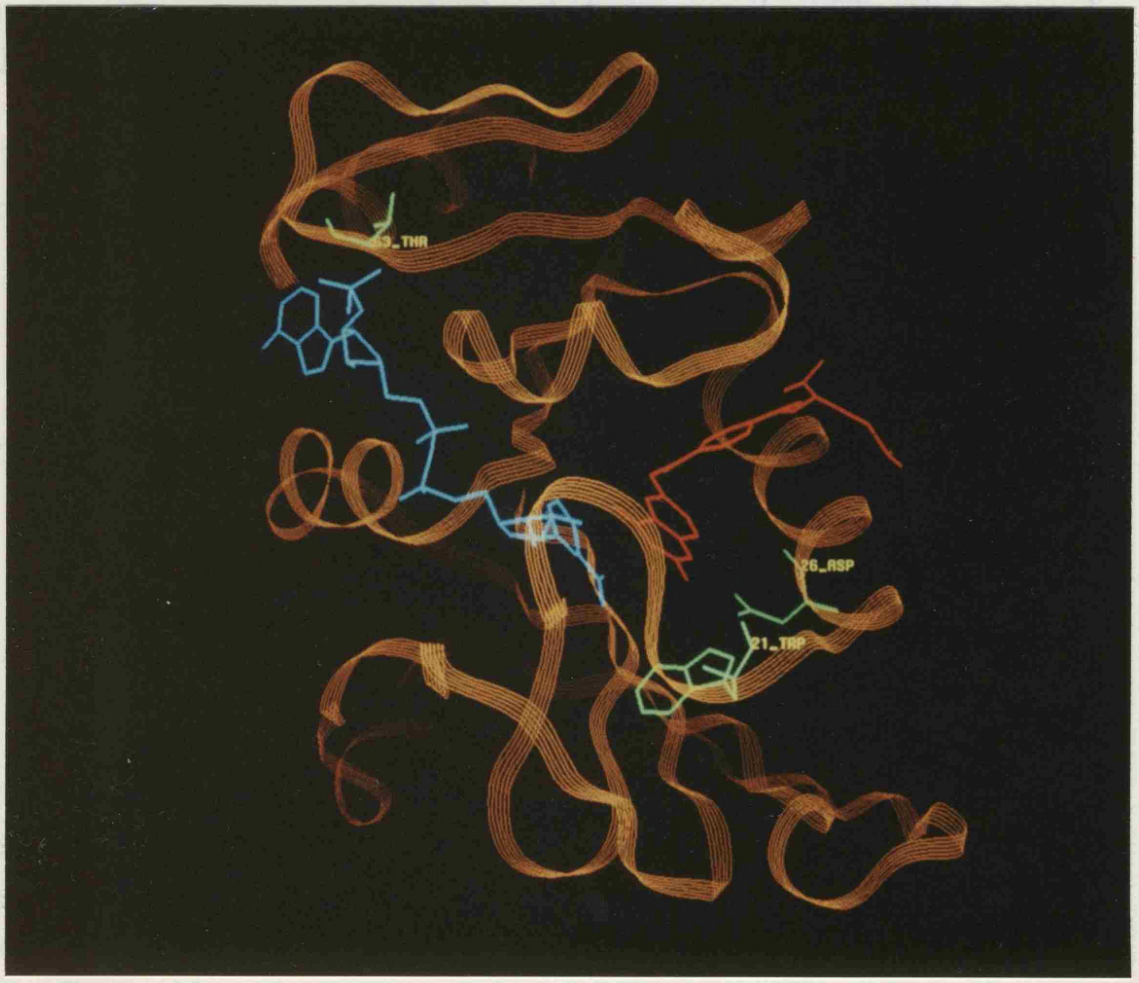

CHAPTER 2. MUTAGENESIS

2.1. INTRODUCTION

The DHFR gene from *L. casei* has been cloned into *E. coli* (Andrews *et al.*, 1985) and mutagenesis protocols have been developed (Andrews *et al.*, 1989), using a gapped-duplex DNA approach (Kramer *et al.*, 1984).

Two mutagenesis methods have been used for this research which differ in the type of vectors used.

1. The original method, carrying out mutagenesis in M13, followed by recloning the mutated gene into an expression vector.

2. In the second method a similar protocol is used, but mutagenesis is carried out in a plasmid, thus eliminating the need to reclone the gene into an expression vector.

An overview of these protocols is shown in figure 2.1.

A) M13 protocol

The M13 mutagenesis protocol uses the bacteriophage M13 vectors, M13mp8 and M13mp18 (Messing, 1983). The mp series of vectors consist of M13 DNA with a short insert of *E.coli* DNA containing the *lac* operator and a portion of the *lacZ* structural gene corresponding to the first 146 residues of the β-galactosidase. The host (e.g. JM101) carries the F' plasmid which contains a defective *lacZ* gene lacking amino acids 11-41. Transformation of this host with the vector results in production of blue plaques on a medium containing IPTG and X-gal, due to α-complementation of the defective gene and the peptide to form an active β-galactosidase enzyme. The gene to be cloned is inserted into the *lacZ* region of the vector and so eliminates the α-complementation, giving rise to colourless plaques and providing a simple screen for recombinant DNA.

The difference between M13mp8 and M13mp18 is that the former has an amber mutation in the selectable marker gene that codes for ampicillin resistance, whereas the latter does not. An "amber" mutation is one in which a base has changed such that a stop codon is created in the gene, preventing its full expression. Thus the host strain can not grow in the presence of ampicillin. However, a "suppressor" strain (e.g. *supE* or *supF* such as JM101, see appendix) can survive because it has a tRNA with a mutated anticodon and therefore can insert an amino acid at this stop codon allowing the gene to be expressed.

One strand of M13mp8, with the DHFR gene cloned into it (the template strand), and one strand from M13mp18 (without the DHFR gene) are annealed together to form a gapped duplex. An oligonucleotide containing the required mutation is annealed to the template strand and the gaps are filled in using Klenow polymerase and ligase. In choosing the oligonucleotide for making the mutant five factors were considered;

1. No accidental loss or addition of restriction sites.
2. The priming specificity; it is preferable to have at least two CG base pairs on the ends for strong hybridisation.
3. The position of the mismatch; preferably in the centre of the oligonucleotide.
4. The oligonucleotide must be complementary to the reading frame.
5. Using two base changes rather than one makes hybridization selection easier.

The resultant plasmid is transformed into a repair deficient suppressor strain (e.g. mutS, supE), so that strand segregation and replication can occur without repair of the mutation. The resultant mixed population of mutant and wild type phage are then transformed into a suppressor$^-$ strain grown on ampicillin so that the phage containing the wild type gene will not grow (since they have an amber mutation in the ampicillin resistance gene). The cells that grow will be those transformed with DNA derived from the mutant strand, M13mp18.

The mutants are then identified using selective colony-hybridisation by the radiolabelled oligonucleotide (with the mutant DNA), followed by sequencing the entire gene. The mutant DNA is then cleaved out of M13mp18 by appropriate restriction enzymes and ligated into an expression vector such as pPLc28.

B) pMa/c protocol

Another protocol has recently been used which uses the pMa/c series of vectors. The pMa/c vector contains an origin of replication for plasmid replication (ColE1 type) and an origin of replication for f1 phage. The two origins of replication mean that the DNA can replicate as either plasmids or as phage rods (called phasmids) (Dente *et al.*, 1983). However, because the plasmid does not code for the proteins required to package the DNA into phage, the presence of "helper phage" is necessary to produce these proteins. Thus the vector is usually present as plasmid DNA and the host cells are infected with helper phage in order to produce single stranded DNA used for sequencing.

Figure 2.1. Gapped Duplex Mutagenesis Protocol

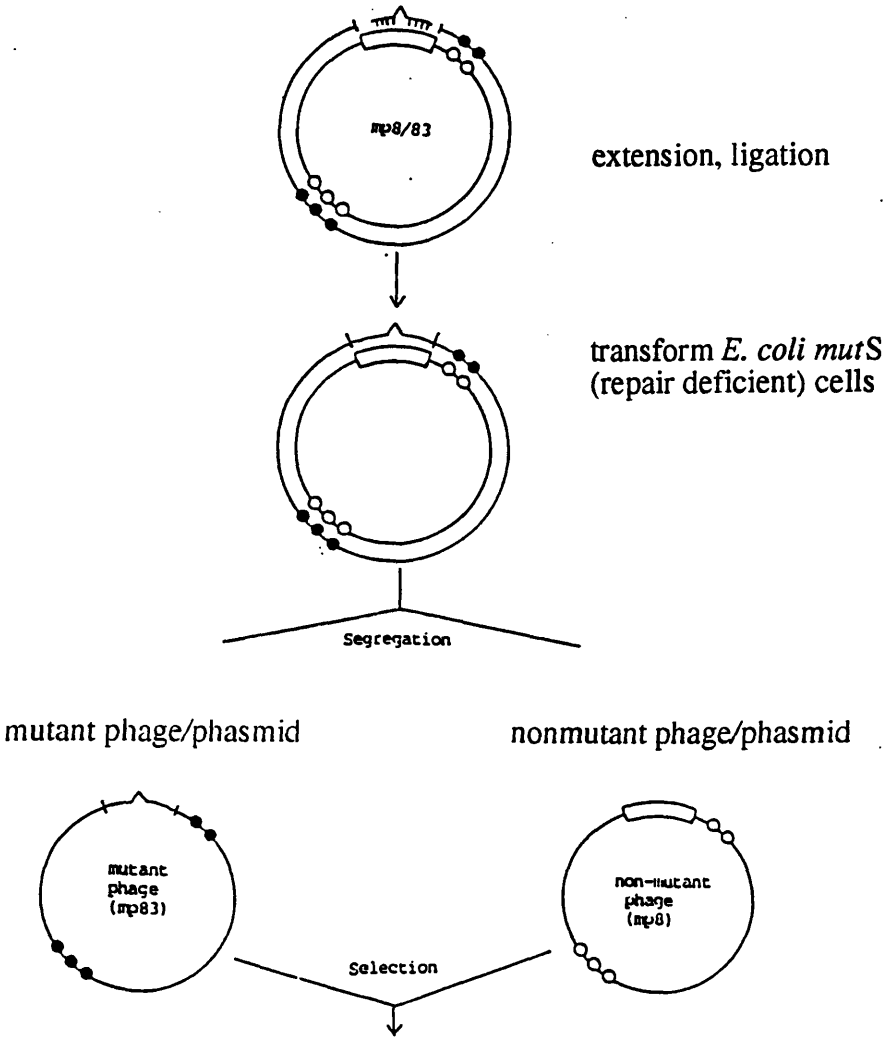

The main advantages of the pMa/c system over M13 are;

* the recombinants can be used for mutagenesis and expression, which omits the recloning procedures
* several rounds of the mutagenesis protocol can be used to make multiple mutations
* the vector DNA exists as plasmids but can also replicate as packaged single stranded phage under certain conditions.

The pMa/c5-14 plasmid used for this protocol also has a P_L promoter so that high levels of expression of the cloned gene can be obtained under the control of the λ cI_{857} temperature sensitive repressor.

To enable several rounds of mutagenesis to be carried out there are two selectable markers; a *cat* gene, conferring chloramphenicol resistance, and a *bla* gene conferring ampicillin resistance. Two plasmids are constructed complementary to each other except for an amber mutation in one or other of these genes. Thus one strand of the gapped duplex can only code for ampicillin resistance (pMa) and the other can only code for chloramphenicol resistance (pMc) unless in a suppressor strain that can read through the amber mutation. This method provides a positive selection (using antibiotic resistance) for the phasmid containing the mutant gene. If a mutation is constructed on the pMa strand a second round of mutagenesis can be carried out using the complementary pMc strand as the vector.

2.2. PROTOCOLS

All the basic methods used to make the mutants (Andrews *et al.*, 1989 and personal communication) are detailed in the appendix in the order described, and these protocols described were used to make the following mutants;

Tryptophan-21⇒Histidine (W21H)
Threonine-63⇒Alanine (T63A)

In addition to my own preparations (described below), gapped duplex DNA, plasmids and phosphorylated linear pMa DNA have also been kindly provided by Dr Andrews.

2.2.1. Threonine63⇒Alanine (T63A)

The oligonucleotide used in the preparation of T63A was:

```
                                Ala
5'  C.  TTC.  CTG.  ATG.  CGC. CAA. AAC. AAC.  3'
                          GGT
                          Thr
```

The codon CGC (entailing two base changes for the mutation) was chosen since it is probably the most abundantly used in coding for alanine in *E.coli* and it has two noncomplementary bases. Non-complementarity makes hybridisation selection easier because there is a greater difference between the melting temperatures of the oligonucleotide with wild type and mutant genes.

The oligonucleotide was phosphorylated using polynucleotide kinase and annealed to a gapped heteroduplex DNA (gdDNA) made up of pMa802 (pMa containing the wild type DHFR gene) and pMc as the gapped strand. An extension/ligation reaction was carried out to fill in the gaps. The resultant plasmids were transformed into BMH71-18 *mutS* (a mismatch repair deficient strain) for strand segregation, replication and production of phasmids. The phasmids were transformed into WK6λ (a suppressor$^-$ strain that expresses the λ cI_{857} repressor gene, used for controlling the enzyme expression) and these were plated out on media containing streptomycin and chloramphenicol for selection of the mutant, i.e. because BMH71-18 cells are streptomycin sensitive they will not grow in this medium, the plasmids containing the mutant gene express chloramphenicol resistance and so selection is for WK6λ transformed with the pMc/T63A plasmid.

200 colonies were picked into storage media in microtitre plates and left to grow at 37°C overnight. Colonies were replica plated onto agar plates and the trays were stored at 20°C. The agar plates were grown overnight at 37°C.

The colonies were transferred to nitrocellulose filters, lysed, and the probe (the mutagenic oligonucleotide radiolabelled with ^{32}P) was hybridised to the DNA. The mutants were detected by washing at a temperature high enough so that only if the probe exactly matched the DNA would it remain bound (the thermal dissociation temperature or T_d). The temperature for selection was determined using the equation:

$$(4 \times N^o \text{ of } G/C) + (2 \times N^o \text{ of } A/T) = T_d \,^\circ C$$

For T63A, T_d was calculated to be 66°C. The hybridised colony DNA was washed at (T_d-2)°C to remove most of the background, followed by a wash at T_d. The hybridised DNA which remained was detected by autoradiography, indicating which colonies contained the mutant gene. This treatment gave 21 probable T63A mutants, thus a probable mutation rate of 10% was achieved.

Ten putative mutants were grown from the microtitre trays in culture broth containing chloramphenicol (giving selective pressure for the plasmid because it expresses chloramphenicol resistance). Glycerol stocks and plates were made for storage of these strains. Template and plasmid preparations were made from single colonies for restriction digests and sequencing. Restriction digests were carried out to check that the plasmid contained the gene (EcoRI and HindIII cuts either side of the gene) and that the correct gene had been inserted (there is a unique BglII site within the gene). Having established this, the whole gene was sequenced to confirm that it was the mutant rather than wild type and that there were no further mutations or any deletions/insertions. Sequencing the T63A gene showed that the sequence was correct (Figure 2.2).

To summarise, the T63A gene was located after, and under the control of, the P_L promoter in the pMc plasmid which codes for chloramphenicol resistance. The plasmid was transformed into WK6λ which expresses the temperature sensitive cI_{857} repressor.

2.2.2. Tryptophan21⇒Histidine (W21H)

Similar protocols to those used for T63A were followed, the main difference was that the DHFR gene was manipulated in M13 rather than the pMa/c system. However, the gene cannot be expressed in M13, so once sequenced, it was cloned into an expression vector. The vector used was pMa, which has a P_L promoter for expression of the gene, and an ampicillin resistance gene.

The oligonucleotide used for the mutation was;

```
                                  His
3'  CCA. GTA. AAC. GGT.  GTA. GTA. AAT. GGC. C  5'
                         ACC
                         Trp
```

The gapped duplex DNA to which the oligonucleotide was annealed was made from two plasmids, M13mp8 and M13mp18. These are complementary to each other except for an amber mutation, described in the introduction to this chapter. The gapped strand was M13mp18 whilst M13mp8 had the wild type DHFR gene cloned into it and carried the amber mutation.

The gaps were filled in by extension/ligation reactions and BMH71-18 *mutS* (a mismatch repair deficient suppressor strain) was transformed with the plasmid for strand segregation and replication. The resultant phage were used to transfect a suppressor$^-$ strain, W71-18. Only M13mp18 derived DNA containing the mutant gene could be replicated to form plaques.

Colony hybridisation was carried out to find probable mutants, as previously described for T63A. The T_d calculated for W21H was 74°C. W21H showed 21 probable mutants from 200 colonies picked, i.e. a mutation rate of 10%.

The mutants were grown up and given to Dr Andrews' laboratory for sequencing. A W21H mutant has been sequenced and transferred to the pMa expression vector and is (at the time of writing) ready for study.

2.2.3. Threonine63⇒Glutamine (T63Q)

The T63Q mutant was made previously by Dr J. Andrews. The results described in the nmr and kinetics chapters led to some concern as to whether an additional mutation had occurred with or without the T63Q mutation reverting back to wild type and so it was decided to resequence the gene. In order to do this the gene was transferred from the pPLc28 vector and into the pMa plasmid. This meant that single stranded sequencing could be carried out and the gene would be in a convenient vector for further manipulation if required.

The T63Q plasmid was purified from a 1 litre culture by the large scale plasmid preparation method. Restriction digestions were carried out on a sample to ensure the purity of the preparation and the efficiency of the restriction enzymes. The enzymes used were EcoR1 and HindIII which cleave either side of the gene, and BglII which cleaves within the gene. Once it was ascertained that the digestions were working, a large scale EcoR1/HindIII restriction digest was set up to excise the 650 base pair fragment containing the T63Q DHFR gene. The fragment makes up approximately one sixth of the plasmid and so 12μg was digested to ensure approximately 1μg of fragment was obtained, conservatively estimating a 50% yield.

A preparative agarose gel was run to separate the insert from the rest of the plasmid. The bands of insert were cut out and the DNA was electro-eluted from the agarose. The ethidium bromide bound to the DNA then had to be removed by purification on a NACs column (a ready prepared ion exchange column from Pharmacia). For this column the buffer had to be changed, so the DNA was precipitated by ethanol, dried, and resuspended in the low salt loading buffer.

To estimate the final concentration of the insert, half of this purified DNA was run on a gel, where it is possible to visually estimate the amount of DNA in a band using controls for comparison. In this way, half of the T63Q fragment preparation was estimated to be 500ng.

The insert was ligated with phosphorylated pMa vector DNA using various ratios of vector to insert from 10:1 to 1:1, in order to find the conditions required for achieving one insert per plasmid. The resultant recombinant plasmid was used to transform competent WK6λ. Plasmid and template DNA were made for restriction digestions and sequencing.

Sequencing showed that the mutation was T63Q and that there were no other mutations in the gene.

Figure 2.2. The sequence of the L. casei wild type DHFR gene.

```
  GGGGTCTCG.AAT.GAC.CGC.ATT.TTT.ATG.GGC.ACA.GGA.TCG.CGA.TGG.C
      START  M   T   A   F   L   W   A   Q   D   R   D   G

TT.AAT.TGG.CAA.AGA.TGG.TCA.TTT.GCC.ATG.GCA.TTT.ACC.GGA.TGA.TT
L   I   G   K   D   G   H   L   P   W   H   L   P   D   D   L

T.ACA.TTA.TTT.CCG.GGC.GCA.GAC.AGT.TGG.TAA.GAT.CAT.GGT.CGT.TGG
   H   Y   F   R   A   Q   T   V   G   K   I   M   V   V   G

.TCG.GCG.CAC.CTA.TGA.AAG.TTT.TCC.TAA.ACG.TCC.TTT.ACC.TGA.GCG.
  R   R   T   Y   E   S   F   P   K   R   P   L   P   E   R

AAC.CAA.TGT.TGT.TTT.GAC.CCA.TCA.GGA.AGA.CTA.TCA.AGC.GCA.AGG.T
 T   N   V   V   L   T   H   Q   E   D   Y   Q   A   Q   G

GC.CGT.GGT.CGT.GCA.TGA.TGT.TGC.GGC.GGT.TTT.TGC.TTA.TGC.TAA.GC
A   V   V   V   H   D   V   A   A   V   F   A   Y   A   K   Q

A.GCA.TCC.CGA.TCA.GGA.ACT.GGT.CAT.TGC.TGG.CGG.TGC.ACA.GAT.CTT
   H   P   D   Q   E   L   V   I   A   G   G   A   Q   I   F

.TAC.GGC.GTT.TAA.AGA.TGA.TGT.CGA.TAC.GTT.ACT.GGT.AAC.ACG.TTT.
  T   A   F   K   D   D   V   D   T   L   L   V   T   R   L

GGC.TGG.CAG.TTT.TGA.AGG.CGA.TAC.GAA.AAT.GAT.TCC.ATT.AAA.CTG.G
 A   G   S   F   E   G   D   T   K   M   I   P   L   N   W

GA.TGA.TTT.TAC.CAA.AGT.CTC.CAG.CCG.CAC.CGT.TGA.AGA.TAC.CAA.TC
D   D   F   T   K   V   S   S   R   T   V   E   D   T   N   P

C.GGC.GCT.GAC.GCA.CAC.TTA.TGA.GGT.TTG.GCA.AAA.GAA.GGC.TTAAGC
   A   L   T   H   T   Y   E   V   W   Q   K   K   A  STOP
```

3. DHFR EXPRESSION AND PURIFICATION

3.1. INTRODUCTION

DHFR is expressed in a temperature dependent system in which the DHFR gene is cloned in a plasmid next to the P_L promoter. The plasmid is transformed into an *E. coli* strain that expresses a temperature dependent cI repressor which binds to the P_L promoter preventing transcription of the gene. If the temperature is raised above 40°C the repressor does not bind to the promoter and DHFR is expressed.

For the wild type and each mutant DHFR the conditions for growth and expression were ascertained to achieve high yields, first by using small scale shake cultures and then scaled up for fermentation on a 10 to 13 litre scale.

The cells were harvested and the DHFR was extracted and purified using a modification of the published protocol (Dann *et al.*, 1976). For each mutant the appropriate purification scheme had to be found and suitable assays established in order to follow the purification.

3.2. METHODS

3.2.1. DHFR Expression

Strains were maintained as described in the appendix. Unless stated otherwise, the culture media was L-broth supplemented with the appropriate antibiotic.

The T63Q, T63A, and D26N mutants were tested for expression by inoculating 500µl of a fresh overnight culture into 40ml L-broth in shake flasks. The cultures were grown at 30°C to an OD_{595} of 1 when the temperature was raised to 40°C. After 1 hour the cells were spun down and resuspended in 2ml cold Tris-sucrose buffer (20mM Tris-HCl, 20% sucrose, pH7.4).

The cells were broken open by sonicating for 3 x 20 seconds at a peak amplitude of 8-12 microns. The suspension was spun and the supernatant was transferred to a fresh tube. The supernatant was assayed for DHFR activity. If no activity was detected then the supernatant was analysed by protein SDS-polyacrylamide gel electrophoresis (SDS-PAGE) using purified wild type DHFR as the standard.

Conditions were determined to give good yields of DHFR. For this, a similar procedure was followed, but samples were taken at time intervals after temperature induction. These were assayed either by SDS-PAGE or by activity. The conditions varied were;

1) broth composition, by doubling the strength of the broth.

2) induction conditions, by inducing enzyme production at different temperatures (39°C, 40°C, 42°C, and 40°C for 1 hour followed by 30°C or 37°C until harvesting), and at different phases of growth.

3) varying the time after temperature induction before harvesting.

Large amounts of DHFR were produced in 10-13 litre fermentations by a direct scale up from the shake flasks. The stir rate was 850rpm, oxygen levels were set for almost continuous air sparging at 10-15 litres/minute, and antifoam (polypropylene glycol) was added to prevent the build-up of foam which would block the air filters and prevent transfer of gases. The pH was maintained between 6.0 and 7.5 by adding 1M NaOH or 1M HCl when required.

250ml of a fresh overnight culture was used to inoculate the broth. Samples were taken at intervals after induction and assayed to check for DHFR expression. At the predetermined time (from the shake flask experiments) the cells were harvested by centrifugation in 400ml buckets in a Beckman J2-21 centrifuge. Since this is a slow process because of the large volume, during the centrifugation steps the temperature of the cell culture remaining in the fermenter was reduced as quickly as possible by turning down the fermenter temperature as low as possible. Once this temperature was reached the culture was collected into buckets and placed in the cold room. In this way the culture was cooled quickly to reduce the amount of enzyme lost by proteolysis. Harvesting using this procedure took between 1.5 and 2 hours. A continuous flow head was also tried but harvesting using this method took a similar length of time but there was a loss of cells because some remained in the broth.

The cells were either stored frozen or were used immediately for DHFR purification.

3.2.2. DHFR Purification

The purification protocol is outlined in figure 3.1

Figure 3.1 The Purification Scheme

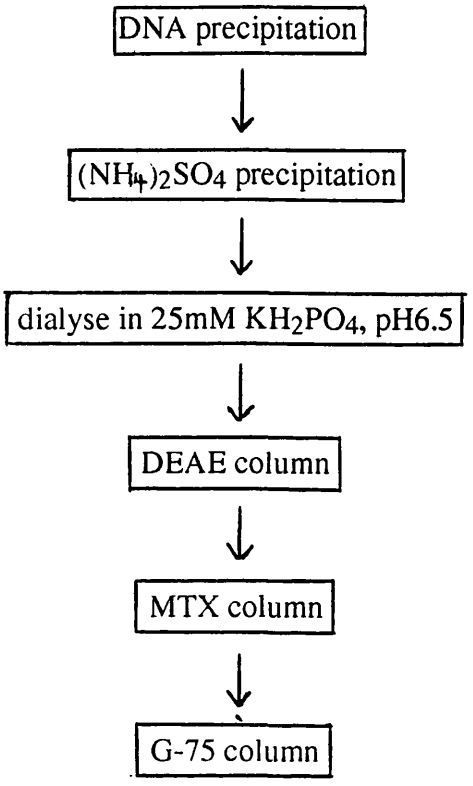

All the procedures were carried out on ice or in a 4°C cold room keeping DHFR as cold as possible to minimise loss.

The purification procedure was followed by assaying activity or, where activity was too low, by PAGE electrophoresis.

The cells were resuspended in 300ml of ice cold 0.05M Tris-HCl pH 7.4, per 100 g of wet cells. The suspension was passed twice through a cold French press to break open the cells and the cell debris was removed by centrifugation at 18000rpm in a MSE Prepspin-50 centrifuge.

To lower the viscosity, nucleic acids were removed by precipitation using polyethyleneimine (PEI) or streptomycin sulphate. The amount of PEI required to

precipitate the nucleic acids without precipitating DHFR was determined by titration of a small batch of the cell extract first. Streptomycin sulphate was added by dropwise addition of a 20% solution to make a final concentration of 4%. The resultant DNA precipitate was spun down by centrifugation at 10000rpm and discarded.

DHFR and proteins which co-precipitate were then concentrated by ammonium sulphate precipitation using 600g ammonium sulphate per litre and stirred overnight. The precipitate was centrifuged down at 10000rpm (the supernatant discarded) and could be stored frozen.

The ammonium sulphate precipitate was redissolved in 25mM KH_2PO_4, pH 6.5, and dialysed against this solution over 24 hours in 4 x 2 litre batches. Any remaining precipitate was removed by centrifugation.

The first column in the purification was a DEAE ion exchange column. The ion exchanger used was Whatman DE23 cellulose prepared as recommended by Whatman, the final equilibration buffer being 25mM KH_2PO_4 pH 6.5. The prepared matrix was stored with 0.2% benzalkonium chloride in the equilibration buffer and was washed before use. The dialysed protein solution was pumped onto a 200ml DEAE cellulose anion exchange column and eluted with a salt gradient made from 500ml each of 25mM KH_2PO_4 and 25mM KH_2PO_4, 100mM KCl, both at pH 6.5. The fractions containing DHFR were pooled and either stored at -20°C after lyophilisation or were immediately applied to a methotrexate (MTX) affinity column.

MTX affinity agarose was packed into a 100ml column and extensively washed with equilibrating buffer (50mM KH_2PO_4, 100mM KCl pH 6.5) until the A_{302} of the eluate was zero. The enzyme solution was applied to the column by downwards flow and washed with 30ml equilibrating buffer. The column was then washed with high salt buffer (50mM KH_2PO_4, 2M KCl pH 6.5) until a peak at A_{280} was eluted (or overnight). The flow was reversed (since reversing the flow has been found to give cleaner separations, Dann *et al.*, 1979) and after at least one bed volume of high salt buffer the enzyme was eluted with folate eluting buffer (50mM Tris-HCl, 1M KCl, 2mM folate, pH 8.5). The eluate was immediately dialysed against 10mM KH_2PO_4, 100mM KCl, pH 6.5 and the column was re-equilibrated. The fractions containing DHFR were pooled and lyophilised.

The enzyme from the affinity column was redissolved in a small volume (usually 10-20ml) and applied to a sephadex G-75 column to remove the remaining folate, change the buffer and separate a high molecular weight impurity. Sephadex G-75 was swollen in 10mM KH_2PO_4, 100mM KCl, pH 6.5 and poured into a 400ml column. To check the column was packed well a 1% Blue Dextran 2000 solution was run down the column.

Since the dye can be seen passing down the column the flow of the dye can checked and the column repoured if the flow was uneven (which would result in poor separation of protein bands). The enzyme solution was loaded onto the column, washed with buffer and the fractions containing DHFR were pooled and freeze dried.

To assess protein purity three methods were used; native and SDS polyacrylamide gel electrophoresis to look for protein contaminants and UV absorption spectra to look for low molecular weight impurities. SDS-PAGE gels (15%) contained 0.1% SDS and were run in tris-glycine buffer with 1% SDS. Native PAGE gels (10%) were run in tris-glycine buffer pH 8.3 and the enzyme was run with and without MTX/NADPH. Staining of both gel types was with Coomassie Brilliant Blue.

For purification of mutants, small batches were purified first to check the columns were giving a similar purification to wild type. Cells from a fermentation were spun down, the nucleic acids were removed and the proteins were ammonium sulphate precipitated. The precipitate was then split into several batches and applied to small scale DEAE (20ml) and MTX (10ml) columns to determine any necessary adjustments to the protocol.

3.3. RESULTS AND DISCUSSION

3.3.1. DHFR Expression

The assay for DHFR activity, used to estimate DHFR production, was not very precise when used on the cell extracts; there was a lot of variability in the results and so were only useful as a rough guide. This was probably due to a combination of factors such as;

1. the presence of other proteins having FH_2 reductase or NADPH oxidation activity,

2. other proteins binding the substrates,

3. DNA binding weakly to DHFR, reducing its activity,

4. the high viscosity making accurate measurement of assay volumes difficult.

However, the assay was more precise than PAGE gels and so was generally used.

The amount of DHFR produced over time is shown in table 3.1. For the wild type there was an increase in production with time up to 5 hours, the level remaining constant thereafter. Cells containing the wild type enzyme were therefore harvested between 5 and 20 hours. For the T63Q mutant there was an increase in production over time up to 5 hours and then the amount of enzyme decreased to a negligible amount by 20 hours. The mutant therefore appears to be more labile than wild type. Cells containing the T63Q enzyme were therefore harvested at 5 hours after induction. D26N had no detectable activity and was therefore assayed by PAGE electrophoresis. This showed a similar expression profile to wild type and so indicates that the D26N mutation has not affected the stability of the protein but has greatly affected the activity.

Table 3.1. Enzyme production when induced for different lengths of time.

time after 40°C induction (hrs)	wild type units/ml	T63Q units/ml
1.5	0.14	0.01
3	0.15	0.11
5	0.27	0.13
9	0.24	0.10
20	0.28	0.001

E. coli expressing T63A did not produce any measurable quantity of the enzyme as detected by both activity and PAGE assay. It was thought the *E. coli* strain (WK6λ) could be at fault. To check this, the plasmid containing the gene was transformed into a fresh culture of the same strain and into a strain which does not express the repressor (W71-18) so the gene would be constitutively expressed. It was found T63A was not expressed in WK6λ but was expressed in W71-18 at 30°C and showed DHFR activity, but at 40°C activity could not be detected. If the temperature was lowered back to 30°C DHFR activity was again detected. The protein appeared to be heat labile and could only be produced in reasonable quantities at 30°C, so a strain without the cI repressor had to be used. It is probable that DHFR is stabilised in the cell by bound NADPH (as it is *in vitro*) and if the binding constant of NADPH was lower in this mutant it could be expected to be more temperature sensitive.

One batch of T63A was produced in the fermenter, but further fermentations were unsuccessful, presumably because some part of the expression system was deleted. A plausible reason for this could be due to the constitutive expression of the gene. Constitutive expression would create a selective pressure against producing large quantities of a protein which binds its NADPH yet has no useful function for the cell. For future production of T63A the gene needs to be cloned into a different expression system so that control of expression can be maintained. One possible vector is pINIII A1 which uses IPTG as the inducer (Masui *et al.*, 1981) and has previously been used by Dr Andrews (personal communication). However, expression in this vector gives lower yields of DHFR.

To find optimum inducing conditions, enzyme production was induced at different stages of growth (table 3.2). The maximum DHFR yield was obtained when induction

occurred during mid log phase of growth. Lower amounts of enzyme were obtained when cells were induced during early and late log phase of growth.

Table 3.2. Amount of enzyme produced when induction was carried out at different stages of growth, harvesting after 3 hours.

stage of growth	enzyme activity (units/ml)
early log	0.20
mid log	0.31
late log	0.27

The effect of broth concentration on yields of DHFR (table 3.3) was examined. Doubling the broth concentration gave a large increase in cell number yet low DHFR activity, probably because the rich medium encouraged cell growth and discouraged maintenance of proteins unnecessary for growth (which would be rapidly proteolysed), therefore the regular broth concentration was always used.

Table 3.3. Enzyme production when different broth concentrations were used.

LB concentration	enzyme activity u/ml	OD at harvest
1x	0.24	5.5
2x	0.05	7.1

The effect of temperature on DHFR production for the wild type and T63Q enzymes was examined (table 3.4). Optimum yields were obtained when the inducing temperature was maintained at 40°C. It was thought that lowering the temperature to 37°C or to 30°C after an hour would increase the yield as the enzyme is sensitive to high temperatures. However, it was found that enzyme yield was much reduced upon lowering the temperature. The temperature used for induction of DHFR expression was therefore 40°C.

Table 3.4. Enzyme production when induced at different temperatures

temperature °C	wild type u/ml	T63Q u/ml
39	0.06	0.02
40	0.27	0.13
42	0.19	0.0
40 ⇒ 37	0.08	0.03
40 ⇒ 30	0.04	0.01

In summary, all *E. coli* cultures (except T63A discussed above) were grown in 1x LB at 30°C and DHFR production induced by increasing the temperature to 40°C when the cell culture had reached a cell optical density at A_{595} of at least 1.0.

3.3.2. DHFR Purification

To remove DNA from the cell extract PEI precipitation (Dann *et al.*, 1976) was initially used, but this required time consuming titration of a small sample before use because it precipitates DHFR when used in large amounts. Streptomycin sulphate was tried as an alternative and worked well with no detectable loss of enzyme and was therefore used in all purifications.

Tables 3.5 and 3.6 show typical purifications of wild type and T63Q respectively. The total measured amount of activity obtained from the MTX column was consistently low because of the presence of residual folate acting as a competitive inhibitor (folate is, of course, a substrate but has a lower turnover number than FH_2).

Table 3.5 A typical wild type DHFR purification from a 12 litre fermentation

purification step	total units of activity	%activity
streptomycin sulphate	2800	100
ammonium sulphate	2221	79
DEAE column	1762	63
MTX column	800	27
G-75 column	990	35

Table 3.6. A typical T63Q purification from a 13 litre fermentation

purification step	total units of activity	%activity
streptomycin sulphate	1500	100
ammonium sulphate	1125	75
DEAE column	950	63
MTX column	360	24
G-75 column	410	27

The MTX and DEAE columns were prepared and used as published by Dann *et al.* (1978). I also tried using the MTX column first, followed by the DEAE column. This worked well, but ultimately no time was saved and the MTX column showed signs of deterioration, so the DEAE column was usually used first.

Following the methotrexate column, the published method described the use of a G-25 column to remove excess folate, followed by a Bio-Rex 9 column to remove a low molecular weight impurity to yield pure DHFR. This protocol was modified by using a G-75 column which was found to separate DHFR from both the folate and the remaining impurities, thus eliminating the need for the Bio-Rex 9 column (on which there was a large loss of DHFR). This protocol also had the advantage of eluting the DHFR in a suitable buffer for nmr and kinetics.

The purification of the T63Q mutant followed the same procedure as for the wild type enzyme. Reductase activity was detectable in the crude extract so the purification could be followed by activity assay.

D26N had no activity detectable in the crude extract so the purification was followed by PAGE electrophoresis. The MTX affinity column was expected to be difficult since the MTX binding site was altered by the mutation. However, the affinity column was in fact used successfully. D26N did not bind tightly to the column but it was retarded sufficiently well to afford a good purification. The protein solution was pumped onto the column and washed with high salt buffer. D26N DHFR was washed down the column more slowly than contaminating proteins. Once the impurities were washed off the column, the folate buffer was applied and D26N came off in a concentrated band at the first trace of folate. The rest of the purification followed the same procedure as for the wild type enzyme.

4. NMR CHARACTERISATION OF MUTANT DHFR'S

4.1. INTRODUCTION

4.1.1. Mutations

DHFR is highly specific for NADPH as the coenzyme; the K_M for NADPH is 100 fold lower than that for NADH (Feeney *et al.*, 1975). This specificity is of interest both in the specific context of DHFR and more generally in terms of understanding the coenzyme specificity of dehydrogenase enzymes. Mutants of DHFR have therefore been designed to test hypotheses regarding the binding of the 2' phosphate of NADPH, since it is this which must provide the specificity for NADPH over NADH.

From the refined crystal structure of the DHFR/MTX/NADPH complex (Filman *et al.*, 1982), it was observed that the side chains of threonine-63, argenine-43, and glutamine-65 and the peptide NH of histidine-64 interact with the 2' phosphate group by hydrogen bond interactions. The residue at the position equivalent to position 63 (Thr63) in the *L. casei* enzyme, is conserved as a threonine or a serine in DHFR from all species for which sequences are available. In the crystal structure the hydroxyl group forms an hydrogen bond with the 2' phosphate group. It was decided that this residue would be a target for mutagenesis to study the role of this hydrogen bond in ligand specificity. To study the role of Thr63 two mutants have been made to date; in one it has been changed to glutamine (T63Q), in the other to an alanine (T63A). The relevant side chains are;

Threonine

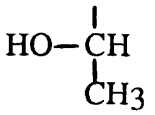

Alanine

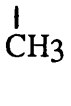

Glutamine

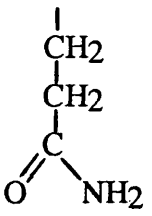

The T63Q mutant had been cloned by Dr. Andrews and given to me to study its structure and function. Glutamine is perhaps not an obvious choice for replacing a threonine since it is not a conservative mutation but it was chosen for two reasons;

1) its larger size would be expected to cause steric hindrance of the binding of the 2' phosphate and thus NADPH,

2) molecular modelling suggested that the amide group may be able to interact with the 2' hydroxyl of the ribose ring of NADH.

This mutation then, was an attempt to alter the specificity of DHFR by making NADPH less able to bind whilst making NADH better able to bind to the enzyme.

T63A was made and studied in order to help explain the results that were obtained for the T63Q mutant; to ascertain whether the effects seen were due to the loss of the hydrogen bond to the 2' phosphate or due to the increased size of the side chain. T63A is a more conservative mutation, alanine is smaller than threonine and therefore would be expected to fit with little steric hindrance. Any affects on the activity and structure of the enzyme due to this mutation were expected to be mainly caused by the loss of the hydrogen bond between the threonine hydroxyl group and the 2' phosphate, without any steric repulsion or other bonds being engineered in.

4.1.2. NMR Experiments

A 2D ^1H NMR experiment is generally performed by applying an initial preparation pulse (often, as in the case of the experiments used here, a 90° pulse) which is followed by an incremented delay time conventionally referred to as t_1. This is followed by a mixing process (usually a pulse or a cluster of pulses and fixed delays); then the FID is collected during the period referred to as t_2. A series of FIDs is thus collected with incremented lengths of t_1. Fourier transformation of these FIDs (i.e. with respect to t_2) gives a series of spectra which vary due to the different values of t_1 used in recording each one. Another Fourier transform, this time with respect to t_1, then yields a two-dimensional spectrum. In homonuclear experiments (as used in this thesis) this contains a "diagonal", where $f_1 = f_2$, which corresponds to magnetization that is unchanged between t_1 and t_2; i.e. not affected by the "mixing propagator". Other signals that lie off the diagonal, so-called "cross peaks", are indicative of magnetisation that has been transferred from one resonance to another during the course of the pulse sequence. The nature of this transfer depends particularly on the details of the mixing propagator used.

In the COSY (COrrelated SpectroscopY) experiment the mixing propogator is a 90° pulse and the magnetisation transfer depends on direct scalar coupling. Cross peaks appear between resonances from protons that are (usually) two or three bonds apart, and are thus within the same residue. For example, the proton signals from each methyl group of valine will give a cross peak with the β carbon proton resonance due to the transfer of magnetisation between the two, scalar coupled, spins. This connection thus depends only on the covalent structure of the protein. However, by spreading the spectrum out in two

dimensions, the COSY experiment makes it easier to resolve resonances from individual residues. The chemical shift of each proton in the spectrum is determined by its environment, for example if a proton is above an aromatic ring it will be shielded by the π electrons of the ring and will be shifted upfield, whereas if it is at the side of the ring it will be deshielded and shifted downfield. Therefore any change in this environment (eg. by a change in protein structure) will cause a change in chemical shift and the position of cross peaks in the COSY spectrum.

In the HOHAHA (HOmonuclear HArtman HAhn) experiment the mixing process involves a cascade of pulses designed to encourage "isotropic mixing"; this allows magnetization to be passed throughout a scalar-coupled network. Thus cross peaks appear at the same coordinates as in the COSY spectrum, with additional peaks between indirectly coupled signals. Again, these connect signals from protons within the same residue, but are not restricted to directly coupled partners. Cross peaks may occur between all members of a scalar-coupled network. For example a valine residue will give COSY cross peaks between both the γCH_3's and βCH and the HOHAHA will give further cross peaks between the γCH_3's and αCH and between the two γCH_3's.

The NOESY (Nuclear Overhauser Enhancement SpectroscopY) experiment is one of the few that does not involve "scalar coupled transfer". The experiment consists of a "mixing time" (often referred to as τ_m) sandwiched between a pair of 90° pulses (see Neuhaus and Williamson, 1989). During the mixing time inter-nuclear dipolar relaxation occurs. This is an example of the nuclear Overhauser effect (NOE), and becomes increasingly efficient the closer together in space two protons are. For a two spin approximation the volume of the cross peak is proportional to the inverse sixth power of the distance between the protons. In practise this means a nOe is seen up to a maximum distance of about 5 Å, (but see spin diffusion, discussed below). Thus a NOESY spectrum contains cross peaks between signals of nearby protons which may be in different residues and which are thus not necessarily scalar coupled. The NOESY mixing time is an important parameter. As it is increased the cross peaks becomes more intense, since there is more time for the cross relaxation to occur. However in a macromolecule such as a protein the relatively slow tumbling of the molecule in solution makes this such an efficient process that the magnetization rapidly passes from one proton to the next, then the next, and so on, which is "spin diffusion". Cross peaks can thus arise between signals from protons that are not close to each other, but between which such a pathway exists. This seriously degrades the specificity of the information that the NOESY experiment can give. Thus it is important to choose a mixing time such that the cross peaks are large enough to be observed, but not so long as to allow excessive spin diffusion. The mixing time used for DHFR is 100 msec.

The NOESY experiment is an extremely useful tool as it provides detailed structural information about the protein. To study any differences in the mutant structure compared to wild type, a comparison of the peak volumes (or peak intensity in practice) is made. The relationship of peak intensity with distance is $1/r^6$ so a small change in distance can cause a relatively large change in peak height. Therefore, whilst distance changes can be readily observed, the errors in quantification are large. In practice, an impression of whether the peaks are large, medium or small, corresponding to distances of up to 2.5, 3.5 and 5Å respectively is generally used by nmr spectroscopists to obtain distance constraints for structure determination (for example Campbell and Sheard, 1987). However, for studying the changes in the structure of mutant enzymes it would be of more use to have quantitative results, in order to determine the small effects of the mutation. To this end, full density relaxation matrix treatments, which allow for indirect magnetisation transfer, are currently being developed.

Distances that can be obtained from the NOESY spectra are those between the backbone protons (between NH-NH and αCH-NH, the fingerprint region), the intra-residue protons (between αCH, NH, and the side chain protons of a residue) and inter-residue protons (between αCH, NH and the side chain protons of neighbouring residues and residues close to each other in space). The backbone NOE's can give information on secondary structure, for example if the protein is helical one would expect to see NH-NH NOE's between progressive residues along the chain, whereas in a β-sheet the distances between the NH's are too great to see NOE's beyond the nearest neighbour. The inter-residue NOE's describe the tertiary structure of the protein, i.e. the NOE's between protons of residues that are close together in space because of the protein folding and yet are not necessarily close in sequence.

There are a number of assigned inter-residue NOE's in the DHFR spectra and these act as important indicators of the structural changes in the mutants. The largest number of inter-residue NOE assignments are those between the aromatic and high field methyl protons since these are comparatively well resolved. For comparison of the mutant spectra the basic strategy was to compare, firstly NOE's from residues that have some change in chemical shift, and then all the other NOE's which have been assigned and lastly to look for obvious changes in NOESY peak sizes in unassigned regions of the spectra.

Phosphorus nmr experiments are another aid for analysis of structure by providing information regarding the environment of this nucleus when phosphorus containing ligands bind to the protein (Verkade and Quin, 1987, Gorenstein, 1989). For example phosphorus nmr has been used to study the binding of the 2' phosphate and the pyrophosphates of a number of coenzyme complexes (Feeney *et al.*, 1975, Hyde *et al.*, 1980a,b, Gronenborn *et al.*, 1981a,b).

4.1.3. DHFR Assignments

A complete assignment of the proton resonances to specific residues in the sequence has not been possible to date for any DHFR complex because it is a large protein (in nmr terms), with a molecular weight of ca.18000. Its relatively large size means that a large proportion of the spectrum consists of overlapping peaks which are therefore difficult to assign to particular protons in the molecule. In addition, being a large protein in nmr terms, the linewidth is inherently large (linewidth is inversely proportional to the correlation time which is short for large molecules), reducing resolution. Assignments are also hindered because DHFR is relatively labile and cannot be subjected to extremes of pH (changes in pH gives information on ionisable groups and their neighbours) or temperature (which can be used to move resonances and the water peak thus helping to overcome resonance degeneracy).

However, a significant number of assignments have been made both of the protein and the bound ligands (Birdsall *et al.*, 1990, Searle *et al.*, 1986, Hammond *et al.*, 1986, Feeney *et al.*, 1989) and the number of assignments are increasing as experimental techniques and hardware improve, for example with the advent of two dimensional nmr. These assignments are well spread about the enzyme and so can act as reporter groups, giving information on changes in structure and conformation. Photograph 4.1 shows the residues which have peaks assigned in the spectrum to date.

Photograph 4.1. Crystal structure of L. casei DHFR in ternary complex with MTX (red) and NADPH (blue). Residues with proton assignments in the nmr spectra are shown in orange, residues with no assignments are shown in pale green.

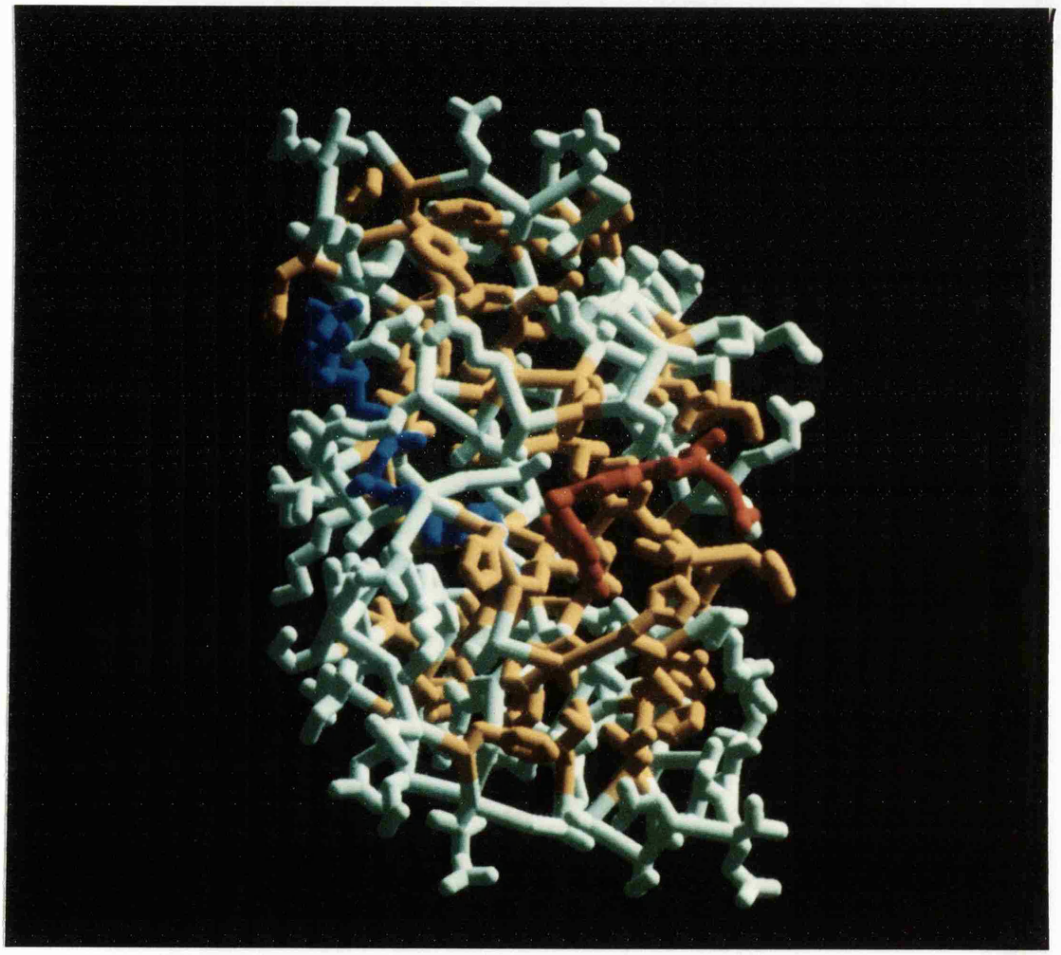

4.2. METHODS

4.2.1. Sample preparation

Enzyme concentrations were between 0.5 and 2mM. 0.1µl of 1mM dioxan was added to the sample for the chemical shift reference (the dioxan resonance is 3.75ppm downfield of 5,5-dimethyl-5-silapentane-2-sulphonate at 308K). Spectra were recorded at 308K for all complexes except for those with the T63A mutant which were recorded at 298K. Since the amount of this mutant was limited and it had been found to be labile at 40°C during its production, the temperature was kept lower than the "standard" 308K that has been generally used in previous DHFR nmr studies (Birdsall *et al.*, 1990). For comparison of the spectra with wild type DHFR some spectra of complexes of the wild type were also recorded at 298K.

For studies of the binary complex with methotrexate, approximately 14mg DHFR and 3 to 5 fold molar excess MTX were dissolved in 1.5ml H_2O. The solution was dialysed against several changes of 10mM phosphate, 100mM KCl, pH 6.5 and made up to a final volume of 2ml. The sample was lyophilised and then exchanged twice against D_2O (i.e. a cycle of redissolving in D_2O and lyophilising). The sample was made up to a final volume of 400µl with D_2O to give a 2mM solution in a buffer of 50mM KH_2PO_4, 500mM KCl pH*6.5 [pH* indicates pH values measured in D_2O uncorrected for the deuterium isotope effect on the glass electrode]. If necessary, the sample was centrifuged to remove any undissolved material.

A similar procedure was used for the preparation of the ternary complex with MTX and NADPH. For complexes with MTX and $NADP^+$, the $NADP^+$ was added to the binary complex in a two fold excess without dialysis (since the binding of $NADP^+$ is weak and so it would dialyse away). Similarly, complexes with folate and TMP were not dialysed.

4.2.2. NMR Experiments

The nmr experiments were recorded on a Brüker AM500 spectrometer.

The 2D COSY, NOESY and HOHAHA spectra were recorded with the carrier placed on the residual HDO signal. Quadrature detection in F1 was obtained by incrementation of the phase of the preparatory pulse by 90° after each t_1 experiment, with incrementation of t_1 after every other t_1 file (i.e. a modified version of the system of States *et al.*, (1982). A spectral width of between 5813 and 6410 Hz in both dimensions was used.

1024 or 2048 t_2 data points were recorded for each of 256-512 t_1 data points with between 64 and 120 transients averaged for each t_1 value.

Most COSY spectra were recorded in phase sensitive mode, but some early COSY experiments were recorded in magnitude mode using a $(90\text{-}t_1\text{-}90\text{-}t_2\text{-}d)_n$ pulse sequence with an 8 step phase cycle (Hammond *et al.*, 1986, Wider *et al.*, 1984). The t_1 values were zero filled to 1K data points and multiplied by a sine bell squared or unshifted sine bell window function prior to Fourier transformation.

For the NOESY experiment the mixing time was 100msec since this gives a good compromise between obtaining optimum peak size with minimal spin diffusion effects. The mixing time was not randomly varied since zero quantum coherence effects (Neuhaus and Williamson, 1989) were not observed to have any significance in this work. The NOESY data was multiplied by Gaussian window functions in both dimensions and zero filled to 1-2K data points prior to Fourier transformation.

HOHAHA spectra were recorded using the MLEV-17 mixing pulse with trim pulses (Bax and Davis, 1985). The spin lock periods (mixing times) were between 20-50msec. Initially HOHAHA experiments could not be recorded because the available hardware was unsuitable. The data was multiplied by Gaussian window functions in both dimensions and zero filled to 1-2K before Fourier transformation.

The spectra of the mutant complexes were compared with those of the wild type by overlaying the plotted spectra and also by direct comparison of corresponding rows and columns of the spectra on the data station. Detailed comparisons of the assigned peaks in the spectra were made and these were used as "reporter groups" of structural changes in the protein. These regions where most assignments are available are mainly the "high field methyl" and the aromatic regions. The "high field methyl" region consists of resonances from methyl protons that lie close to the face of aromatic rings and so have unusually up-field chemical shifts due to ring current effects. Conversely, protons in aromatic rings have chemical shifts at a lower field than aliphatic protons and so are separated from the main envelope of resonances and, being relatively few in number, the aromatic proton resonances are generally well resolved from each other. The aromatic region has now been fully assigned during the period of this work (Birdsall *et al.*, 1990)

Phosphorus spectra were recorded using a spectral width of 5KHz, 16K data points and 400 scans. The fid was multiplied by an exponential function to improve the signal to noise ratio. The chemical shift scale was referenced to external trimethyl phosphate in D_2O.

4.3. RESULTS

4.3.1. Binary Complexes With MTX

For each mutant, the first nmr experiments were on the binary complex with methotrexate. This complex was chosen because it had the most assignments and, importantly, it was expected to be a stable complex since the mutations were some distance from the methotrexate binding site. Studying the enzyme without NADPH bound also allowed an assessment of the protein structure independent of any effects caused by the changes in NADPH binding.

4.3.1.1. T63Q COSY Experiments

When comparing the COSY spectra of the T63Q and wild type binary methotrexate complexes the most striking feature was their similarity. It was immediately clear that very few resonances had a different chemical shift in the mutant as compared to the wild type, indicating the mutation has not greatly affected the protein structure.

Detailed analysis was carried out to localise the effects of the mutation. The high field methyl and the aromatic regions of the COSY spectrum of wild type DHFR in binary complex with methotrexate are shown in figures 4.1 and 4.2 respectively, with the positions of cross peaks that have moved in the T63Q spectra indicated. The assigned proton resonances are labelled.

The threonine region of the mutant spectrum was compared with the wild type spectrum to assign the resonances from Thr63, however there were no peaks obviously missing, suggesting that these peaks lie in a degenerate region of the spectrum.

The residues that have at least one proton resonance whose chemical shift differs between mutant and wild type by at least 0.02ppm (it is not possible to be certain that smaller changes than this are real), are listed in table 4.1. The residues directly around the site of mutation whose resonances have been assigned are Tyr68, Leu62, Val60, and Val61, and proton resonances from these residues have the same chemical shift as wild type. This is unexpected since it is generally assumed that a mutation is likely to affect the local region of the protein in most cases.

Figure 4.1. High field methyl region of the COSY spectrum for wild type binary MTX complex, superimposed are all the peaks which have a different chemical shift in the T63Q complex.

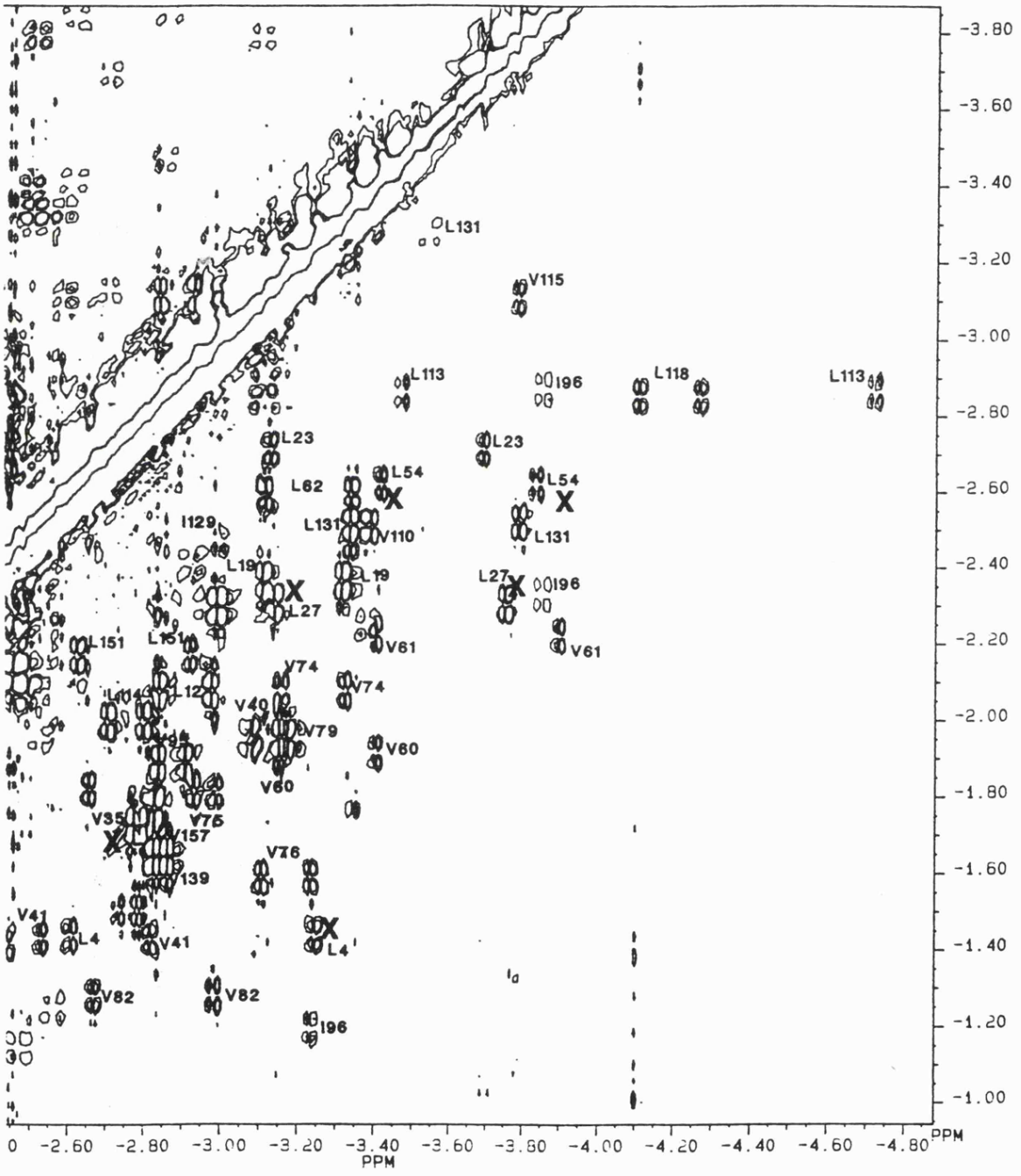

Figure 4.2. Aromatic region of the COSY spectrum for wild type binary MTX complex, superimposed are all the peaks which have a different chemical shift in the T63Q complex.

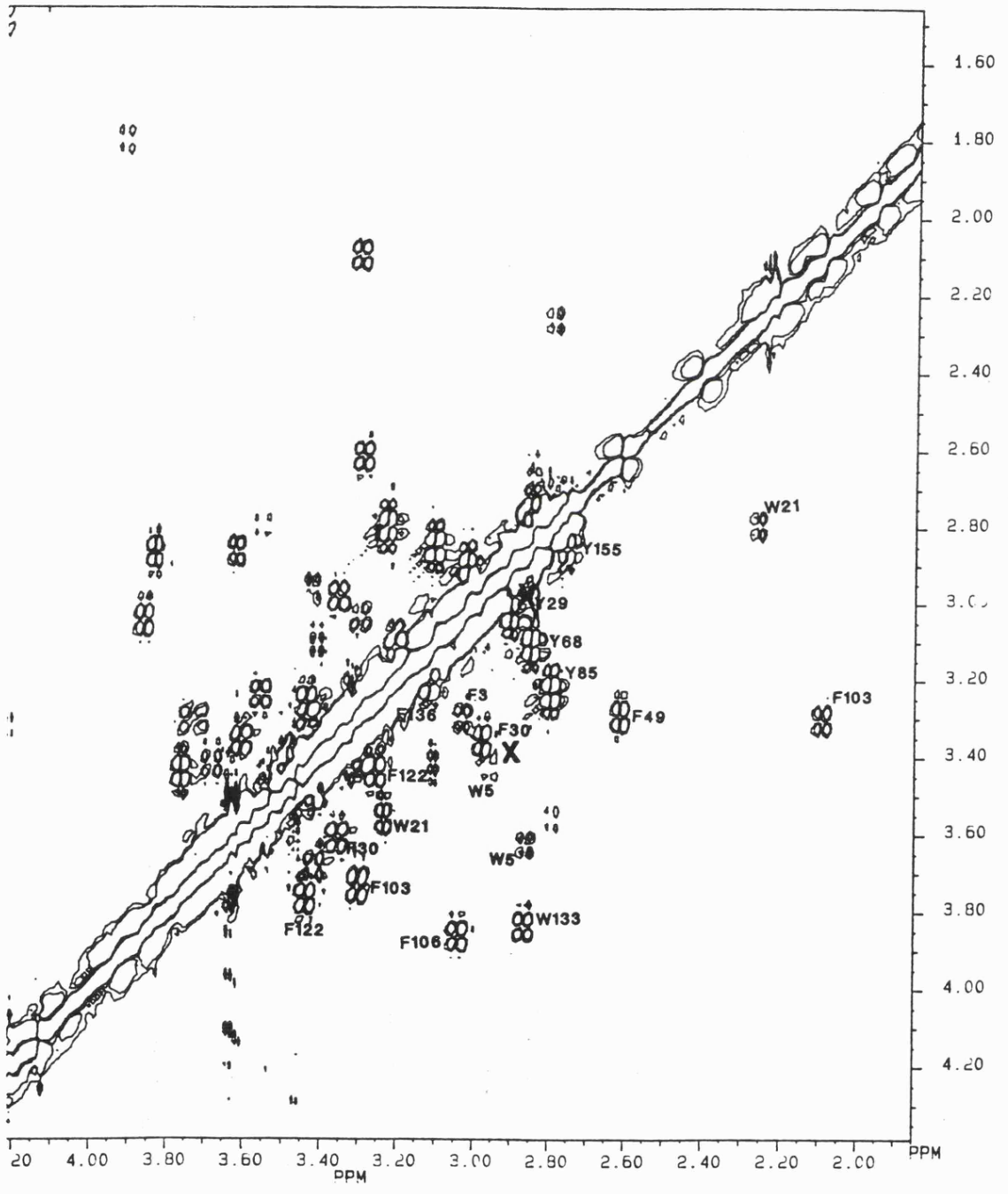

Table 4.1. Proton chemical shifts from residues which have at least one proton chemical shift difference when comparing the wild type and T63Q binary MTX complex.

RESIDUE	^1H	δ WT(ppm)	δT63Q(ppm)	Δδ (ppm)
Phe49	H3'5'	3.31	3.28	0.03
	H2'6'	2.63	2.62	-0.01
	H4'	3.42	3.42	0
Phe30	H2'6'	3.00	2.90	-0.1
	H3'5'	3.38	3.36	-0.02
	H4'	3.63	3.63	0
Tyr29	H2'6'	3.03	3.00	-0.03
	H3'6'	2.92	2.87	-0.05
Leu54	$C\delta H_3$	-3.83	-3.9	-0.07
	$C\delta H_3$	-3.41	-3.45	-0.04
	CγH	-2.62	-2.6	0.02
Leu 4	$C\delta H_3$	-3.25	-3.29	-0.04
	$C\delta H_3$	-2.60	-2.62	-0.02
	CγH	-1.43	-1.45	-0.03
Leu27	$C\delta H_3$	-3.75	-3.78	-0.03
	$C\delta H_3$	-3.17	-3.21	-0.04
	CγH	-2.29	-2.33	-0.04
Val35	$C\gamma H_3$	-2.77	-2.72	0.05
	$C\gamma H_3$	-2.79	-2.74	0.05
	CβH	-1.72	-1.69	0.03
MTX	H7	4.14	4.21	0.07

By studying the crystal structure using the Frodo software on the Evans and Sutherland graphics work station, the residues in table 4.1 were all seen to lie near the MTX binding pocket some distance from the mutation (Photograph 4.2), a surprising result, especially since the mutation site had hardly been perturbed.

Photograph 4.2. αCarbon backbone of L. casei DHFR showing MTX (red) and the side chains of all the residues with assigned protons resonances that have a different chemical shift in the binary MTX complex of the T63Q mutant compared to the wild type spectra. Threonine-63 is shown in green.

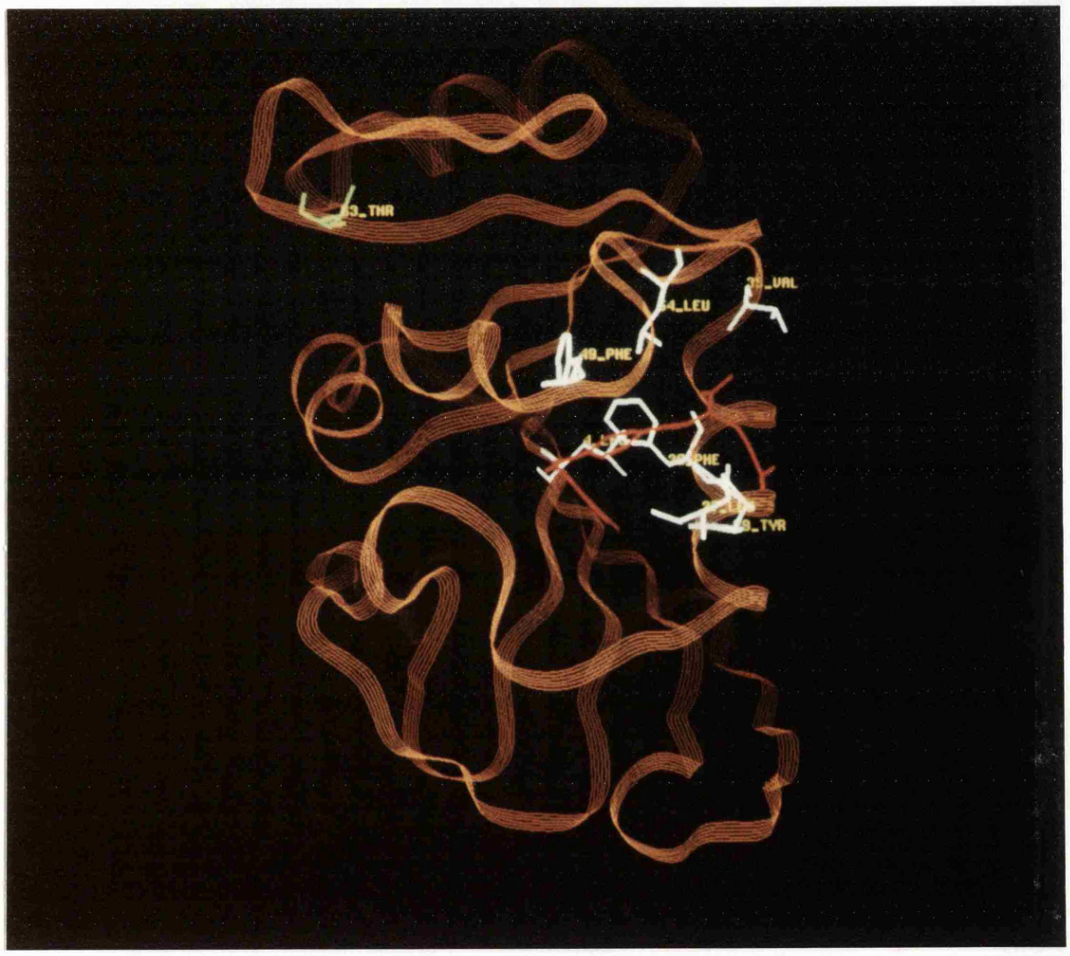

4.3.1.2. T63Q NOESY Experiments

The NOESY experiment is useful since it provides detailed structural information as described in the introduction to this chapter. The chemical shift data obtained from the COSY and HOHAHA spectra can be used to indicate regions of the protein where some structural changes have occurred and the NOESY data can be used to further describe these changes; the chemical shift is affected by a number of parameters so it is impossible to determine exactly what has happened to the protein structure, only that something in that region has altered, whereas the NOESY can give information that two protons have moved closer or further apart.

A major problem with using the NOESY spectra for comparing mutant and wild type DHFR is the inherently limited peak resolution obtained from a protein of this size (the advent of three dimensional techniques will make this less of a problem in future). For comparison it is essential for the peak to be well resolved from other peaks in both the wild type and mutant spectra, a criteria a large number of the NOESY peaks do not meet. However the combination of the obtainable NOESY data and the COSY data provide a powerful approach to determining structural changes of the mutants in solution.

Figure 4.3 shows the regions of the wild type and T63Q NOESY spectra which contain a number of the assigned NOESY cross peaks between the aromatic and aliphatic side chain protons. The NOE's mentioned in the text are labelled.

The assignment for the pteridine H7 of bound MTX can be made in the NOESY spectra because of its NOE's to Leu27 and Leu19, and because it is resolved as a sharp singlet in the 1D spectrum. The signal of H7 has moved by 0.06ppm from 4.27 to 4.21ppm in the T63Q complex. A comparison of the size of the NOESY cross peaks to H7 was not possible because of the presence of artifacts (caused by a gross local distortion of the baseline; tailing from the sharp peaks in the spectrum) in this region of both the wild type and T63Q spectra. The chemical shift change suggests some change in this region of the protein even though H7 is some distance from the mutation.

The assignment for SCH_3 of Met128 can be confirmed in the NOESY spectrum and its chemical shift and NOE's with Trp5 and Phe3 are the same, to be expected since the mutation is not nearby.

The Tyr46 COSY cross peak is not resolved from the diagonal and so it is difficult to assign in the COSY spectrum. However assignment can be made in the NOESY spectrum because Tyr46 H2'6' has NOE's with Leu61 $C\gamma H_3$ (near the mutation) and Phe49 H2'6'. The Tyr46 H2'6' resonance is at the same chemical shift as in the wild type and the

NOE's are apparently the same, thus the mutation has not affected this part of the protein, despite Leu61 being relatively near the mutation.

The NOE's from residues that have proton resonances with altered chemical shifts were examined to determine the possible structural changes causing the shifts:

Phe49-Leu54 NOE's

The NOESY cross peaks between the H3'5' of Phe49 and $C\delta H_3$ from Leu54 at −3.90ppm is not resolved in the wild type spectrum. The NOESY cross peaks of Phe49 H2'6' with all Leu54 protons are in a region of the spectra where there is a large amount of "tailing" from strong peaks on the diagonal and the cross peaks are obscured so their relative peak sizes could not be compared.

Phe49-Phe30

Examination of the crystal structure shows that the side chains of Phe49 and Phe30 are within a few angstroms of each other and so a NOESY cross peak should be seen between them. However, this cross peak is not generally seen in the wild type spectrum. In the T63Q spectrum this NOE is again not seen so no comparison can be made, except to say that these protons have not moved in such a way as to give a cross peak.

Phe49-Tyr46 NOE's

Phe49 has a NOE with Tyr46 which is the same intensity in both the wild type and T63Q spectra, further evidence that no structural changes have occurred in the protein near Tyr46 (see above)

Phe30-Leu54 NOE's.

The NOESY cross peaks between Phe30 H2'6' and H3'5' with Leu54 $C\delta H_3$ at −3.83ppm are not resolved in the wild type spectra and so relative peak sizes were not able to be compared.

Leu4 and Val35 NOE's

The NOE's with Leu4 and Phe30 and Tyr29 (Leu4 is also near the MTX pteridine ring) are in a crowded region of the spectrum and so are not assigned. However there are no readily detected changes in this region of the spectrum. There are no NOE's assigned to Val35 and so none could be compared.

Figure 4.3. NOESY spectra of the wild type and T63Q MTX binary complex. The NOE's mentioned in the text are labelled, where the peaks are below the threshold used for the plot the position of the peak is marked with a cross.

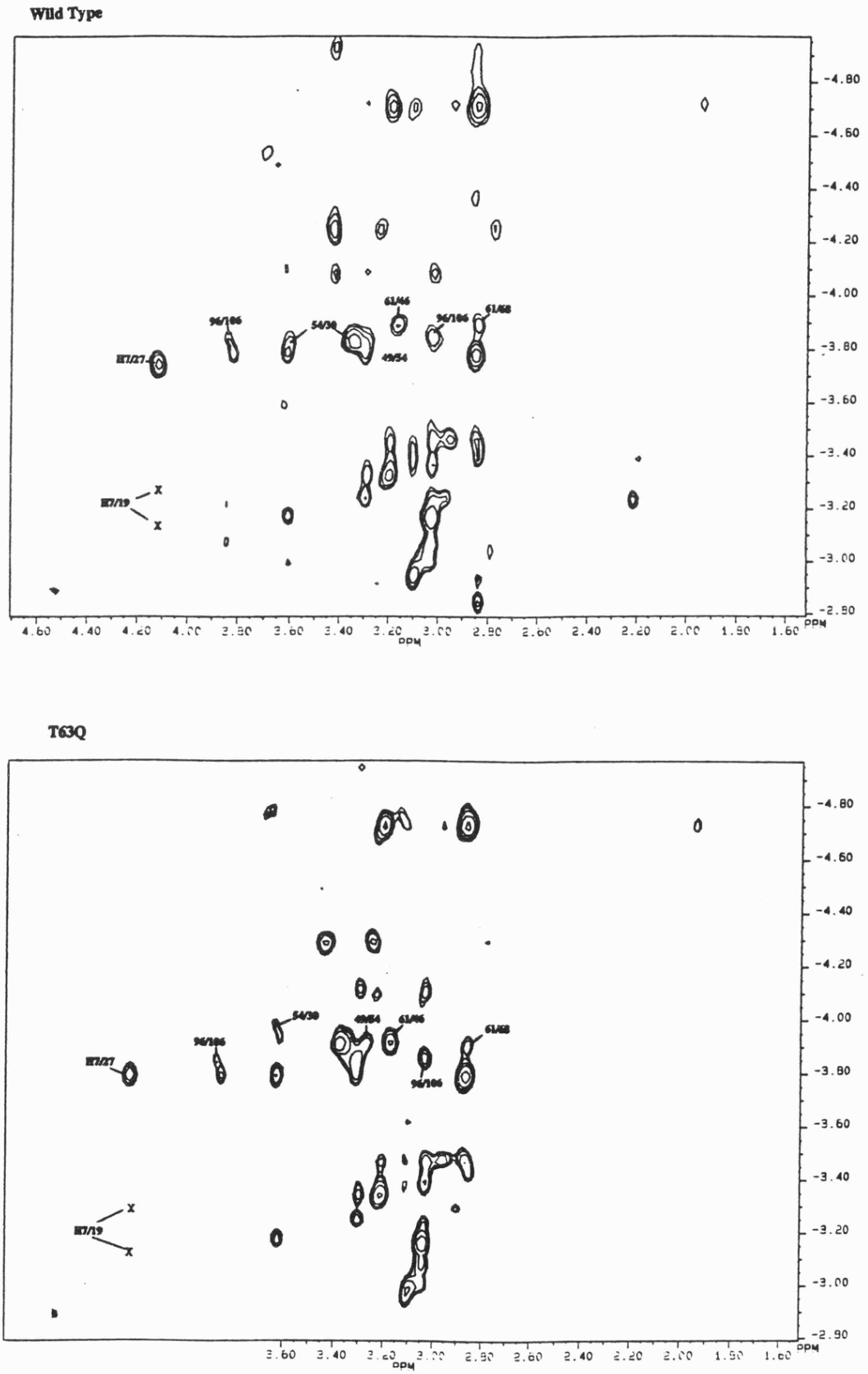

The assigned residues near the mutation include Leu61, Tyr68, Ile96, and Phe106 and their NOE's were not affected by the mutation, which was also suggested by the fact that these residues had no changes in chemical shift. The NOE between Val61 $C\gamma H_3$ and Tyr68 H2'6' is the same as in the wild type spectra (the COSY data showed their chemical shifts had not changed). The NOE's and chemical shifts between Val61 $C\gamma H_3$ and Tyr46 H2'6' were also the same as wild type. The NOE's between Ile96 $C\gamma H_3$ and Phe106 H2'6' and H3'5' are not well resolved so their relative sizes cannot be compared. Since the NOESY peaks from residues near the site of the mutation are the same in the mutant as wild type, the implication is that there is very little perturbation around the mutation, the glutamine side chain fitting into the same pocket and making similar interactions. However, the structure is not identical to wild type because effects are seen at a site distant from the mutation.

The other NOE's from assigned proton resonances that had no change of chemical shift were compared with wild type and revealed no significant changes. These include NOE's from residues Leu118, Trp21, Leu113, Trp5, Phe3, Leu131, Phe136, Phe133 and Trp158. In addition, overlaying the NOESY spectra showed very few differences in the unassigned NOESY cross peaks, however, in regions where there is poor resolution it cannot be certain that changes have not occurred.

To summarise, the NOESY data corroborates the COSY results in that the mutation has caused very little changes to the protein structure. The differences which are seen are not close to the mutation but are at the substrate binding site, far removed from the mutation.

4.3.1.3. T63A COSY and HOHAHA Experiments

Like the T63Q mutant, there were markedly few changes in chemical shifts of COSY and HOHAHA cross peaks compared to wild type. Figure 4.4 illustrates the differences between the high field methyl regions of the wild type and T63A COSY spectra. Figure 4.5 illustrates the differences between the aromatic regions of the wild type and T63A HOHAHA spectra, all the assigned resonances are labelled.

All the assigned residues which have a proton resonance with a different chemical shift from wild type are listed in table 4.2, all the proton resonances in each residue are listed.

Figure 4.4. High field methyl region of the COSY spectrum for wild type binary MTX complex, superimposed are the positions of all the peaks which have a different chemical shift in the T63A complex.

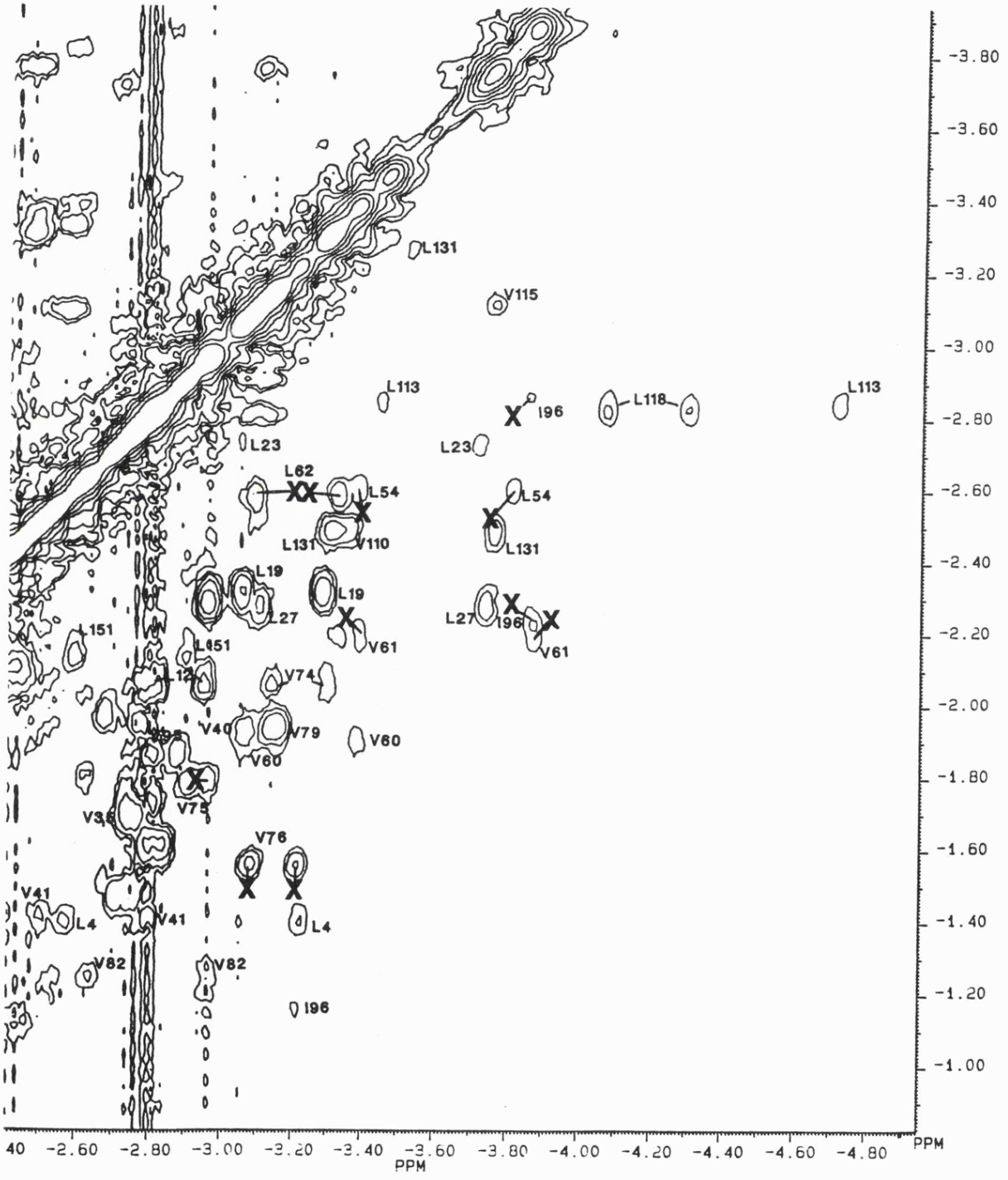

Figure 4.5 Aromatic region of the HOHAHA spectrum for wild type binary MTX complex, superimposed are the positions of all the peaks which have a different chemical shift in the T63A complex.

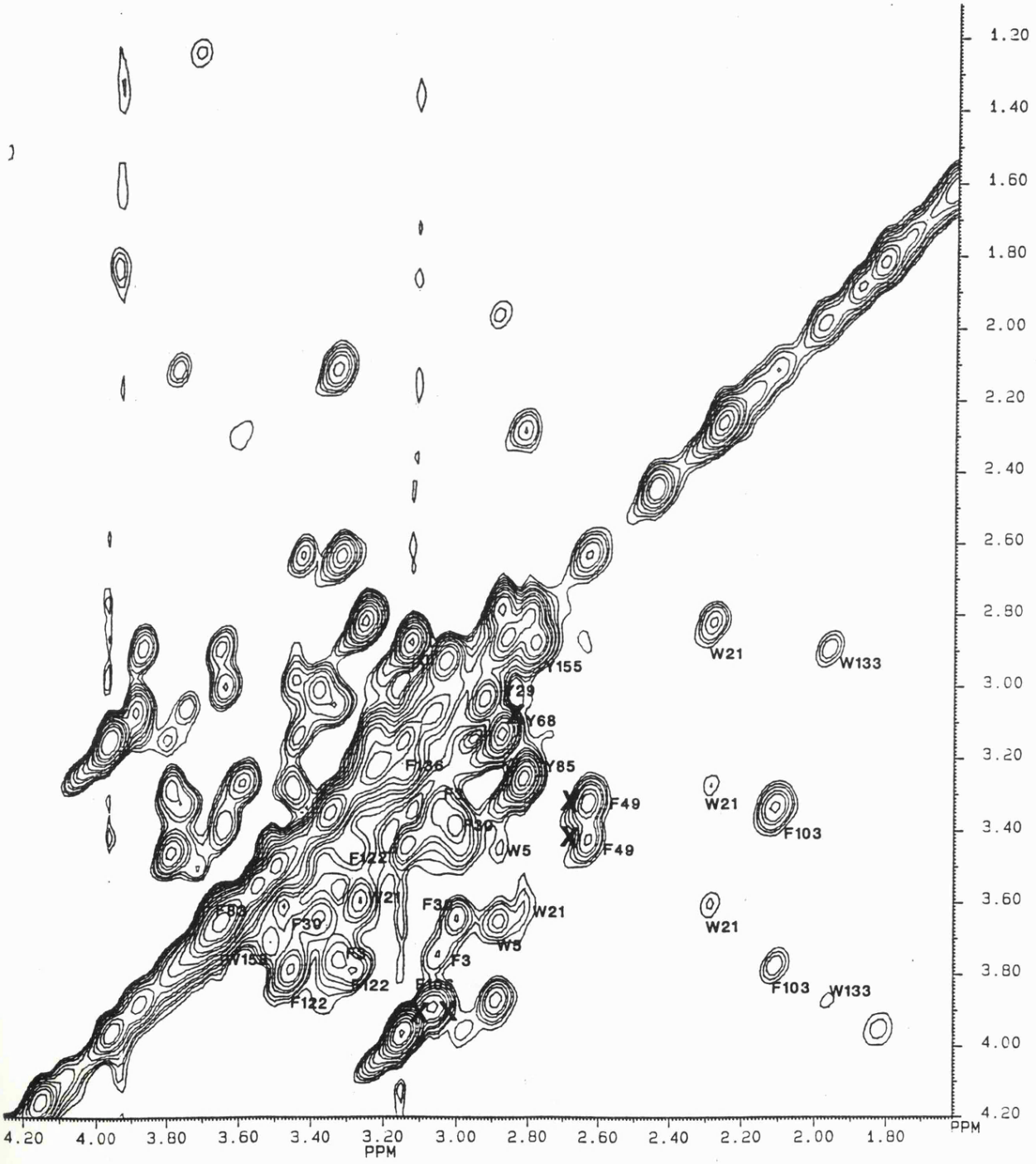

Table 4.2. ***Proton chemical shifts of all the protons in a residue that has a difference of at least one proton chemical shift when comparing the wild type and T63A binary MTX complex.***

RESIDUE	^1H	δ WT(ppm)	δT63A(ppm)	Δδ (ppm)
Val61	$C\gamma H_3$	-3.89	-3.94	-0.05
	$C\gamma H_3$	-3.39	-3.28	0.11
	$C\beta H$	-2.22	-2.24	-0.02
Leu62	$C\delta H_3$	-3.10	-3.21	-0.11
	$C\delta H_3$	-3.34	-3.24	0.10
	$C\gamma H$	-2.62	-2.62	0
Leu54	$C\delta H_3$	-3.39	-3.41	-0.02
	$C\delta H_3$	-3.83	-3.77	0.06
	$C\gamma H$	-2.62	-2.54	0.08
Ile96	$C\delta H_3$	-3.87	-3.80	0.07
	$C\gamma H$	-2.88	-2.82	0.06
	$C\gamma H$	-2.25	-2.31	-0.06
Val75	$C\gamma H_3$	-2.93	-2.98	-0.05
	$C\gamma H_3$	-2.91	-2.91	0
	$C\beta H$	-1.80	-1.80	0
Val76	$C\delta H_3$	-3.10	-3.10	0
	$C\delta H_3$	-3.21	-3.21	0
	$C\beta H$	-1.58	-1.52	0.06
Phe49	H2'6'	2.63	2.67	0.04
	H3'5'	3.34	3.34	0
	H4'	3.45	3.45	0
Phe106	H2'6'	3.91	3.93	0.02
	H3'5'	3.07	3.03	-0.04
	H4'	3.07	3.10	0.03
Tyr46	H2'6'	3.20	3.14	-0.06

4.3.1.4. T63A Noesy Experiments

Figure 4.6 shows the region of the NOESY spectra of T63A and wild type MTX complexes containing a number of assigned NOESY cross peaks between the aromatic and aliphatic side chain protons. The NOE's mentioned in the text are labelled.

Figure 4.6. NOESY spectra of the wild type and T63A MTX binary complex. The NOE's mentioned in the text are labelled, where the peaks are below the threshold used for the plot the position of the peak is marked with a cross.

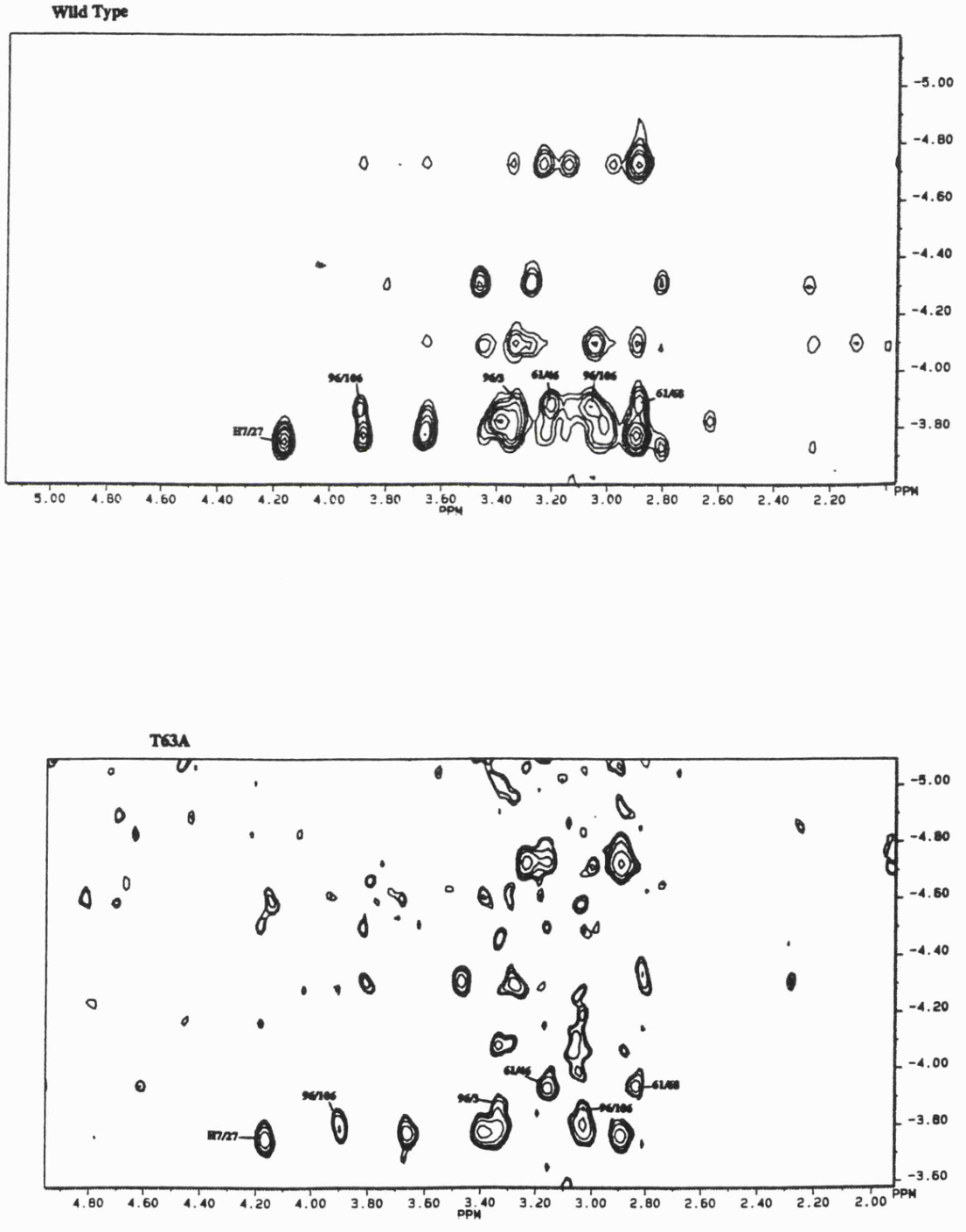

The assignment for the Pteridine H7 of MTX was made (as for T63Q) and the chemical shift of this proton was found to be the same as in the wild type spectra. The spectra had artifacts in this region caused by baseline distortion so it was not possible to compare the sizes of the NOE's with Leu27 and Leu19.

The assignment of Met128 SCH_3 was made and these protons were found to have the same chemical shift as wild type. The NOE's with Trp5 and Phe3 were the same as in the wild type spectrum as expected since these residues are not close to the mutation.

Tyr46 H2'6' was assigned and the proton chemical shift was at 3.14ppm as opposed to 3.20ppm in the wild type spectra, a change of -0.06ppm.

The NOE's from proton resonances with different chemical shifts from wild type were examined to determine the possible structural changes causing the shifts:

Phe49-Tyr46 NOE

The NOE between Phe49 H2'6' and Tyr46 H2'6' was the same for both the wild type and T63A complexes suggesting no structural change in this region.

Phe49-Leu54 NOE's

The Noe between Phe49 H2'6' and Leu54 $C\delta H_3$ at -3.83ppm was the same in both wild type and T63A so the cause for the change in Phe49 chemical shift is not caused by changes in this region either. The NOE's with the other protons of Leu54 were too small for a reliable comparison. The NOE between Phe49 H3'5' and Leu54 $C\delta H_3$ at -3.83ppm is not resolved from other peaks in the spectrum so could not be compared.

Phe49-Phe30

As was explained for the T63Q results the NOE with Phe30 is not seen in the wild type spectra and remained elusive in the T63A spectra, again suggesting that these two residues had not moved significantly closer.

The NOESY data suggests, with the proviso that all the NOE's could not be compared, that the immediate region around Phe49 has not been perturbed structurally despite the difference in chemical shift of some of the Phe49 proton resonances. There are a number of factors that contribute to the chemical shift of a proton besides the relative positions of the nearest neighbours and these are mentioned in the discussion.

Photograph 4.3. αCarbon backbone of L. casei DHFR showing MTX (red) and the side chains of all the residues with assigned protons resonances that have a different chemical shift in the binary MTX complex of the T63A mutant compared to the wild type spectra. Threonine-63 is shown in green.

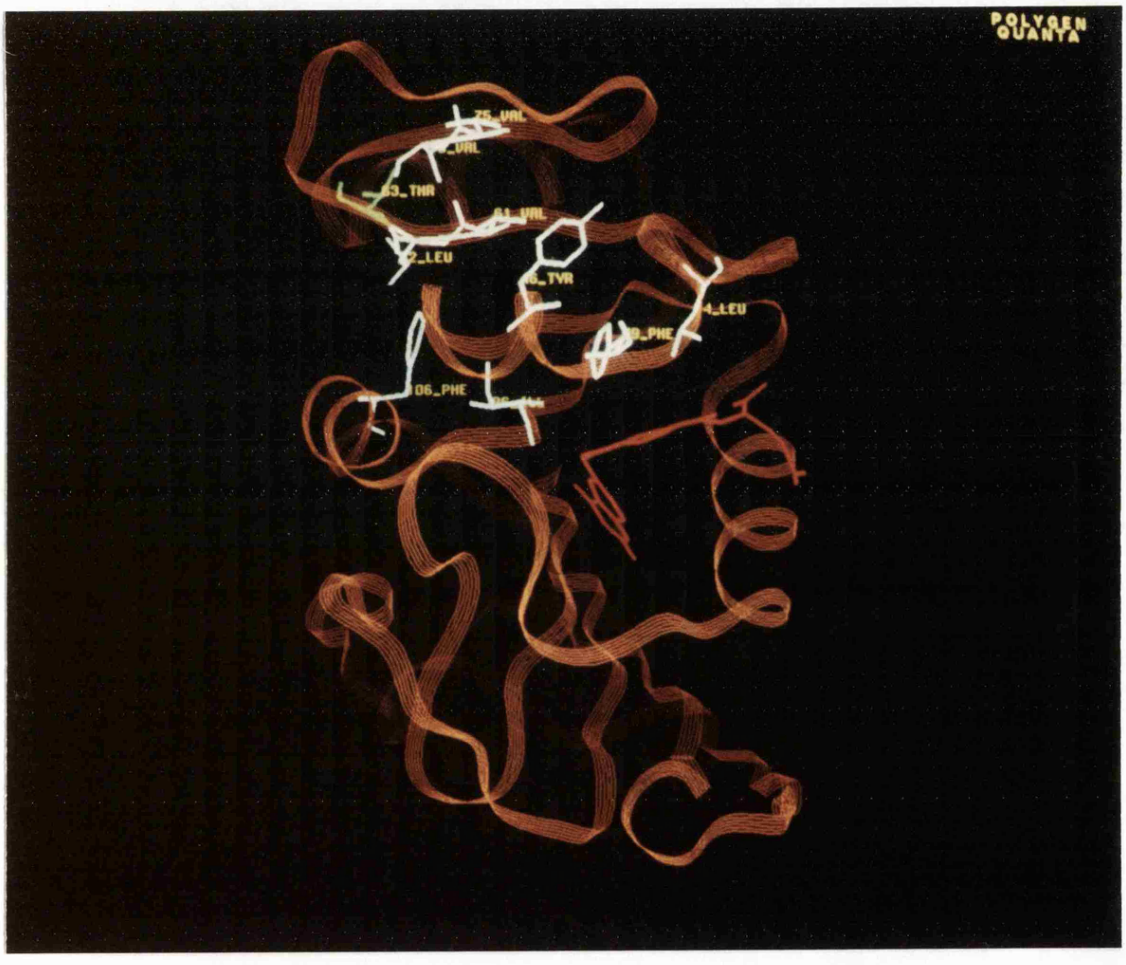

Leu54-Phe30

The NOE's between Leu54 CδH3 and Phe30 H2'6', H3'5', and H4' were not well enough resolved to be compared.

Ile96-Phe106

The NOE's of Ile96 $C\delta H_3$ with Phe3 H3'5', Phe 106 H2'5' and H3'5' are all present but poor resolution from other peaks means the relative sizes cannot be compared. An NOE is expected to be seen with Phe106 H4' but the 4' and 3'5' are not resolved in the wild type spectra so this NOE has not been assigned. The resolution of these peaks in the T63A spectra (due to changes of chemical shift changes in this region) should allow this NOE to be resolved, however the NOE is not seen in the T63A spectra. Due to the degeneracy in the wild type spectrum it is not clear if this absent NOE is significant.

Tyr46-Val61

The NOE between Tyr46 H2'6' and Val61 $C\gamma H_3$ at -3.83ppm is the same as wild type.

Val61-Tyr68

The NOE between Val61 $C\gamma H_3$ at -3.83ppm and Tyr68 H2'6' is the same as in the wild type spectra. The NOE's suggest that no changes in structure have occurred at the region around Tyr46, Leu61 and Tyr68, all relatively near the mutation.

The NOE's with Leu62, Val75 and Val76 are all in the crowded region of the spectrum so their NOE's cannot be compared.

The other NOE's from assigned proton resonances that had no change in chemical shift were compared with wild type and revealed no differences between the wild type and T63A spectra. These residues include those from Leu118, Trp21, Phe122, Met128, Trp5, Phe3, Trp133, Trp158, and Phe136. The NOE's from Leu54, Leu131, Leu27, and Leu23 all overlap, no changes in NOE's were apparent but the poor resolution made it difficult to assess.

4.3.2. TERNARY COMPLEXES WITH $NADP^+$

COSY, NOESY, and HOHAHA spectra were recorded for ternary complexes with MTX and $NADP^+$. The NOESY spectra were examined to compare the exchange peaks (i.e. between free and bound nicotinamide and adenine moieties of $NADP^+$) between mutant and wild type complexes. Exchange cross peaks are seen in NOESY spectra, (provided that the exchange rate is slow on the nmr time scale) because the magnetisation is passed between the bound and free ligand (Hyde *et al.*, 1980a, 1980b). Further analysis on this complex was not carried out because the wild type spectra have relatively few assignments.

In the T63Q/MTX/$NADP^+$ complex the exchange cross peaks for all the adenine proton resonances had similar chemical shifts to wild type. The nicotinamide protons N2, N4, N5, and N6 had small chemical shift differences when compared to wild type. (table 4.3).

Table 4.3. Chemical shifts of proton resonances from the adenine and nicotinamide moieties of $NADP^+$ when bound to wild type and T63Q DHFR in ternary complex with MTX.

Proton	δ WT (ppm)	δ T63Q (ppm)	Δδ (ppm)
A2	3.64	3.64	0
A8	4.31	4.31	0
N2	6.34	6.37	0.03
N4	6.16	6.11	-0.05
N5	5.34	5.29	-0.05
N6	6.31	6.28	-0.03

In the T63A/MTX/$NADP^+$ complex no exchange peaks were observed, probably because the exchange rate had increased from slow to intermediate exchange, in which case the lines would be too broad to see.

4.3.3. TERNARY COMPLEXES WITH NADPH

COSY, NOESY, HOHAHA, and phosphorus nmr experiments were carried out on the enzyme/MTX/NADPH complexes.

4.3.3.1. T63Q COSY and HOHAHA Experiments

As with the binary results, the spectra of the T63Q and wild type complex were strikingly similar suggesting that very little of the protein structure is perturbed by the mutation. Figure 4.7 shows the high field methyl region of the wild type COSY spectrum, superimposed are the positions of peaks that have moved in the T63Q spectra, figure 4.8 shows the aromatic region of the wild type HOHAHA spectrum, superimposed are the position of peaks that have moved in the T63Q spectra, all the assigned proton resonances are labelled.

The assigned resonances of protons close to the mutation site include those from Val61, Leu62, Tyr68, Ile102, and Val115. All these are seen at the same chemical shift (or within 0.02ppm) in the mutant and wild type complex. This was an unexpected result since it is was assumed that the mutation would at least cause local changes in the protein structure, particularly with the coenzyme bound which constrains the structure in this region.

Table 4.4. Proton chemical shifts of all the protons in a residue that has a difference of at least one proton chemical shift when comparing the wild type and T63Q ternary complex with MTX and NADPH.

RESIDUE	^{1}H	δ WT(ppm)	δ T63Q(ppm)	Δδ (ppm)
Leu54	$C\delta H_3$	-3.83	-3.95	-0.12
	$C\delta H_3$	-3.41	-3.44	-0.03
	$C\gamma H$	-2.62	-2.60	0.02
Leu27	$C\delta H_3$	-3.75	-3.80	-0.05
	$C\delta H_3$	-3.17	-3.23	-0.06
	$C\gamma H_3$	-2.29	-2.33	-0.04
Phe49	H2'6'	2.63	2.68	0.05
	H4'	3.42	3.42	0
	H3'5'	3.32	3.32	0
Phe30	H2'6'	2.99	2.89	-0.10
	H3'5'	3.47	3.51	0.04
	H4'	3.63	3.65	0.02
Tyr29	H2'6'	3.02	2.98	-0.04
	H3'5'	2.91	2.88	-0.03
MTX	H7	4.19	4.28	0.09

The locations of these residues in the crystal structure are shown in photograph 4.4.

Figure 4.7. High field methyl region of the COSY spectrum of the wild type ternary MTX/NADPH complex, superimposed are the positions of all the peaks which have a different chemical shift in the T63Q complex.

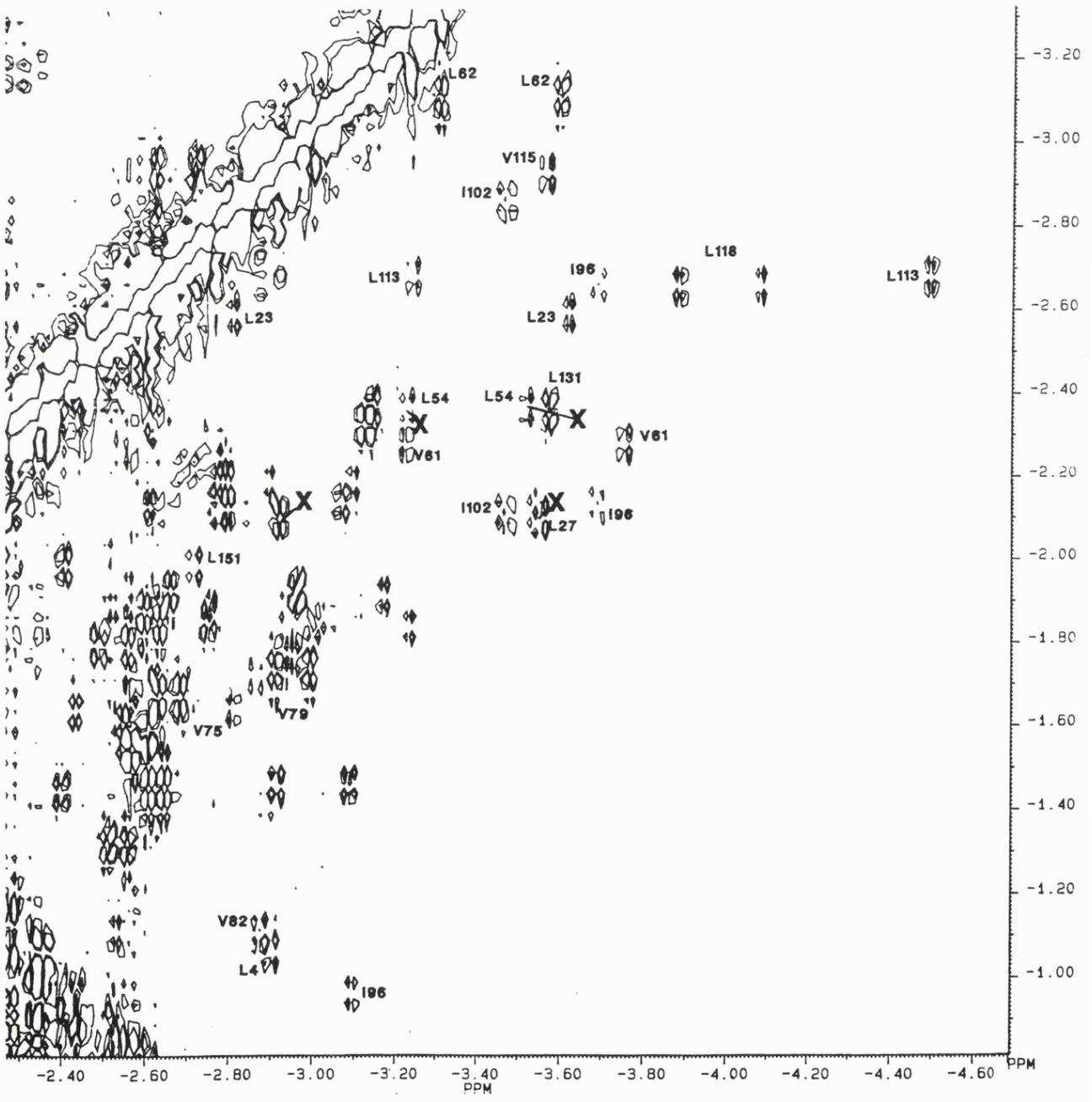

Figure 4.8. Aromatic region of the HOHAHA spectrum of the wild type ternary MTX/NADPH complex, superimposed are the positions of all the peaks which have a different chemical shift in the T63Q complex.

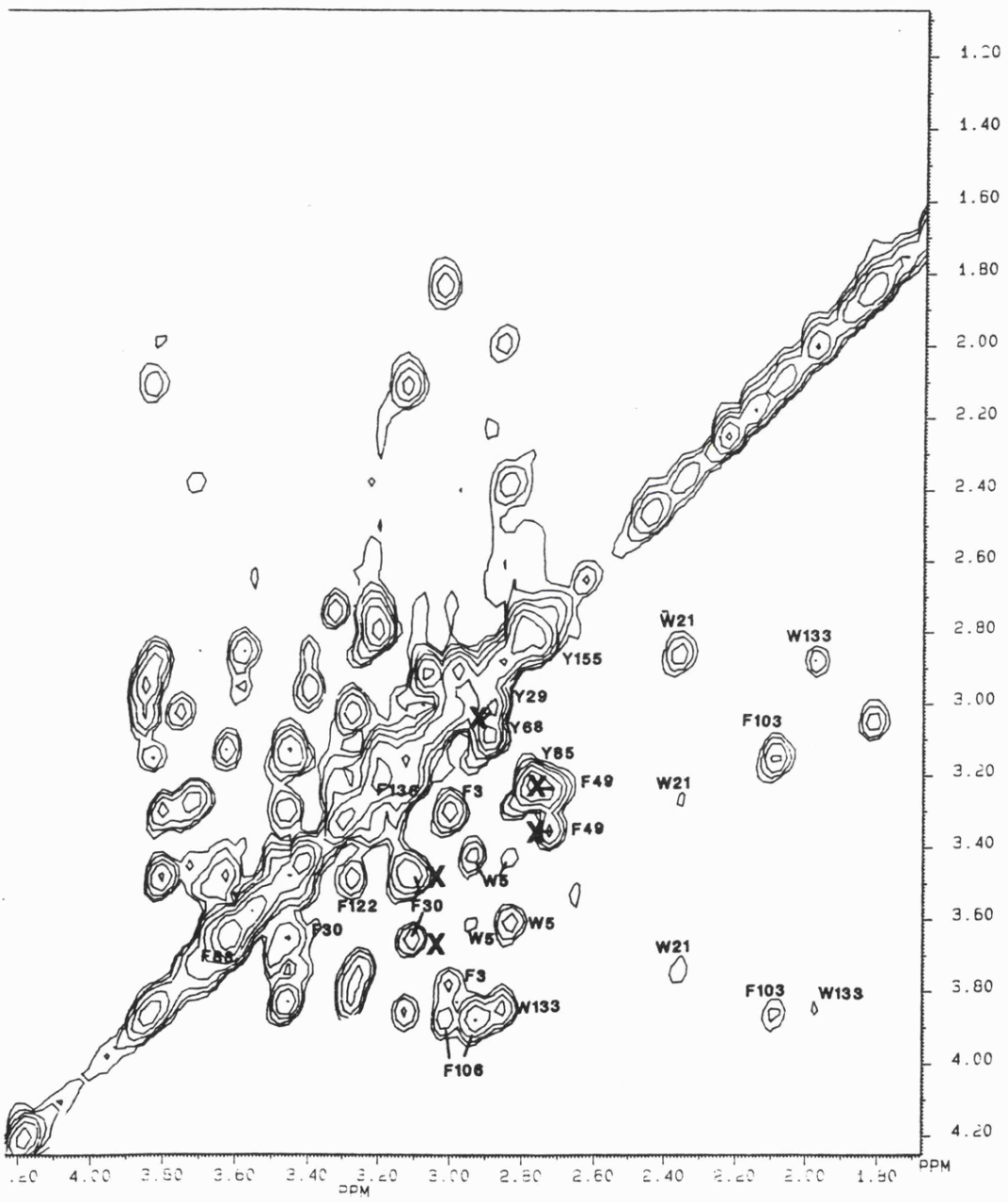

Photograph 4.4. αCarbon backbone of L. casei DHFR showing MTX (red) and NADPH (blue) with the side chains of all the residues with assigned protons resonances that have a different chemical shift in the ternary MTX/NADPH complex of the T63Q mutant compared to the wild type spectra. Threonine-63 is shown in green.

4.3.3.2. T63Q NOESY Experiments

Figure 4.9 shows a region of the NOESY spectra of T63Q and wild type MTX NADPH ternary complexes where a number of assigned NOESY cross peaks reside. The NOE's mentioned in the text are labelled.

From the T63Q NOESY spectrum it was seen that the chemical shift from the pteridine H7 proton resonance of MTX had moved from 4.19ppm in the wild type to 4.28ppm in the T63Q mutant.

The proton resonances of the adenine H2 and H8 of NADPH were found to be at the same chemical shift in the T63Q and the wild type spectrum despite being near the mutation. The chemical shifts of Tyr46 H2'6', and Met128 SCH_3 were also the same but this was to be expected since these residues are not close to the mutation.

The NOE's from residues that had different proton chemical shifts in the COSY spectrum were compared with the wild type:

Pteridine H7 NOE's

The NOE's with Leu27 $C\delta H_3$ at -3.75ppm and Leu19 both $C\delta H_3$'s are all smaller by approximately 50% in the T63Q spectra providing positive evidence that there is some structural change at this region of the substrate binding site some distance from the mutation.

Phe49-Tyr46 NOE's

The NOESY peak between Phe49 H2'6' and Tyr46 H2'6' is not resolved in both mutant and wild type spectra so could not be compared.

Leu54-Phe30 NOE's

Leu54 $C\delta H_3$ has NOE's with Phe30 H2'6', H3'5', and H4' which are assigned. The NOE's with Phe30 H3'5' and H4' are resolved in both the wild type and T63Q spectra and these were the same intensity in both spectra, the other NOE's are not resolved so could not be compared.

Leu54-Phe49 NOE's

The NOE's between Leu54 $C\delta H_3$ at -3.83ppm and Phe49 H3'5', and H4' are bigger in the T63Q spectra (figure 4.10). The NOE's correspond to the residues moving closer together by 12 to 18%. The NOE's between all Leu54 sidechain protons and Phe49 H2'6' are too small in the wild type spectrum to be able to quantify the change in size but it is significantly larger in the T63Q spectrum, again providing positive evidence the substrate binding site has been structurally affected by the mutation whereas the region local to the mutation appears unaffected.

Figure 4.9. Noesy spectra of T63Q and wild type ternary complexes with NADPH and MTX, Noesy cross peaks mentioned in the text are labelled.

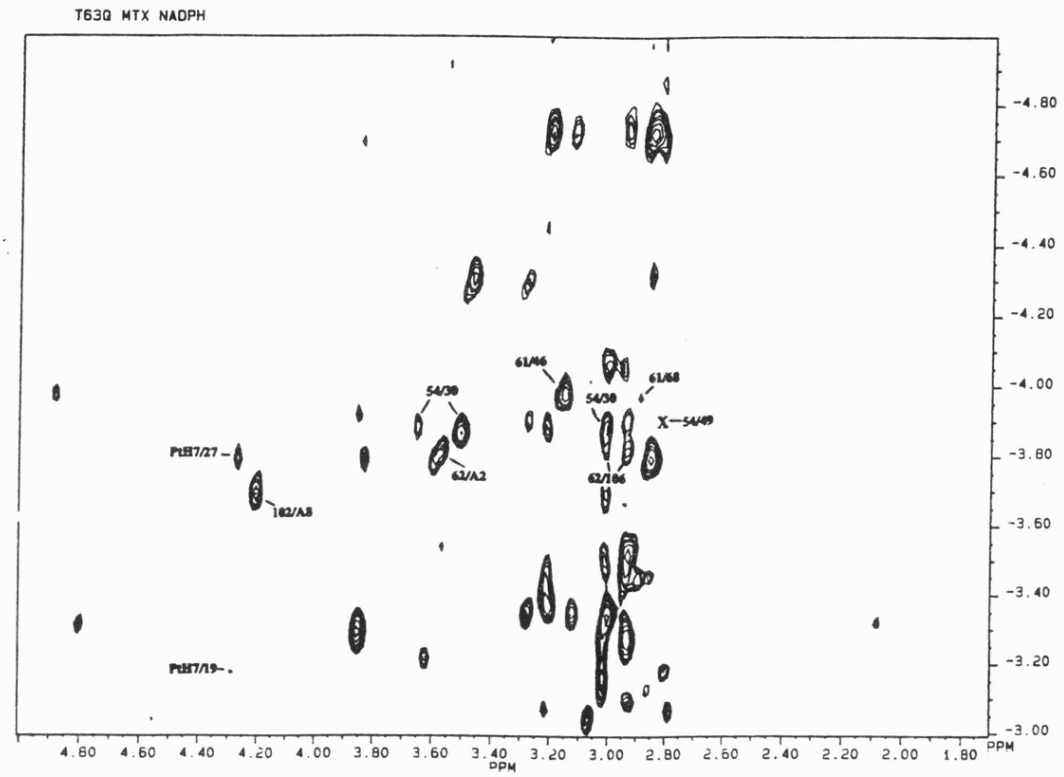

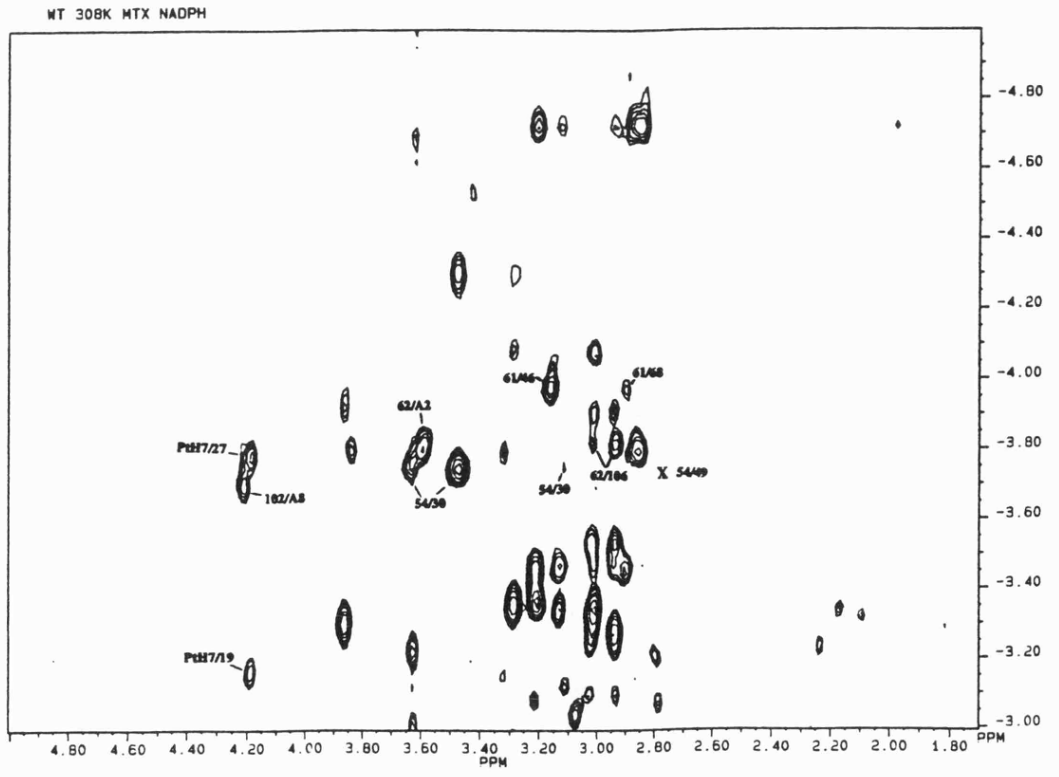

Figure 4.10. Selected rows from the wild type and T63Q NOESY spectra of the ternary complex with MTX and NADPH showing the relative sizes of the NOESY cross peaks between Phe49 H2'6', H4', H3'5' and Leu54 CδH3.

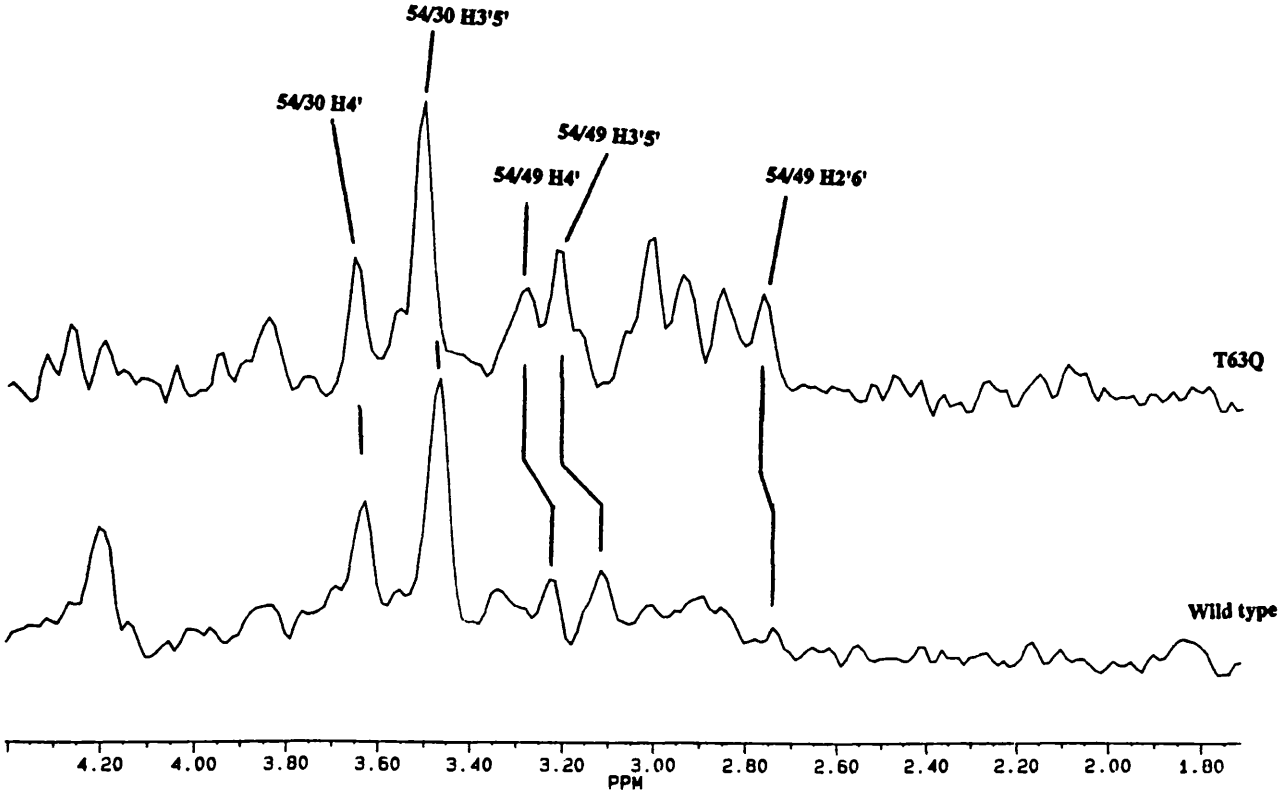

The NOE's in the T63Q spectrum of residues near the mutation were compared with the wild type spectrum:

The NOE's between Tyr68 H2'6' and Val61 $C\gamma H_3$ at -3.96ppm, Ile102 $C\delta H_3$ and Adenine H8, Leu62 $C\delta H_3$ and Phe106 H3'5' and H4' are the same in both wild type and T63Q spectra. All these provide evidence that little has changed near to the mutation. The NOE between adenine H2 and Leu62 $C\delta H_3$ is not resolved from other peaks so could not be compared.

The other assigned NOE's were compared in the T63Q and wild type spectra and no differences were found. These include NOE's from protons in residues Leu113, Phe136, Tyr85, Trp5, Trp21, Leu118, Met128, Phe3, Phe122, Trp133, and Leu131.

4.3.3.3. T63Q ^{31}P Experiments

The resonance from the 2' phosphate group was assigned on the basis of its singlet structure (the pyrophosphates being spin coupled give rise to two doublets), and its chemical shift was to low field of the pyrophosphate ^{31}P resonance position (figure 4.11).

The resonances of the 2' PO_4^{2-} group and pyrophosphates are the same in both the wild type and T63Q complexes.

Figure 4.11. Phosphorus nmr spectra of the wild type, T63Q, and T63A enzymes in ternary complex with MTX and NADPH. A is the resonance of the 2' phosphate, B and C are the resonances of the bound pyrophosphates, B is also where both pyrophosphates of the free NADPH resonate.

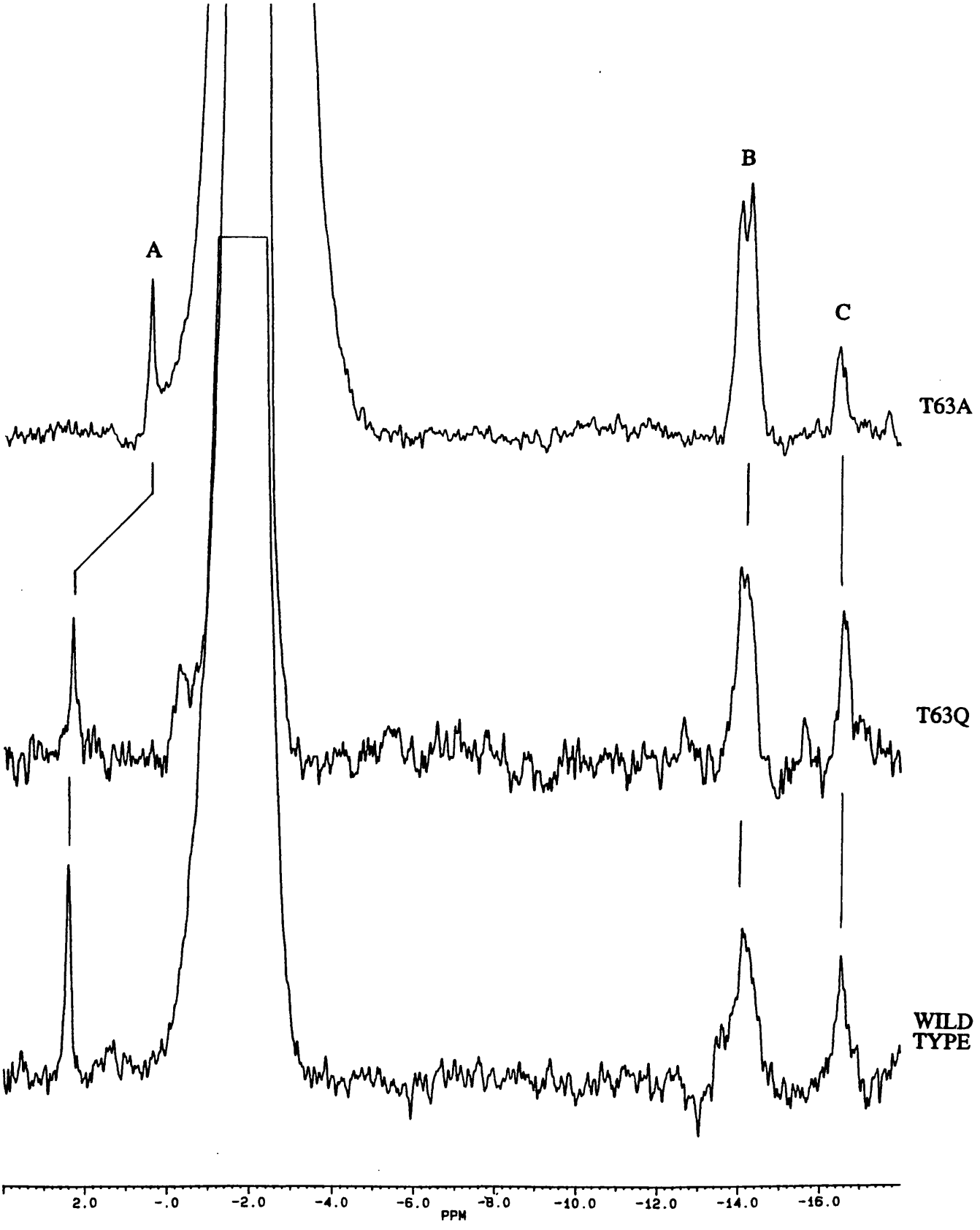

4.3.3.4. T63A COSY and HOHAHA Experiments

Again, as in the binary complex and the T63Q complexes, the spectra for the T63A ternary MTX/NADPH complex were very similar to wild type. Figure 4.12 shows the high field methyl region of the wild type COSY spectrum, superimposed are the positions of peaks that are different in the T63A spectra. Figure 4.13 shows the aromatic region of the wild type HOHAHA spectrum, superimposed are the position of peaks that are different in the T63A spectra. All the assigned cross peaks are labelled.

The residues in the T63A complex that have a different chemical shift to wild type are listed in table 4.5, all the assigned proton resonances for each residue are included. Unlike the T63Q complex the protons with changes of chemical shift are mostly in residues that are near to the mutation (photograph 4.5).

Figure 4.12. High field methyl region of the COSY spectrum for the ternary wild type, MTX, NADPH complex. Superimposed are the positions of all the peaks which have a different chemical shift in the T63A complex.

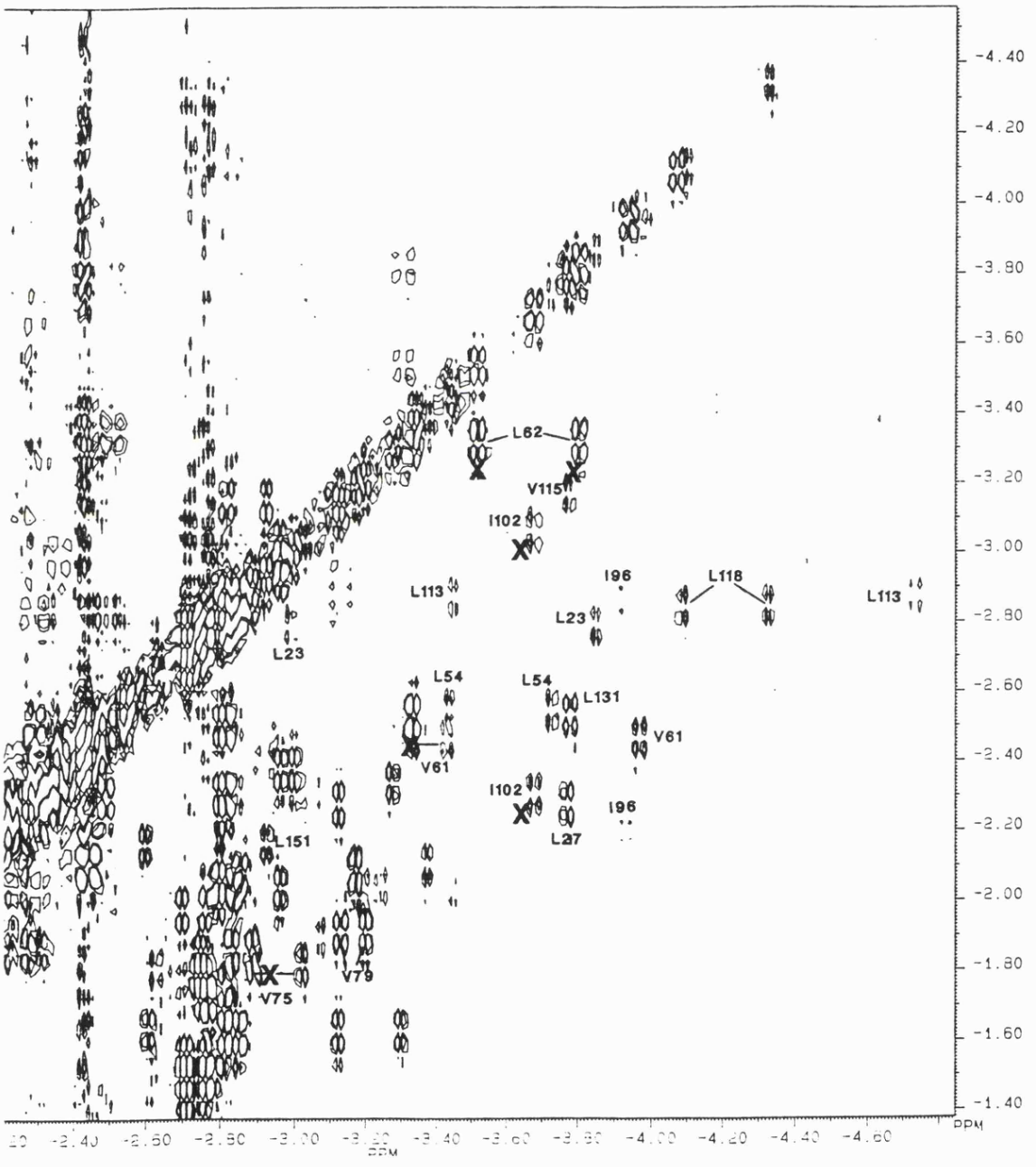

Figure 4.13. Aromatic region of the HOHAHA spectrum for the ternary wild type, MTX, NADPH complex. Superimposed are the positions of all the peaks which have a different chemical shift in the T63A complex.

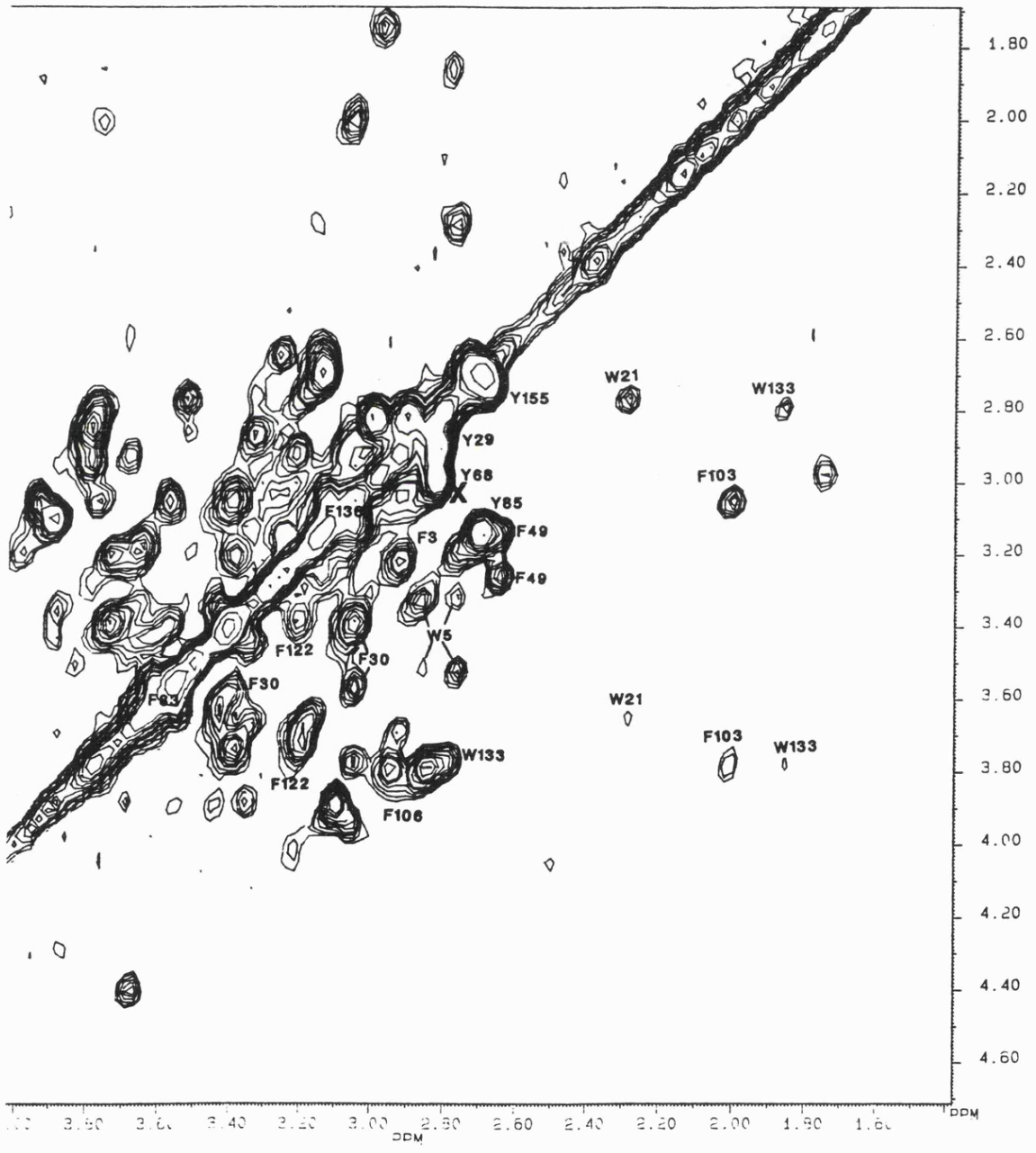

Photograph 4.5. αCarbon backbone of <u>L. casei</u> DHFR showing MTX (red) and NADPH (blue) with the side chains of all the residues with assigned protons resonances that have a different chemical shift in the ternary MTX/NADPH complex of the T63A mutant compared to the wild type spectra. Threonine-63 is shown in green.

Table 4.5. Proton chemical shifts of all the protons in a residue that has a difference in at least one proton chemical shift when comparing the wild type and T63A ternary complex with MTX and NADPH.

RESIDUE	^{1}H	δ WT(ppm)	δ T63Q(ppm)	Δδ (ppm)
Tyr68	H2'3'	3.09	3.15	.06
	H3'5'	2.92	2.87	-.05
Leu62	$C\delta H_3$	-3.80	-3.78	-.02
	$C\delta H_3$	-3.51	-3.51	0
	CγH	-3.28	-3.18	.1
Ile102	$C\delta H_3$	-3.67	-3.63	.04
	CγH	-3.03	-2.98	.05
	CγH	-2.28	-2.24	.04
Val61	$C\gamma H_3$	-3.96	-3.96	0
	$C\gamma H_3$	-3.43	-3.32	.11
	CβH	-2.43	-2.43	0
Tyr46	H2'6'	3.16	3.11	-.05
Val75	$C\gamma H_3$	-3.02	-2.93	.09
	$C\gamma H_3$	-2.89	-2.93	-.04
	CβH	-1.77	-1.77	0
NADPH	A8	4.26	4.14	-.12
	A2	3.60	3.57	-.03

4.3.3.5. T63A NOESY Experiments

Figure 4.14 shows a region of the NOESY spectra of T63A and wild type MTX NADPH ternary complexes where a number of assigned NOESY cross peaks reside. The NOE's mentioned in the text are labelled.

The assignment for the Pteridine H7 of MTX was made and its chemical shift was the same as the wild type. The NOE's with Leu27 and Leu19 were the same in both wild type and T63A spectra. The chemical shift for Met128 was also the same in the T63A and wild type spectra. None of these residues are near the mutation, suggesting that the protein structure is similar to wild type.

The chemical shift of the adenine-H8 proton resonance was different in the T63A spectrum, changing from 4.26ppm in the wild type spectrum to 4.14ppm in the mutant. The adenine-H2 proton resonance had moved upfield but only by 0.03ppm (table 4.5). The chemical shift of Tyr46 H2'6' had also moved from 3.16 to 3.11ppm.

The NOE's of residues that had a change of proton chemical shift were compared with the wild type:

Leu62-Adenine H2

The NOE's of Leu62 CδH_3 at -3.51 and Leu62 CγH with adenine H2 are resolved and the NOE with CγH is clearly smaller (figure 4.15), indicating some change in the binding site of the adenine moiety of NADPH. The NOE between Leu62 CδH_3 at -3.8ppm and the adenine-H2 is not resolved from other peaks in the spectrum.

Ile102-A8

The NOE between the adenine H8 of NADPH (A8) and Ile102 CγH_3 is approximately 50% smaller in the T63A spectrum (figure 4.16) providing evidence that the structure of the NADPH binding site has been affected by the mutation.

Leu62-Phe106

The NOE's between Leu62 CδH_3 at -3.80ppm and Phe106 H2'6', H3'5', and H4' are all the same in the wild type and T63Q spectra, evidence that this region of the protein, although close to the mutation, is not affected.

Val61-Tyr68 NOE's

The NOE's between Val61 CγH_3 at -3.96ppm and Tyr68 are not resolved in the wild type spectra at this temperature and so the size of these NOE's cannot be compared with the mutant.

Val61-Tyr46 NOE's

The NOE between Val61-CγH_3 at -3.96ppm and Tyr46-H2'6' is the same size in the wild type and mutant spectra, again providing evidence that this region of the protein, despite being close to the mutation, is not affected.

Val75 has no assigned NOESY cross peaks because they are in a very crowded region of the spectrum.

The other assigned NOE's were compared in the two spectra and no differences were found. These include NOE's from residues Leu118, Met128, Trp5, Trp133, Leu113, Leu23, Leu131, Leu96, Phe106, Trp21, Phe122, and Phe3.

Figure 4.14. Noesy spectra of T63A and wild type ternary complexes with NADPH and MTX, Noesy cross peaks mentioned in the text are labelled.

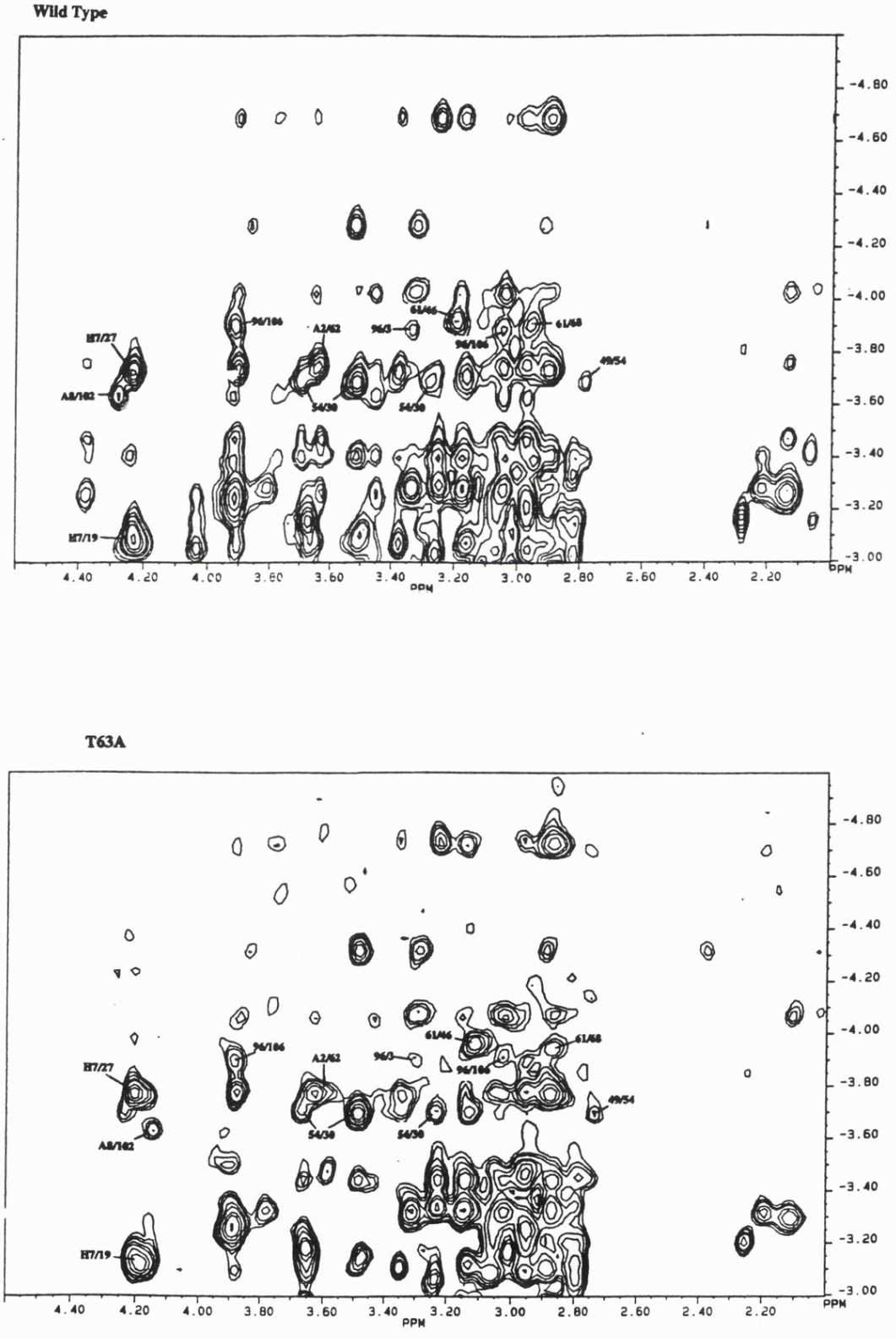

Figure 4.15. Stacked plot representations of the NOESY spectra of the wild type and T63A ternary complexes with MTX and NADPH showing the NOESY cross peaks of adenine H2 (labelled A2) and Leu62.

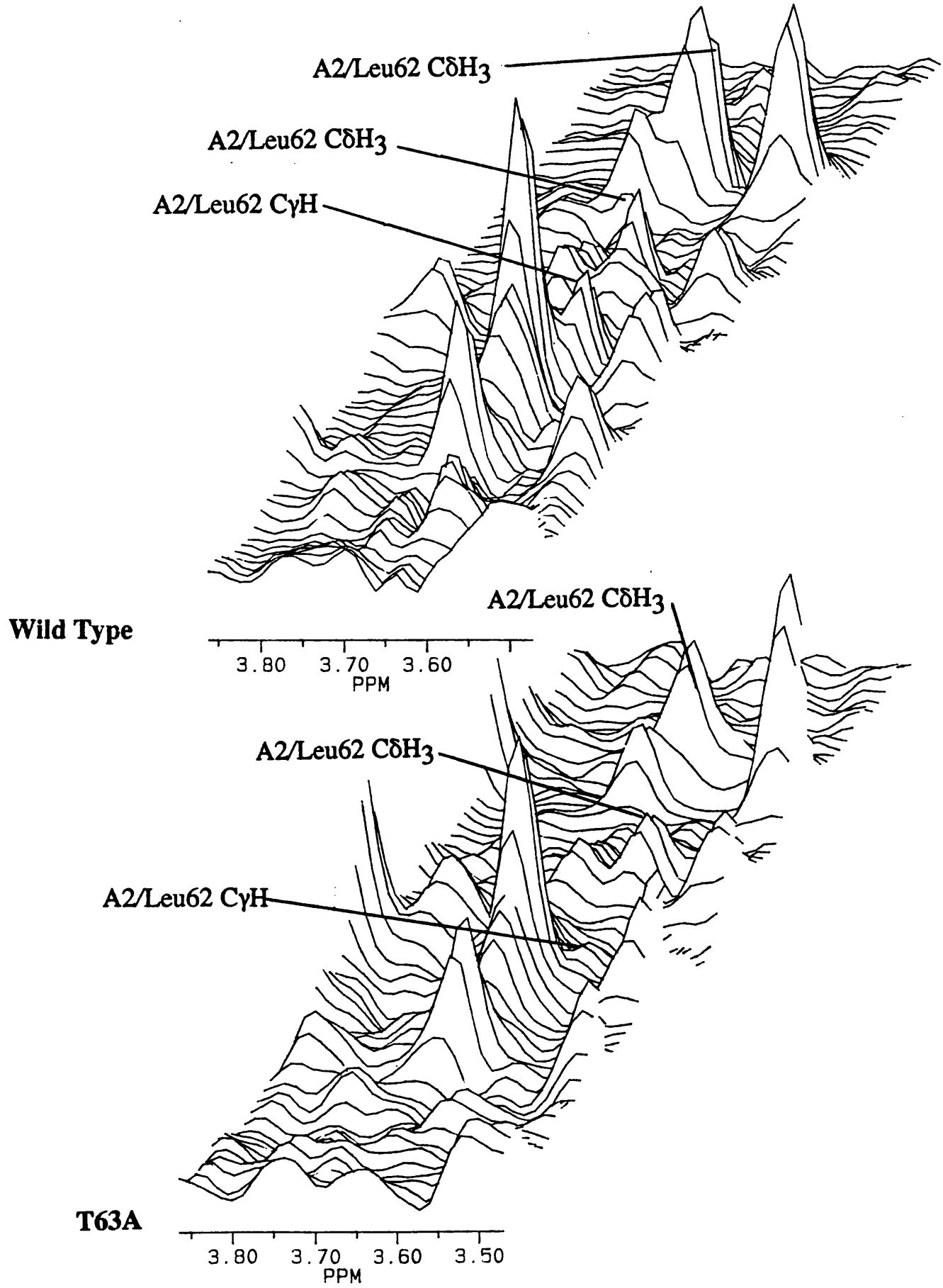

Figure 4.16. Stacked plot representations of the NOESY spectra of the wild type and T63A ternary complexes with MTX and NADPH showing the NOESY cross peaks of adenine H8 (labelled A8) and Ile102 CδH3.

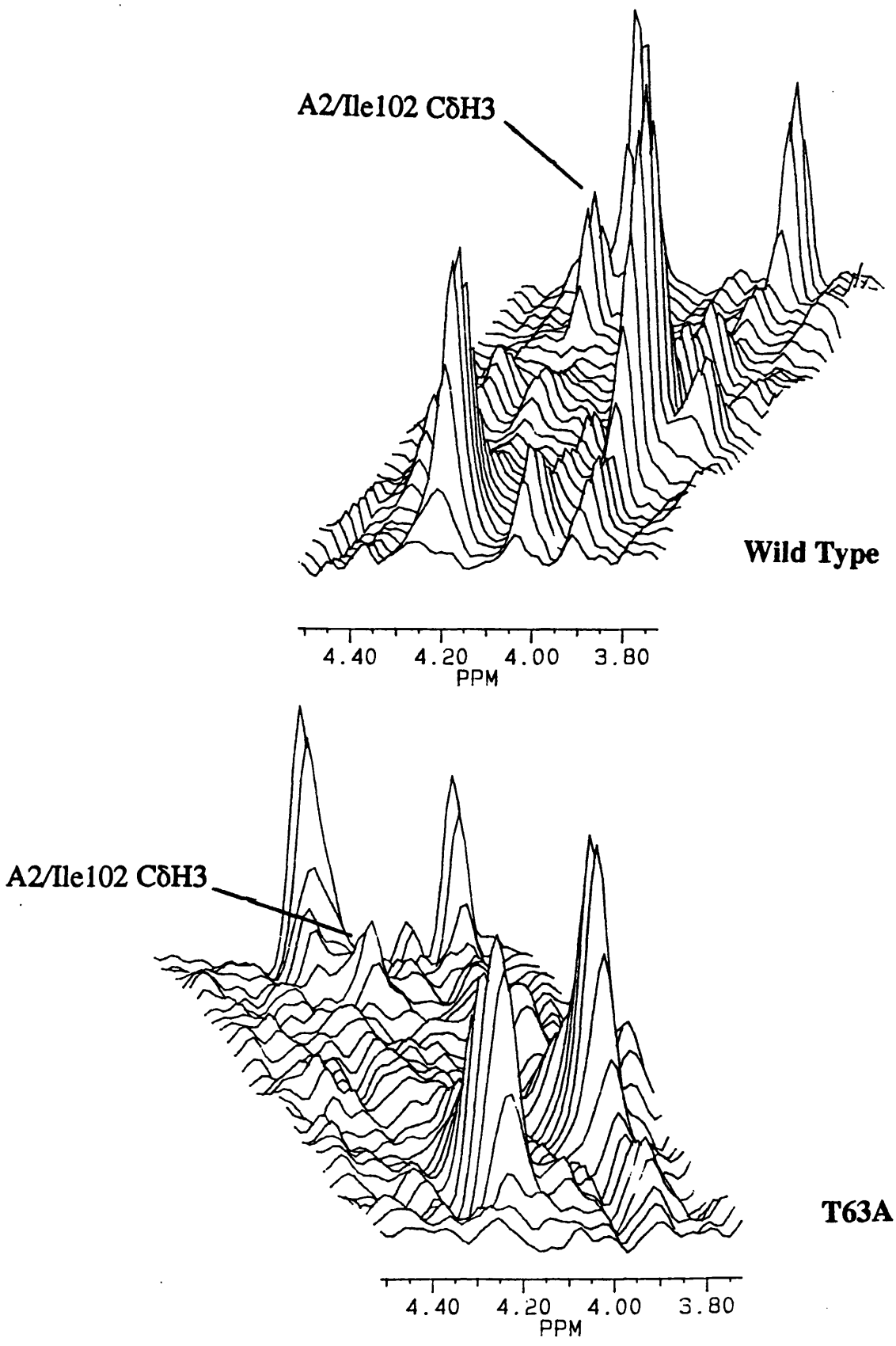

4.3.3.6. T63A ^{31}P Experiments

The one dimensional phosphorus spectra of the ternary complexes are shown in figure 4.11 (page 93). The 2' phosphate resonance from the T63A complex has shifted by 2ppm relative to wild type, indicating that the phosphate moiety binds differently in the mutant complex. The pyrophosphate chemical shifts are similar to the wild type complex suggesting their binding is unaffected by the mutation. Peak B of the pyrophosphates appears larger because of the presence of some free NADPH which has the same chemical shift.

4.4. DISCUSSION

4.4.1. General Discussion

In the results section the lists of proton chemical shift changes include all the changes of assigned peaks in the spectra, including the very small changes. [It should be noted that the assignments available at that time were fewer and now the whole spectrum of the binary MTX complex has been almost completely assigned (Birdsall, Carr, Feeney, personal communication)]. However, it is debatable whether the smaller changes are enough to indicate significant differences in protein structure. Initially it was thought that a "cutoff" point would be used, below which the changes in shift would be considered irrelevant. Using a cutoff is rather arbitrary and perhaps not realistic since the sensitivity of the chemical shifts to structural changes will vary from proton to proton. For these reasons a strict cutoff has not been used, instead, less emphasis has been placed on the smaller chemical shift changes, i.e. below 0.05ppm.

Interpretation of the chemical shift changes in the mutants is fraught with difficulties. A chemical shift change provides evidence that there is some structural difference around the proton but gives little information about what the change is. The proton itself may not be in a different position relative to wild type structure; there are a number of factors contributing to the chemical shift, not all of which are fully understood. Therefore the NOE data is essential to shed light on what is causing the shift changes.

The difficulty with relying on NOE's to provide structural information is in obtaining sufficient data to interpret the precise changes. The problems lie in the relatively small number of resonance assignments compared to the total number of protons in the protein and in finding NOESY cross peaks which are well resolved in both the wild type and mutant spectra to be able to see if the peak intensities have changed. Thus the chemical shift data, with more assignments and chemical shift changes more easily seen, was relatively more "complete" but could not give information on exactly what had happened to the structure. On the other hand there was less NOE information but what there was gave detailed information on what had happened to the structure; if an NOE changes in intensity there has to be a change in distance to cause this, assuming the peak does not arise as a result of spin diffusion (see the introduction to this chapter).

In calculating distance changes and in data interpretation, the crystal structure coordinates were used and for this purpose they were assumed to be accurate. The general consensus is that the crystal structure is very similar to the solution structure, supported by nmr evidence (Hammond *et al.*, 1986, Birdsall et al., in press). Nmr provides the time

averaged position of protons and x-ray crystallography provides a fixed position which may not accurately depict the structure in solution due to crystal packing constraints. Therefore neither technique necessarily provides the true structure and so calculation of distances is precarious and may produce large errors. A great deal of effort is being exercised in developing methodologies for the calculation of structures from nmr data, reviewed by Clore and Gronenborn (1989), and Wuthrich (1989). However, where possible, numbers were calculated for distance changes between protons, more out of a need to give an impression of the magnitude of the distance changes rather than to provide an accurate number.

4.4.2. T63Q

The 2D nmr spectra of the T63Q complexes were very similar to those of the wild type enzyme, indicating there were no gross structural changes caused by the mutation. The most interesting observation is that the changes seen were all some distance from the mutation and were at the substrate binding site rather than, as was expected, the coenzyme binding site. An alternative explanation to those described below for structural changes remote from the mutation is that the mutant was not really T63Q, or that an additional mutation had occurred in the protein. This possibility was explored as described in the mutagenesis chapter and the mutation was confirmed to be T63Q.

When NADPH binds to the binary enzyme/MTX (E.MTX) complex, the chemical shifts of protons from some residues change substantially due either to the proximity of NADPH or to conformational changes in the protein. These spectral changes seen in the wild type complexes were also seen in the T63Q complexes, providing strong evidence that the coenzyme binds in a very similar fashion to the wild type enzyme. Even the residue adjacent to the mutation, Leu62, has identical proton chemical shifts in the wild type and mutant spectra of both complexes. The assigned residues which show large proton chemical shift changes when the coenzyme binds to DHFR are Leu62, Val61, Ile102, Leu23, Tyr68, Phe49, Phe30, and Trp21. The pteridine H7 of MTX also shows a change of chemical shift when coenzyme binds. Of these, only H4' of Phe49, H2'6' and H3'5' of Phe30 and the MTX pteridine-H7 had a different chemical shift between at least one of the wild type and T63Q complexes. The results were studied to ascertain if the changes in these protons are due to an altered coenzyme binding and if not, to determine what was causing them. The observations are;

1. Phe49 had similar proton chemical shifts in T63Q and wild type enzymes in the binary MTX complex, only H3'5' having a small chemical shift

difference of 0.03ppm. In the ternary complex however, the H2'6' resonance was at a different chemical shift, i.e. the shift difference of the H2'6' proton, on going from the binary to the ternary complex, was greater for the mutant than the wild type enzyme. This suggests that the coenzyme binding causes the ternary complex to adopt a slightly different conformation from wild type at or near Phe49 H2'6', (15Å away from the mutation). There is no detectable change near the mutation with or without NADPH bound so it is not immediately clear how the affect is propagated through the protein to this site 15Å away.

2. The Phe30 H3'5' protons of the T63Q mutant have a different chemical shift from wild type in both complexes but the chemical shift is altered in different ways. In the binary complex the resonance is shifted relative to the wild type by -0.02ppm (although this may not be considered significant) but is shifted in the opposite direction by 0.04ppm, in the ternary complex. Thus the difference in chemical shift of Phe30 H3'5', between the binary and ternary complexes, is greater for the mutant than the wild type. This could be interpreted to indicate that the mutation causes a small change in structure at or near Phe30 H3'5' in the binary complex and that the coenzyme binding exerts a conformation change which is slightly different from that of the wild type complex. Phe30 H2'6' protons have a different chemical shift from the wild type in both the binary and ternary complex and in this case the difference from wild type was the same in both complexes, i.e. the difference in chemical shift of Phe30 H2'6', on going from the binary to the ternary complex, was the same in the mutant complex as the wild type. The results could be interpreted to indicate that the mutation causes a change in structure at or near Phe30 and the change, being the same in both the binary and ternary complexes, appears not to be affected by coenzyme binding. The result for the H2'6' contradicts that of the H3'5' and depicts how precarious over interpretation of chemical shift data can be. The chemical shift of proton resonances vary in their sensitivity to structural changes and so all that can be realistically deduced from the results is that the protons of the Phe30 side chain are in a different environment in the mutant compared to the wild type enzyme in both the binary MTX and ternary NADPH/MTX complexes. The fact that Phe30 has been affected by the mutation is striking since it is approximately 21Å away from the site of the mutation at the MTX binding site.

3. Similar to the results for Phe30 H2'6', the chemical shift of MTX H7 is different in both complexes of the T63Q mutant compared to wild type but the shift change on NADPH binding is comparable in each case. Thus the binding of NADPH to the binary E.MTX complex apparently changes this part of the

protein structure in the same way in the mutant and wild type enzymes. Since there is a change in H7 proton chemical shift the mutation is affecting the protein at or near the pteridine end of MTX, 19Å away from the mutation, which must be propagated through the protein since there is apparently no change in coenzyme binding.

To summarise observations 1 to 3, the mutation has significantly affected the chemical shifts of proton resonances from residues Phe30 and MTX H7 in the binary complex, indicating the mutation has affected protein structure in the absence of coenzyme. Since the residues affected are at the MTX binding site, some distance from the site of the mutation the protein must be adopting a slightly different structure compared to wild type in order to propagate these affects. The mutation has significantly affected the chemical shifts of protons in residues Phe30, MTX H7, and Phe49 in the ternary complex all of which are again at the MTX binding site, distant from the mutation. Since residues were affected in both the binary complex where coenzyme is absent, and the ternary complex, it is likely that the affects are propagated to the MTX binding site through the protein rather than through the coenzyme. However, coenzyme binding does appear to affect the structure because different chemical shift changes are seen in the mutant compared to wild type when NADPH binds therefore it could be that the binding of the nicotinamide ring, next to MTX, is changed slightly because of the affect of the mutation on the MTX binding site.

The other residues with assigned resonances that have chemical shift changes in the mutant spectra include those in side chains of Leu54, Leu4, Leu27, Tyr29, and Val35 in the binary complex and Leu54, Leu27, and Tyr29 in the ternary complex (Leu4 and Val35 are not assigned in the ternary complex). Since these residues are all found at the MTX binding site they add weight to the argument that the mutation has altered the protein structure in some way, leading to the change at the MTX binding site. The NOE's of Leu4, Val35 and Tyr29 were all unresolved or unassigned so could not be examined to determine what had changed in the protein structure at these residues. The NOEs of the other residues are discussed below.

Leu27 has proton chemical shift changes in both binary and ternary complexes. The side chain protons from the two $C\delta H_3$'s and the $C\gamma H_3$, although shifted by up to 0.06ppm in T63Q, have a similar chemical shift with and without NADPH bound, thus the structural change is probably not caused by different NADPH binding. Leu27 is near to the pteridine ring of MTX and a NOE is seen between Leu27 $C\delta H_3$ at -3.75ppm and the pteridine H7. Comparison of the NOE in the ternary T63Q spectrum showed that it was smaller than in the wild type spectrum by approximately 50%. The distance between H7 and Leu27 is 3.9Å in the wild type complex thus the distance change is less than 0.1Å (since the peak size is inversely proportional to the sixth power of the distance, see the introduction to this

chapter). This provides direct evidence that there is a small structural change in the MTX binding site.

Leu54 CδH_3's and CγH all have chemical shifts which differ from the wild type but the CδH_3 at -3.83ppm has a bigger chemical shift difference in the ternary complex. Leu54 is near the MTX binding site, next to Phe49. As discussed above, the protons of Phe49 also show chemical shift changes, so one possibility is that these two residues have moved with respect to each other. In the NOESY spectra of the binary MTX complex the NOESY cross peaks between Phe49 and Leu54 could not be compared because of peak overlap. Detailed analysis of peaks in the ternary complex spectra was however possible, and revealed that the NOE's between Leu54 and Phe49 were bigger, corresponding to the two residues moving closer by 12 to 18% of the distance in the wild type enzyme. The average distance between Phe49 and Leu54 is approximately 4Å so this corresponds to a distance change of 0.4 to 0.7Å. This provides further evidence that there is a change in binding of MTX despite there being little change at the site of mutation. The Phe49 proton resonances have an unusual chemical shift caused by the proximity *p*-amino benzoyl ring of MTX exerting a ring current affect. Thus the chemical shift of the proton resonances from Phe49 would be very sensitive to the orientation of this ring.

Leu54 also has NOE's with Phe30, and although these were not resolved in the binary complex, two of the three NOE's with Leu54 CδH_3 at -3.83ppm were resolved well enough in the ternary complex to ascertain that they were the same for both wild type and T63Q enzyme. Therefore the change in distance found between Phe49 and Leu54 has not affected the distance between Phe30 and Leu54 and the changes of proton chemical shift seen for Phe30 are not because it has moved with respect to Leu54. This suggests that Phe49 not Leu54 has moved. The changes occurring at the MTX binding site must be small because otherwise it is difficult to see how Leu54 and Phe30 could remain the same distance apart, this is also supported by the fact that there are no gross chemical shift and NOE differences between the two enzymes. The differences in chemical shift seen for Phe30 may be due to a slight change in orientation of MTX in the binding site.

Another observation is that the proton chemical shift changes of Phe49 were small, the largest being 0.05ppm yet there is clearly a structural change around this residue compared with wild type. This highlights the fact that the sizes of chemical shift changes cannot be easily interpreted to suggest what has happened to the protein structure. This also casts doubt on the interpretation that if there is no change in chemical shift there is no change in structure. However where a large number of resonances are the same it is unlikely that there is a structural alteration.

The observations that distances have changed between Phe49 and Leu54, and Leu27 and MTX pteridine H7, provide positive evidence that the protein structure has been altered by the mutation. Surprisingly the change in structure is seen at least 15Å away from the mutation yet there are no observable structural changes in residues that are much closer to the mutation. The reason the changes are not seen is not because of a limited number of assignments, there are a substantial number of residues with proton resonance assignments which lie between the mutation and the substrate binding site, including protons from side chains of residues Tyr68, Leu61, Val60, Tyr46, Tyr85, Phe106, His77, Leu62, and Ile102 (see photograph 4.6). These were all at the same chemical shift in the mutant spectra as wild type and so are probably in the same environment. Further powerful evidence that the mutation of T63Q does not have a significant effect on local protein structure comes from the NOE data. NOESY cross peaks from Leu61, Tyr68, Ile96, Ile102 and Phe106 were all the same relative size in the wild type and mutant binary complex spectra. Thus the evidence is that the affect of the mutation on nearby residues is minimal. Despite this there must be a change in this region in order to effect the change remote from the mutation and so the affect must be on a limited number of unassigned residues.

The phosphorus nmr experiment provides yet more evidence that the 2' phosphate binding site of the coenzyme is not affected by the mutation. The chemical shift of the phosphorus nucleus is most sensitive to the electron distribution in the phosphate group providing local information specific to the phosphate group (e.g. bond angles, ionisation state, and electrostatic interactions) so acts as another probe and may show changes in the mutant structure not detected by proton nmr. The phosphorus nmr spectrum was the same as wild type indicating the environment of the 2' phosphate and the pyrophosphates were not affected by the mutation. Thus it appears the hydrogen bonding and ionisation state may be the same and glutamine may still be forming an hydrogen bond with the 2' phosphate, just as threonine does in the wild type. These conclusions are supported by the T63A results (see later).

The nmr results on the ternary MTX/$NADP^+$ complex showed that the mutation causes some change to the coenzyme proton chemical shifts although it should be noted that it is the oxidised rather than the reduced coenzyme being studied in this case. The adenine protons, near the site of mutation, have the same chemical shift as wild type thus again supporting other evidence that this region is not greatly affected by the mutation. The adenine end of the $NADP^+$ binds in a very similar way to NADPH (there is a small chemical shift difference in the A8 proton, Hyde *et al.*, 1980). The nicotinamide protons do have some different chemical shifts in the T63Q spectrum, the larger changes being to the N4 and N5 protons. In studies of the wild type enzyme, Hyde *et al.*, (1980) found these resonances are shifted the most when MTX binds to the E.NADPH complex. The nicotinamide protons are next to the MTX pteridine ring and their resonances are affected

by the ring current affects of the pteridine ring of MTX. Therefore, any structural change in the position of the pteridine ring will cause a change in chemical shift of the nicotinamide protons. In addition, the nicotinamide ring itself may be moved slightly. Nicotinamide ring movement with respect to wild type is not likely to arise as a result of a movement along the coenzyme binding site; none of the protons from residues along the coenzyme, nor the phosphorus nuclei of the coenzyme, have altered chemical shifts. A shift change could arise as a result of the differences in MTX binding. However too much emphasis should not be placed on these results since the nicotinamide ring does not bind the same in the oxidised and reduced form of the coenzymes and shows a reduced cooperativity with MTX compared to NADPH (Hyde *et al.*, 1980). The assigned side chains of Trp5, Trp21 and Phe103 are all near the nicotinamide ring and their proton chemical shifts and NOEs are the same as wild type suggesting there is probably very little difference in nicotinamide binding in the ternary NADPH/MTX complex.

The crystal structure coordinates were examined to find the possible channels by which the mutation could make changes to the protein structure. Given the number of residues which must be in the same environment as wild type, it was very difficult to find a route which could cause the structural effects, the assignments in the protein were sufficient to eliminate many of the possible pathways.

A feasible route was found via Arg43. The mutated Gln63, being larger than Thr63, may force the Arg43 side chain (resonances unassigned) to move due to unfavourable steric interactions. This movement could be transmitted along the backbone of helix C, which begins at Arg43, along to Phe49 at the end of this helix. This movement would cause Phe49 to move closer to Leu54 (as observed from the nmr data). The side chain and backbone protons of residues in helix C are shown in photograph 4.5, together with residues around the mutation site which have not been affected by the mutation, and Thr63. The difficulty with this hypothesis is that Tyr46 lies along this helix yet the resonances of this side chain do not show chemical shift or NOE changes. However it is conceivable (clearly seen in the photograph) that the packing of the side chains is such that the Tyr46 ring can remain unaffected by the movement of this backbone. This can be predicted as long as the proposed backbone movement is small. Since the effects of the mutation appear to be small (as determined by changes in chemicals shifts of resonances and the NOE's between them) and limited to only a few residues, this suggestion is feasible. The residues just a few Å away from the residues affected by the mutation (as found by the nmr analysis) include Leu131, Leu113, Leu118, Met128, Trp21, Trp5, Phe3 and Tyr46. None of these residues have side chain resonances with chemical shift changes or changes in NOE intensities. Most notably the NOE between Phe30 and Leu54 is the same despite the distance between Leu54 and Phe49 being smaller. The structural change in the protein around Leu54 must therefore be small or else it is difficult to see how the distance between

Leu54 and Phe30 is the same in the wild type and T63Q enzymes yet the distance between Leu54 and Phe49 is smaller. All the evidence taken together suggests that the changes in protein structure are small and supports the suggested movement of helix C.

In summary, there are no changes to the orientations of a large number of residues around the site of mutation and up to 15Å away. There is a small change in structure at the MTX binding site, as proved by NOE and chemical shift changes of protons in a limited number of residues and MTX itself. The changes at the MTX binding site may have caused a small change in NADPH nicotinamide ring orientation, as indicated by very small chemical shift changes of the nicotinamide protons of $NADP^+$. Since there are structural changes at the MTX binding site, there must also be an undetected structural change at the site of mutation, hence it must be at unassigned residues. As there is an overwhelming amount of evidence that very little has changed around the mutation and that the coenzyme binding near the mutation has not been affected, the structural change is probably very small and specific to only a few residues. The hypothesis suggested is that Arg43 is the residue directly affected by the mutation and the movement of this residue is transmitted along the C-helix backbone to Phe49 causing a small change of the MTX binding site.

Photograph 4.5. The position of residues in the crystal structure of L. casei DHFR in complex with NADPH (blue) and MTX (red) which were not affected by the T63Q mutation (white), and residues in helix C believed to have been affected by the mutation (green) with threonine-63 shown in yellow.

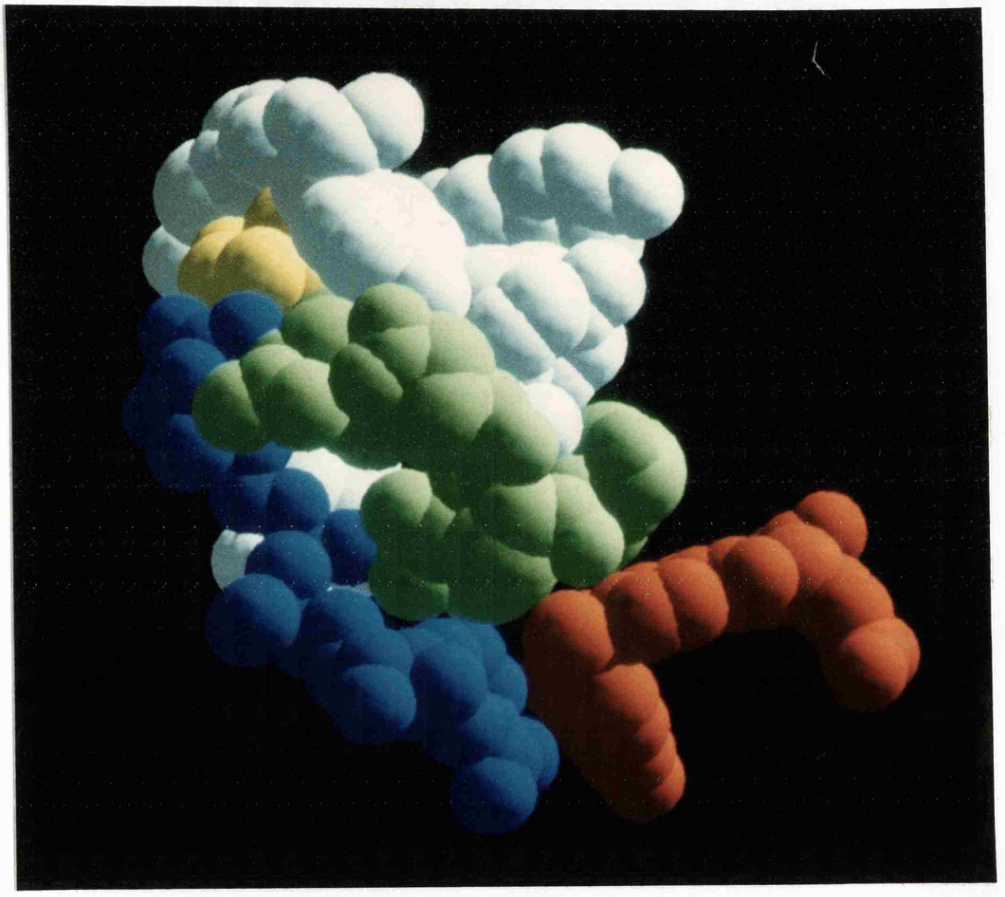

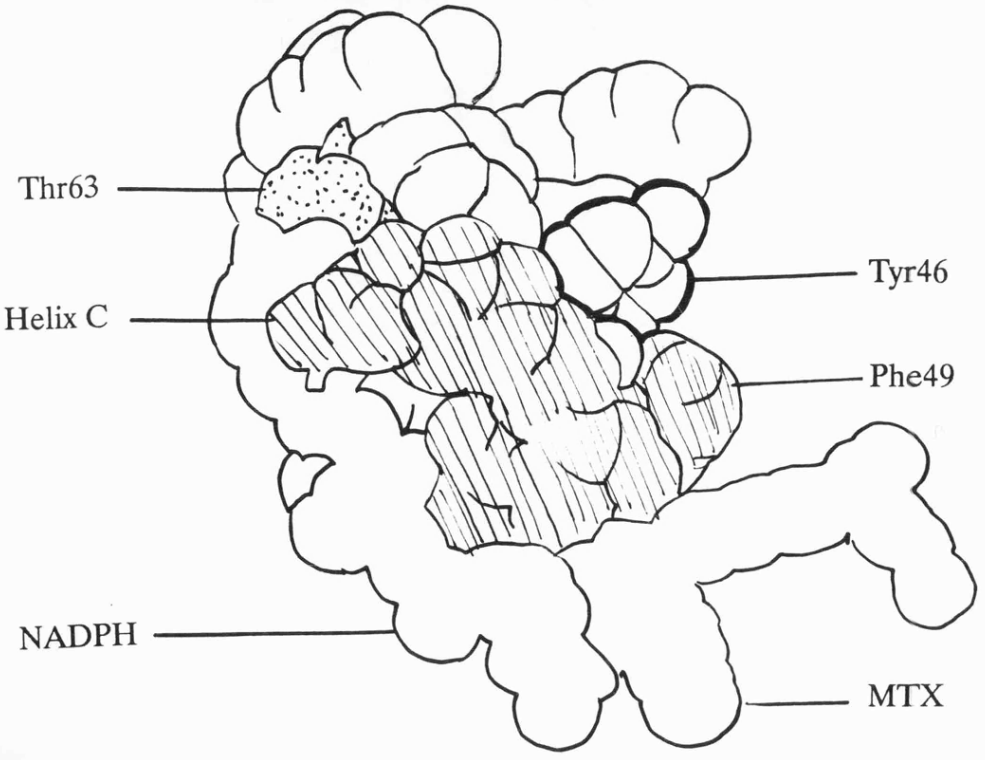

4.4.3. T63A

The T63Q mutation produced intriguing results but did not provide any clues as to the importance of the hydrogen bond to coenzyme specificity. The mutation T63A, a subtractive mutation, was made to determine if the affects seen in the T63Q enzyme were due to the presence of the larger glutamine residue and whether the hydrogen bond is important to NADPH specificity.

The T63A results were similar to T63Q in that the changes in the spectra were small and restricted to protons in a relatively few residues. In contrast to T63Q the spectral changes seen were from residues around the mutation.

Proton chemical shifts in a larger number of residues were affected by the mutation in the binary complex compared to the ternary, and the residues which were affected in both complexes had different changes in chemical shift in each complex, apart from Tyr46. All the protons of the Val61 side chain had different chemical shifts compared to the wild type in the binary complex whereas only one $C\gamma H_3$ (at -3.32ppm) had a chemical shift change in the ternary complex. In Leu62 the two $C\delta H_3$s were at a different chemical shifts in the binary complex, whereas it was the CγH that had a different chemical shift in the ternary complex. Only one $C\gamma H_3$ of Val75 had a chemical shift change in the binary complex whereas in the ternary complex both $C\gamma H_3$s did. The side chain protons in residues Leu54, Ile96, Phe106 and Phe49 showed some proton chemical shift differences in the binary complex compared to wild type but none in the ternary complex. Val76 is not assigned in the ternary complex so could not be compared with the binary complex.

It appears from this data that the mutation affects the protein structure to a greater extent in the binary MTX complex and the binding of NADPH to form the ternary complex helps to maintain the enzyme structure in a manner more similar to the wild type. In addition to analysis of proton chemical shifts of the protein, the chemical shifts of the adenine protons of NADPH were found to be different from wild type, suggesting the binding of NADPH may be different.

To determine what structural affects were causing the chemical shift changes, the NOESY data were analysed. The residues that have resonances with chemical shift differences all lie in one region of the protein around the site of mutation, and in the binary MTX complex this region extends to two residues at the MTX binding site (Phe49 and Leu54). A network of NOE's is seen between these residues, those NOEs which are sufficiently well resolved to be compared in both the mutant and wild type binary MTX, and/or ternary NADPH/MTX spectra include those between Tyr68-Val61-Tyr46-Phe49-

Leu54 and these are discussed below. The NOEs of the other residues with chemical shift changes were not resolved well enough in one or both of the enzymes to be compared.

The NOEs between the side chain protons of Val61 and Tyr68 were the same as wild type in the binary complex, despite the chemical shift differences of Val61 (although next to the site of mutation, the chemical shift of Tyr68 is not affected in the binary complex), but could not be compared in the ternary complex. This means the relative positions of these two residues, at least in the binary MTX complex, are not altered and the chemical shift must be affected by some other structural affect. The NOE between Tyr46 and Val61 is the same intensity as wild type in both complexes, thus the change of their chemical shifts is not because of a movement of these residues relative to each other. The NOESY cross peak between Phe49 and Tyr46 (the chemical shift of resonances from Phe49 were not affected in the ternary complex) was the same intensity as wild type again, therefore the chemical shift changes of protons in these two residues are not because of a movement relative to each other. Since Phe49 and Val61 are the two nearest neighbours to Tyr46 and the NOEs between them have not changed, it appears Tyr46 has not altered its position relative to the structure in the wild type enzyme. The NOE's between the proton resonances between the Phe49 aromatic ring and Leu54 (the chemical shifts of protons from these residues were not affected in the ternary complex) are the same as wild type and these residues have not moved relative to each other.

Phe49 and Leu54 protons had chemical shift differences in the binary MTX complex. Since these residues are at the MTX binding site the chemical shifts and NOESY cross peaks of protons from other residues around this site were carefully studied and were found to be the same as wild type (unlike the T63Q spectra) including the pteridine H7 of MTX and many other residues. It is likely that the chemical shift changes of the resonances from these two residues are caused by structural changes at a site distant from the MTX binding site.

The mutation has caused resonances to have altered chemical shifts and so there must be some structural alteration in the protein. The resonances that have been compared are resolved from the rest of the resonances in the spectrum in order to be assigned and for comparison of their NOE's. The reason they are resolved is because the resonances have unusual chemical shifts due to their local environment (e.g. caused by ring current affects when close to an aromatic ring). This means that the shift of these resonances is going to be very sensitive to any small changes in the structure of the enzyme. Therefore, although a number of residues had proton resonances affected by the mutation this does not necessarily mean that there is a large change in structure. Analysis of the NOESY spectra of the binary MTX complex has not elucidated what the structural alteration is in this complex and therefore must be at residues in this region of the protein which have no

resonances assigned to them, e.g. residues Arg43, Glu47, and Arg52. It is notable that Arg43 was also the residue hypothesized to have moved in the T63Q mutant aswell.

For the binary MTX complex it is apparent that the structural alterations causing the chemical shift changes in the T63A mutant must be small and appear not to include Phe49, Tyr46, Phe106 and Leu54, even though they have small chemical shift changes of their proton resonances, since the measured NOEs of these residues are the same as wild type. The structural modification that has occurred to the protein could not be determined since none of the assigned, resolved NOESY cross peaks were different from wild type.

Aswell as the above analysis of the protein structure, in the ternary NADPH/MTX complex the interaction of the protein with the coenzyme can be studied to elucidate structural affects. Focusing on the adenine end of NADPH in the ternary complex revealed some interesting observations. The NOEs between the adenine protons A2, with Leu62, and A8, with Ile102, are all smaller by approximately 50%. Thus the mutation has affected the binding of NADPH, the adenine moiety being more distant from Ile102 and Leu62 compared to the wild type enzyme. Leu62 is also close to Phe106 and the NOEs between Leu62 and Phe106 were compared and found to be the same as wild type. Thus the relative positions of Leu62 and Phe106 are the same as wild type but the relative positions of Leu62 and adenine A2 are further apart. This suggests that the protein structure is the same at Leu62 but the adenine is not able to bind as close because of some structural changes in the protein at some other, as yet unidentified residues.

In the ternary MTX/NADPH complex the phosphorus nmr spectra showed the 2' phosphate of NADPH had a different chemical shift in the complex with T63A than in the wild type, evidence to support the other results that the binding of the adenosine portion of the coenzyme is different. The reason for the change in chemical shift is not clear. One possible cause could be due to a different ionisation state of the 2' phosphate. Previous ^{31}P nmr studies (Feeney *et al.*, 1975) have shown that the pK of the 2' phosphate of NADPH is decreased by more than 3 pH units on binding, and its resonance experiences a large downfield shift. The inference drawn was that NADPH is in the dianionic ionisation state when bound to the enzyme. Other ^{31}P nmr studies (Birdsall *et al.*, 1977b) have shown that binding of adenosine 2' phosphate (a "fragment" of NADPH) is 16 fold weaker in the monoanionic state compared to the dianionic ionisation state. The mutation T63A decreases the binding constant of NADPH to the apoenzyme some 600 fold (see the Kinetics chapter), thus it is feasible that a different ionisation state of the coenzyme may be contributing to the change in chemical shift and the weaker binding. However, an additional change is required to explain the very large affect on the binding constant. To see if a change in ionisation state had occurred, a ^{31}P nmr spectrum was obtained at pH 6 (rather than pH6.5) but no difference in the position of the 2' phosphate was seen. Since it

appears the pK is still pH independent this result argues strongly against there being a large enough change in the pK to affect the shift at pH 6.5. Due to the shortage of mutant enzyme, and its relative instability, a more complete pH titration was not carried out.

The chemical shift of the 2'phosphate however does not depend solely on the ionisation state. The chemical shift of the 2' phosphate of bound 2' AMP is lower than that of bound NADPH so other factors must be involved in binding the NADPH to achieve this extra shift, and probably also contribute to the better binding of the NADPH compared to 2' AMP. The chemical shift change of the 2' phosphate in the T63A mutant may be due to a change in any of these factors. Since the parameters contributing to the extra chemical shift are not defined it is not possible to determine what may have changed in the mutant around the 2' phosphate binding site. The extra shift may be due to a combination of changes, such as the magnetic and electrostatic environment, the O-P-O bond angle, and the bond angles of hydrogen bonds of the 2' phosphate with the residues in the protein.

To summarise the ternary T63A/MTX/NADPH complex, the only assigned and resolved NOESY cross peaks that had a different size compared to wild type were those between the protein and the adenine moiety of NADPH. No changes of the protein structure were found despite chemical shift changes in residues around the mutation. Thus it appears the structure is very similar to wild type and the changes in the protein which cause the different binding of NADPH are not known, except they are probably around the mutation. It may be suggested that the only difference in the mutant compared to wild type is the loss of the hydrogen bond between the 2' phosphate and Thr63 with no other conformational affect. However, there is likely to be some structural change in the protein in order to cause the number of changes of proton chemical shifts. In addition the rate of association of NADPH to the mutant enzyme was found to be 50 times slower than for the wild type enzyme (see the kinetics chapter) suggesting that there is some steric hindrance not present in the wild type enzyme. Obviously there has to be some structural difference to produce this affect.

Comparing the structures of T63Q and T63A it appears the two mutations cause quite different affects, despite being at the same residue. The T63Q does not affect the coenzyme binding site whereas T63A does, and vice versa for the MTX binding site. However the structural differences of both mutants, compared to the wild type, are very small and specific to a relatively few residues. From these studies the results suggest that the protein structure is difficult to perturb to any great extent, whether a "sensible" subtractive mutation (T63A) or a more gross mutation (T63Q) is used. As will be seen in the next chapter these innocuous, minor changes can cause relatively dramatic changes in function.

5. KINETIC CHARACTERISATION OF MUTANT DHFR'S

5.1. INTRODUCTION

5.1.1. Equilibrium Binding Constant Determination

For each mutant and wild type DHFR, the equilibrium binding constants of the substrates and selected other ligands were measured. The information obtained then correlated with the structural information, gleaned from the nmr studies, to provide hypotheses regarding the structural origins of changes in the enzyme's affinity for different ligands.

Fluorescence spectroscopy is widely used to measure protein ligand interactions. Proteins contain the fluorophores tyrosine and tryptophan, the latter generally contributing the most fluorescence. The measurement of tryptophan fluorescence is often used in protein binding studies, for example for DHFR the binding constants of many ligands have been determined by measuring the quenching of tryptophan fluorescence upon ligand binding. Alternatively, the fluorescence of the ligand itself may be used to measure binding constants. For example the binding of the coenzyme analogue $\varepsilon NADP^+$ to DHFR was measured by following the enhancement of its fluorescence upon binding to the protein (Birdsall *et al.*, 1980a, 1980b).

A major problem in using fluorescence to measure ligand binding is the inner filter effect, where absorption of the excitation light by the added ligand causes a reduction in the amount of fluorescence emitted; this purely optical affect interferes with the measurement of changes in fluorescence due to ligand binding. Substantial errors in the determination of binding constants can be introduced by the inner filter effect but these can be corrected for by using empirically determined correction factors (Birdsall *et al.*, 1983). When measuring the quenching of protein fluorescence upon addition of the ligand, the correction factors are obtained from a titration of tryptophan with the ligand. Tryptophan was used in the DHFR experiments because it fluoresces at the same wavelength used in the ligand binding experiments yet does not associate with the ligands at the concentrations used. The major disadvantage of tryptophan is its photochemical lability so if necessary, use of an alternative such as *N*-(*p*-aminobenzoyl)-L-glutamate has been reported. The data from the titration is fitted by non-linear regression using the equations described in the Methods section to calculate the correction factors applied to the binding data.

When measuring the enhancement of ligand fluorescence upon binding to the enzyme the fluorescence of the ligand alone can be measured, which increases linearly with concentration in the absence of the inner filter effect. Deviation from linearity due to the inner filter effect can be analysed by fitting the data to equation 5.1 (Birdsall *et al.*, 1983) using non-linear regression analysis to obtain the correction factors.

$$F_{obs} = (F_{corr} + F_{blank})\{\exp(-aL_Td) - \exp(-aL_T)/aL_T(1 - d)\} \qquad \text{Eq. 5.1.}$$

Where F_{obs} is the observed fluorescence, F_{blank} is the background fluorescence, F_{corr} is the true fluorescence, L_T is the ligand concentration, a and d are the correction factors.

a and d are then used to calculate C in equation 5.2. for each ligand concentration. The data from the titration of the protein with ligand is multiplied by C to calculate the fluorescence corrected for the inner filter effect. The data can then be used to find the ligand binding constant after subtraction of the ligand fluorescence in the absence of protein.

$$C = \exp(-aL_Td) - \exp(-aL_T) / aL_T(1 - d) \qquad \text{Eq. 5.2.}$$

5.1.2. Steady State Kinetics

In the absence of a complete kinetic analysis using transient kinetics, steady state kinetic parameters can be measured to provide information regarding the affect of the mutations on catalysis. In the same way as the binding experiments, the kinetic data can be compared with the structural information, obtained by the nmr studies, to find what structural affects are causing the kinetic changes.

The k_{cat} of DHFR can be determined by following the rate of NADPH oxidation and FH_2 reduction by measuring the change in absorbance at 340nm. k_{cat} of DHFR varies with pH (Andrews *et al.*, 1989), so to determine the maximum k_{cat} of the reaction, assays are carried out at a range of pH values, otherwise, if the apparent pK_a changes, the k_{cat} will appear to be different rather than simply at a different pH optimum.

The K_M is defined as the substrate concentration at which the rate of reaction is half the rate achieved at saturating ligand concentrations (k_{cat}). In simple single substrate reactions K_M can often be interpreted as an apparent K_d (see Fersht, 1985). However, for DHFR, the K_M of NADPH is less than the dissociation constant because the reaction

proceeds via multiple steps (Andrews *et al.*, 1989), shown in figure 5.1. The preferred reaction pathway is;

1. FH_2 binds to the enzyme-coenzyme complex
2. the reaction occurs to form $NADP^+$ and FH_4
3. $NADP^+$ dissociates from the enzyme
4. NADPH binds to the enzyme-FH_4 complex
5. tetrahydrofolate product is then released to leave NADPH bound, ready for another cycle.

The dissociation constant of the second molecule of NADPH is almost 90 times greater than that for binding to the free enzyme. Therefore the binding of the second molecule will provide a large contribution to the K_M and comparison of the K_M's for NADPH can provide an indication of its affinity to the enzyme-product complex.

Figure 5.1. Kinetic scheme for <u>L. casei</u> DHFR in KMB buffer, pH 6.5, 25°C.

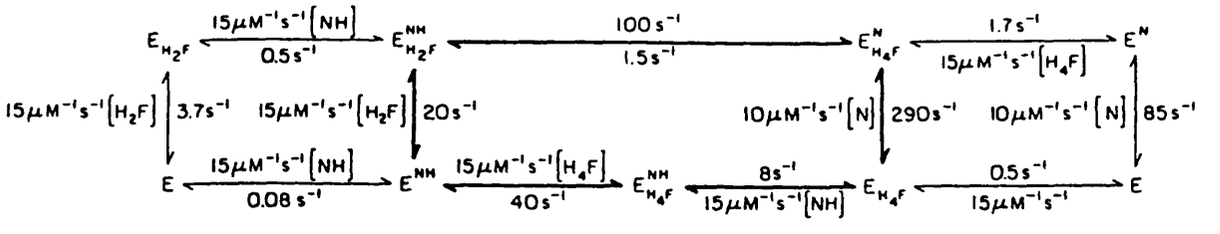

The heavy arrows indicate the preferred kinetic pathway for steady state turnover at saturating substrate conditions. N, $NADP^+$; NH, NADPH. (From Andrews *et al.*, 1989)

Steady state kinetics can also help to identify the rate limiting step. In DHFR there are two major contributions to the rate limiting step, which makes the major limiting contribution depends on pH. The steps are

1. the rate of product release (which is assumed to be pH independent)

2. the rate of hydride ion transfer (pH dependent).

The major rate limiting step at low pH is product release, but the rate of hydride ion transfer decreases as the pH is increased until it is almost completely rate limiting at high pH. The hydrogen of NADPH is transferred to a reaction intermediate during catalysis and at low pH this transfer is relatively fast so that the dissociation of FH_4 is limiting rate. At higher pH the hydrogen transfer (in fact as an hydride ion) is slow and becomes rate limiting.

The contribution of hydride ion transfer to the rate limiting step can be determined by performing deuterium isotope effect experiments. A primary kinetic isotope effect is observed when a rate of reaction is made slower because of a substitution by, for example, a deuterium atom for a hydrogen atom in the substrate, provided the substituted hydrogen is involved in the rate limiting step. The kinetic isotope effect is defined by Cleland (1987) as "the ratio of reaction rates for molecules containing light and heavy isotopes such as k_H/k_D". In DHFR the effect is seen when NADPD is used as coenzyme rather than NADPH. More energy is required to break the C-D bond (zero point energy is 12.5 kJ/mol) than the C-H bond (zero point energy is 17.4 kJ/mol) so, because this step is at least partly rate limiting, the reaction rate is slower when using NADPD as coenzyme. Comparison of the isotope effect can indicate whether hydride ion transfer is rate limiting and if so, whether the mutations have affected the ratios of the rate limiting steps.

5.1.3. Summary of Experiments Performed

T63Q, T63A and wild type DHFR were characterised by a combination of binding, steady state and transient kinetic experiments. The kinetic scheme in figure 5.1 was determined by transient kinetics using a stopped flow fluorimeter (from Andrews *et al.*, 1989). A suitable instrument was not available during the work described here, except for one day on a visit to Applied Photophysics. A complete kinetic analysis was not possible because of the lack of a suitable stopped flow fluorimeter. It was decided the minimum number of experiments should be to determine;

1) the equilibrium binding constants of substrate and coenzyme, to find if the mutations had affected the binding of coenzyme and/or substrate,

2) the steady state kinetic parameters K_M, and k_{cat} and the deuterium isotope effect over a range of pH values.

Other experiments were carried out where possible.

5.2. METHODS

All the assays were carried out at 25°C unless otherwise stated. All experiments on the mutants were repeated with the wild type enzyme in order to compare the data directly rather than using published wild type data (which may not provide a true comparison because of slight differences in experimental method and conditions).

5.2.1. Solutions

NADPH, and NADH are more stable at high pH and so were dissolved in 20mM Tris-HCl, pH 8.5, other ligands were dissolved in KMB buffer (see below) pH 7.0. The concentration of the ligands were calculated spectrophotometrically using the following extinction coefficients; FH_2, 28000 M^{-1} cm^{-1} at 282nm, pH 7.0; NADPH, 6200 M^{-1} cm^{-1} at 339nm, pH 7.5; $NADP^+$, 18000 M^{-1} cm^{-1} at 259nm, pH7.0; NAD^+, 18000 M^{-1} cm^{-1} at 260nm, pH7.0; NADH, 6220 M^{-1} cm^{-1} at 339nm at pH7.5 (all the above from Dawson *et al.*, 1986); MTX, 22100 M^{-1} cm^{-1} at 302nm in 0.1M KOH (Seeger *et al.*, 1949); TMP, 6060 M^{-1} cm^{-1} at 271nm in 0.1M acetic acid (Roth and Strelitz, 1969).

KMB buffer:	MES	50mM
	Tris-HCl	25mM
	KCl	500mM
	Ethanolamine	25mM

MES = 4-morpholineethane sulphonic acid

5.2.2. Determination of DHFR Concentration

The enzyme concentration was estimated by measuring its absorbance at 280nm (ε = 27000 M^{-1} cm^{-1} at 280.5nm, Dann *et al.*, 1976). The extinction coefficients for the T63A and T63Q mutants were determined and found to be the same as that of the wild type enzyme.

For an accurate determination of enzyme concentration a MTX titration was used. MTX binds very tightly (K_d is less than $10^{-9}M^{-1}$) and thus stoichiometrically to the enzyme. The concentration of DHFR could be found by titration of MTX, which quenches the protein fluorescence when bound, provided the binding constant of MTX is not significantly reduced by the mutation.

3ml of 0.2-2μM enzyme in 15mM Tris-HCl, 500mM KCl pH 7.5 was titrated with μl additions of appropriately diluted MTX solution. The quench of protein fluorescence was measured using an excitation wavelength of 290nm and an emission wavelength of 340 to 360nm. MTX was added until no further quench occurred.

The data were plotted as a graph of fluorescence against methotrexate concentration; the intersection of the two straight lines gives the concentration of DHFR in the cuvette (graph 5.1).

Graph 5.1. Determination of DHFR concentration by titration with methotrexate.

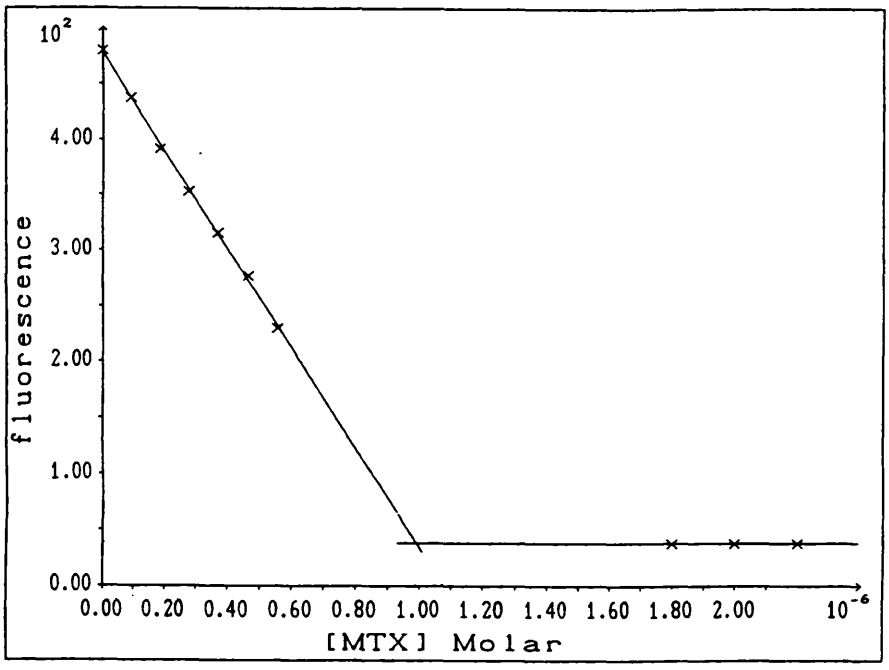

5.2.3. Equilibrium Binding Constant Determination

The equilibrium binding constants of several ligands were measured fluorimetrically by titrating with μl volumes of ligand solution. A Perkin-Elmer LS-5 Luminescence Spectrometer was used with 1cm pathlength cells at 25°C, the buffer was KMB and the enzyme concentration was approximately half the binding constant. 1% lactose was included in the buffer to prevent the enzyme adsorbing to the cuvette. The quenching of protein fluorescence upon ligand binding was measured (Birdsall *et al.*, 1980a,b 1978, Dunn *et al.*, 1978). To correct for absorption of the excitation light by the ligand, a tryptophan solution was titrated using the same slit widths and wavelengths as used for the

protein titration. A curve was fitted to the tryptophan titration data (after correcting for dilution) using equation 5.3 programmed into the Enzfitter software package (Leatherbarrow, 1987) in order to find correction factors a, and d, (Birdsall *et al.*, 1983).

$$F_{obs} = F(\exp(-aL_Td) - \exp(-aL_T) / aL_T(1-d)) \qquad \text{Eq. 5.3.}$$

where F_{obs} is the measured fluorescence, F is the initial fluorescence, and L_T is the ligand concentration.

a and d were used in equation 5.4 to calculate C for each ligand concentration.

$$C = \exp(-aL_Td) - \exp(-aL_T) / aL_T(1-d) \qquad \text{Eq. 5.4.}$$

The true enzyme fluorescence was then calculated from the observed fluorescence data (after correcting for dilution) by multiplying by the correction factor C. This calculated "true" fluorescence data was then used to find the equilibrium binding constant of the ligand by fitting the data using equation 5.5 to the data.

$$F = F_eE_T + (F_c-F_e)\,(\,X- [X^2-E_TL_T]^{1/2}\,) \qquad \text{Eq. 5.5.}$$

where $X = (L_T+E_T+K_d) / 2$, F is the corrected observed fluorescence, F_e is the fluorescence of free enzyme, E_T is the enzyme concentration, F_c is the fluorescence of the complex, L_T is the ligand concentration and K_d is the equilibrium dissociation constant.

The K_d of TMP was determined for each of the mutant and wild type DHFR's at pH 6, 6.5, 7, and 7.5 to ascertain if ligand binding was pH dependent.

5.2.4. Enzymatic Reduction of $NADP^+$ to NADPH and NADPD

To obtain normal and deuterated coenzymes, $NADP^+$ was reduced by $NADP^+$ dependent alcohol dehydrogenase (ADH) (Stone and Morrison, 1982) and NAD^+ was reduced using NAD^+ dependent ADH. Both reactions were carried out by mixing the following;

50-100mg oxidised coenzyme
8ml 20mM triethanolamine, pH 9
1ml ethanol
20-40 units ADH

The pH was brought up to pH 9 by addition of Tris-HCl. The solution was kept dark and occasionally swirled until there was no further increase in absorbance at 340nm (approximately 2 hours).

To make NADPD, d_6-ethanol was used.

The solution was stored at -80°C until required, the coenzyme was purified just before use since it could be stored pure at -80°C only for one week before a breakdown product, which acted as a potent inhibitor of DHFR, became detectable.

5.2.5. NADPH Purification

When stored in frozen solution or as a lyophilised powder NADPH produces an inhibitor, as yet not characterised, which binds tightly to DHFR (Fawcett *et al.*, 1961). This inhibitor is a decomposition product, so NADPH was purified just before required to achieve accurate kinetic measurements. NADPH made as above, and that bought from Sigma, were purified by FPLC (Orr and Blanchard, 1984).

A MonoQ 5/5 column was used to determine the purification conditions, but for larger scale purification (approximately 20mg NADPH per loading), a MonoQ 10/10 column was used. A salt gradient was made with 20mM triethanolamine (TEA), pH 9, with and without 1M KCl (buffer B and A respectively), the pH of the buffer was adjusted by bubbling CO_2 through the solution. The FPLC was programmed so that the MonoQ column was first washed with 2ml buffer A (0% buffer B), then a gradient was started from 10% buffer B to 20% buffer B over 20ml, during which time the NADPH was separated from impurities and $NADP^+$. The column was washed with 100% buffer B for 5ml and re-equilibrated with buffer A for a further 2ml.

1ml fractions were collected and the absorbance at 260 and 280nm was taken. If the ratio of the A_{260}:A_{280} was <2.3 the NADPH was deemed pure and these fractions were pooled.

5.2.6. Steady State Kinetics

When the activity assay was used to follow the purification, a buffer of 50mM KH_2PO_4, 500mM KCl, pH 6.5 was used. When the assay was used for kinetic measurements the buffer used was KMB because this can buffer between pH 5 and 9, eliminating the need to change buffers for assays at different pH values.

The substrate concentrations in the assay were 50μM NADPH and 50μM FH_2 unless otherwise stated.

> 500μl of double concentration buffer was pipetted into the cuvette and made up with water to the required volume so that the total assay volume was 1ml. The buffer was prewarmed in the cuvette to 25°C. NADPH and the enzyme were then added and allowed to equilibrate for a few minutes to form the active conformation of the complex to eliminate hysteresis (Baccanari and Joyner, 1981) and to equilibrate to 25°C. The assay was initiated by the addition of FH_2 with inversion of the cuvette to mix the solution.

The rate of reduction was measured on a Philips PU 8820 UV/VIS spectrophotometer by measuring the change in absorbance at 340nm. NADPH absorbs at this wavelength whereas $NADP^+$ does not, with some additional contribution to the absorbance change from the reduction of FH_2 thus the decrease in absorbance is proportional to number of moles NADPH oxidised, the reaction having a difference extinction coeffient of 11800 M^{-1} cm^{-1} (Stone and Morrison, 1982).

Each mutant and wild type enzyme was assayed at a range of pH values.

> A double concentration buffer was made up at a range of pH values between pH5 and 9. The assay was carried out as above and when completed the pH was measured.
>
> To check whether the enzyme was denaturing at the extremes of pH and therefore giving reduced rates, the enzyme-NADPH solutions were left to equilibrate for varying lengths of time. If the enzyme was denaturing, the activity would be expected to be lower after longer periods of incubation. The results showed there was no detectable denaturation.

NADPH oxidises at a measurable rate at low pH, so the rate of this oxidation was also measured and, where necessary allowance was made in the activity calculation.

The data obtained were fitted to equation 5.6 to find the apparent pK of the reaction.

$$Y = (lim1 + lim2 \times 2.303exp(-pH + pK_a)) / (2.303exp(-pH + pK_a) + 1) \qquad \text{Eq. 5.6.}$$

where $Y=k_{cat}$ at a particular pH value, lim1 is the low pH rate, lim2 is the high pH rate and pK_a is -log of the acid dissociation constant.

The K_M for NADPH of wild type and T63Q DHFR was determined using a fluorimetric assay. The K_M for both substrates binding to wild type DHFR is sub-micromolar so the spectrophotometric assay cannot be used (it is not sensitive enough to detect absorbance at these low concentrations). Fluorescence however has been used successfully to follow the reaction by measuring the decrease in fluorescence with oxidation of coenzyme (Dann *et al.*, 1976). The assay was carried out on a Perkin-Elmer LS-5 Luminescence Spectrometer with an excitation wavelength of 360nm and an emission wavelength of 450nm; the assay buffer was KMB, pH 6 containing 1% lactose. The concentration of FH_2 was maintained at 10μM and the concentration of NADPH was varied. Instability of FH_2 was found to cause errors in the measurements due to the low substrate concentrations used and the sensitivity of the fluorimeter. The rate of decomposition of FH_2 was measured and subtracted from the gradients obtained in the assays. To reduce the errors, at least six measurements for each NADPH concentration were taken and averaged.

The K_M of NADPH for T63A DHFR was measured using the spectrophotometric assay, because the K_M was found to be orders of magnitude higher than for the other enzymes. The concentrations of NADPH used were too high to be measured at 340nm due to the lack of transmitted light, so the assay was recorded at 360, 370 and 380nm, depending on the NADPH concentration. The rates were then calculated using the appropriate extinction coefficient for the wavelength used. The concentration of FH_2 was maintained at 100μM in order to provide sufficient change in absorbance at the higher wavelengths, where the extinction coefficients for the reaction are low (ε_{360} = 6140 M^{-1} cm^{-1}, ε_{370} = 3190 M^{-1} cm^{-1}, ε_{380} = 1180 M^{-1} cm^{-1}).

5.2.7. Kinetic Isotope Effect

Values for k_{cat} using NADPD as the coenzyme were determined at a range of pH values and the kinetic isotope effect was calculated (k_{cat} NADPH / k_{cat} NADPD) for each pH value (Cleland, 1987).

5.2.8. Determination of NADPH Association Rate Constant

The rate of association of NADPH was found for the wild type and T63A mutant DHFRs using a stopped flow spectrometer from Applied Photophysics (model SF.17 MV) by following the rate of decrease of fluorescence. The excitation wavelength was 290nm and fluorescence was measured using a 340nm filter. The buffer was KMB, pH6.5 (see above), the enzyme concentration was 0.2μM and the rate of association was measured at 4 concentrations of NADPH. The data was analysed using an iterative nonlinear regression package supplied by Applied Photophysics. The average of at least 3 runs was used for data analysis of each ligand concentration.

5.3. RESULTS

5.3.1. Equilibrium Binding Constants

Table 5.1 shows the equilibrium dissociation constants for ligands bound to the enzyme in binary and ternary complexes. For T63Q, T63A and wild type, the dissociation constant of methotrexate was too low to measure. Only the binding of NADPH to T63A was affected to a large extent, with a 600 fold increase in K_d. The binding of $NADP^+$ to T63Q may have changed three fold but this change is only just outside the experimental error. The binding of $NADP^+$ to form the ternary complex with MTX however is the same as wild type. The implication of this observation is that if the three fold change in $NADP^+$ binding to the apoenzyme is considered significant, then the cooperativity between the binding of the two ligands (Birdsall *et al.*, 1978) has been increased by the mutation. The binding of NADPH to T63Q was the same as wild type and the binding of TMP and the substrate FH_2 to T63Q and T63A was the same as wild type.

Table 5.1. Equilibrium dissociation constants of ligands binding to the enzyme (E) or enzyme/MTX complex (E.MTX).

Ligand	Enzyme species	K_d (μM)		
		WT	T63Q	T63A
NADPH	E	0.01±.003	0.01±.003	6.0±.2
$NADP^+$	E	15±4	49±5	nd
TMP	E	0.2±.03	0.4±.04	0.3±.03
FH_2	E	0.22±.02	0.32±.02	0.50±.02
ε$NADP^+$	E	17±1	59±1	nd
ε$NADP^+$	E.MTX	2.8±.1	2.6±.1	nd

nd = not determined

The K_d of TMP was measured at pH 6, 6.5, 7, and 7.5 and all gave a K_d between 0.2 to 0.5 μM for each enzyme, i.e. there was no clear cut pH effect on TMP binding for the wild type or mutant DHFRs.

From the equilibrium binding constants, ΔG^o (the Gibbs free energy of binding, equation 5.7) can be calculated. For the binding of NADPH to T63A ΔG^o is 7.1 Kcal/mol,

and for wild type and T63Q it is 10.9 Kcal/mol, thus a change in ΔG^o of -3.8 Kcal/mol is caused by the T63A mutation.

$$\Delta G^o = -RT \ln K_d \qquad \text{eq. 5.7.}$$

5.3.2. Steady State Kinetic Parameters

The K_M for NADPH of T63Q was the same as wild type at 1μM (±0.5μM). The K_M for NADPH of T63A however had been dramatically affected and was 0.8mM (±0.09mM, graph 5.2), almost 100 fold higher than wild type. The mutation T63A had affected the affinity of the enzyme for NADPH. k_{cat} for all three of the enzymes were similar where wild type = 26 ±4 s^{-1}, T63Q, 24 ±4 s^{-1}, T63A = 19 ±1 s^{-1}, thus neither mutation had significantly altered the catalytic rate.

Table 5.2. The K_M for NADPH and k_{cat} of each mutant and wild type enzymes.

Enzyme	K_M μM	k_{cat} s^{-1}
wild type	1 ±0.5	26 ±4
T63Q	1 ±0.5	24 ±4
T63A	800 ±90	19 ±1

Values for k_{cat} were measured for each mutant and the wild type enzyme over a range of pH's between pH 5 and 8.5 (graph 5.3). It was found for T63Q that although the k_{cat} is not affected by the mutation, the apparent pK describing the pH dependence of k_{cat} is altered. The apparent pK_a of T63Q was pH 7.0 compared with pH 7.5 for wild type, i.e. the pKa of T63Q was 0.5 pH units lower than wild type.

The measured k_{cat} for T63A was ten fold lower than wild type, but since the K_M for NADPH is almost 1mM the coenzyme was not at saturating concentration and thus was limiting the rate of reaction. The experiments to find the kinetic isotope effect could not be performed since the highest concentrations of coenzyme that could be used still would not saturate the enzyme and accurate k_{cat} values could not be obtained. The coenzyme would have to be at least 10mM to reach saturating concentration and the absorbance would be

much too high to measure even using higher wavelengths where the extinction coefficient is comparatively low.

To determine the deuterium isotope affect, the values of k_{cat} at a range of pH values were measured for NADPD and the ratio with k_{cat} of NADPH was calculated. The apparent pK_a of the isotope effect for wild type DHFR was pH 7.3 and for T63Q it was pH 6.8 (graph 5.4), a difference of 0.5 pH units. This suggests that the pK of a residue involved in catalysis has been altered by the mutation, despite the mutation being some distance from the catalytic site.

5.3.3. NADPH Association Rate Constant

For a simple association reaction, the observed rate constant under pseudo first order conditions may be approximated by $k_{observed} = k_{on}NADPH + k_{off}$ (k_{on} is the association rate constant and k_{off} is the dissociation rate constant). Thus in a linear plot of k_{obsd} vs NADPH concentration, the gradient is k_{on} and the intercept is k_{off}. In this way the rate of NADPH association to wild type was found to be 2×10^7 $M^{-1}s^{-1}$ (graph 5.5) and to T63A was 4×10^5 $M^{-1}s^{-1}$ (graph 5.6). The rate of dissociation of NADPH was too slow to be measured from this experiment so it was calculated using the relationship between the ratio of k_{off}/k_{on} and the equilibrium binding constant K_d. Free DHFR in solution adopts more than one conformation but NADPH binds only to one, approximated in the scheme below. The equilibrium constant (K_{eq}) between the conformation to which NADPH can bind and the conformations to which it cannot bind is 1 at pH 6.5 (Dunn *et al.*, 1978), consequently the measured K_d should be 2 fold larger than the ratio of k_{off}/k_{on}, equation 5.8.

$$E_2 \underset{k_{-2}}{\overset{k_2}{\rightleftharpoons}} E_1 + L_1 \underset{k_{off}}{\overset{k_{on}}{\rightleftharpoons}} E_1 \cdot L_1 + L_2 \underset{k_{off'}}{\overset{k_{on'}}{\rightleftharpoons}} E_1 \cdot L_1 \cdot L_2$$

$$K_d = (k_{off}/k_{on})[(K_{eq} + 1) / K_{eq}] \qquad \text{eq. 5.8}$$

From this equation the rate of NADPH dissociation for wild type was found to be 0.1 s^{-1} (in agreement with Andrews *et al.*, 1989) and for T63A was found to be 1.2 s^{-1}. Therefore, for T63A the rate of association of NADPH was 50 times slower and the rate of dissociation was 12 times faster than that of wild type.

Graph 5.2. Observed rate as a function of NADPH concentration for T63A, measured in KMB buffer pH 6.5 with 100μM FH_2.

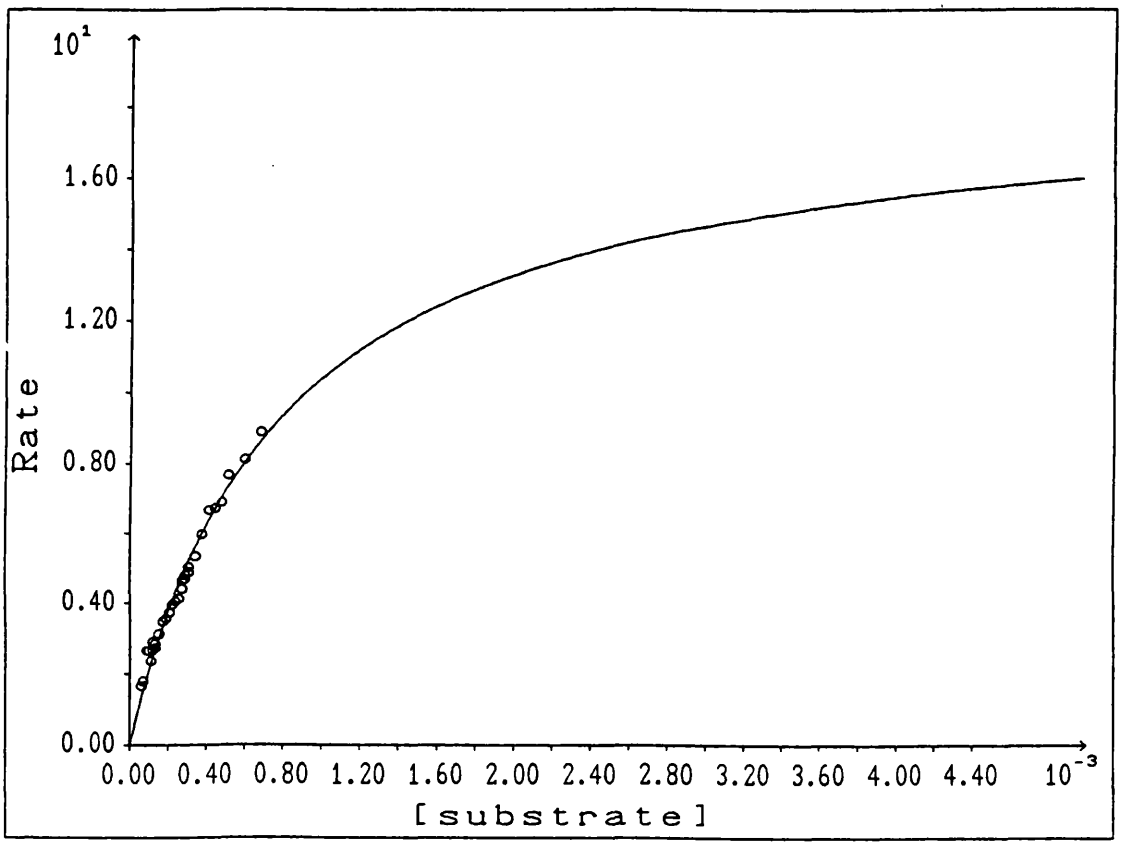

Graph 5.3. Variation of k_{cat} with pH for wild type (WT) and T63Q, measured in KMB buffer with 50μM NADPH and 50μM FH_2.

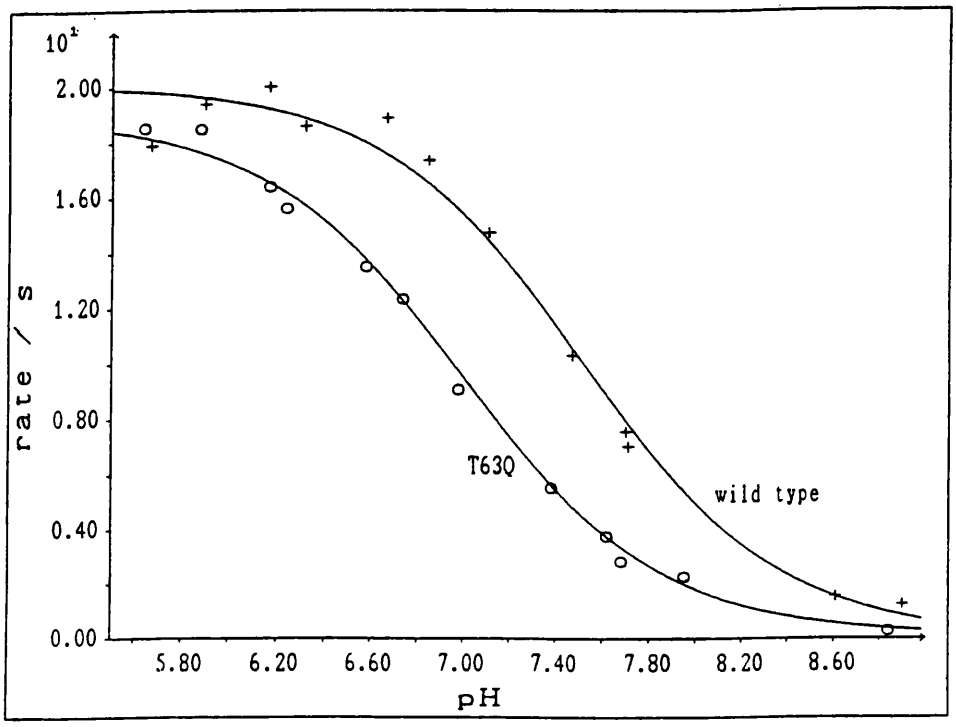

Graph 5.4. Variation of the deuterium isotope affect with pH for wild type and T63Q, measured in KMB buffer with 50μM NADPH or NADPD and 50μM FH_2.

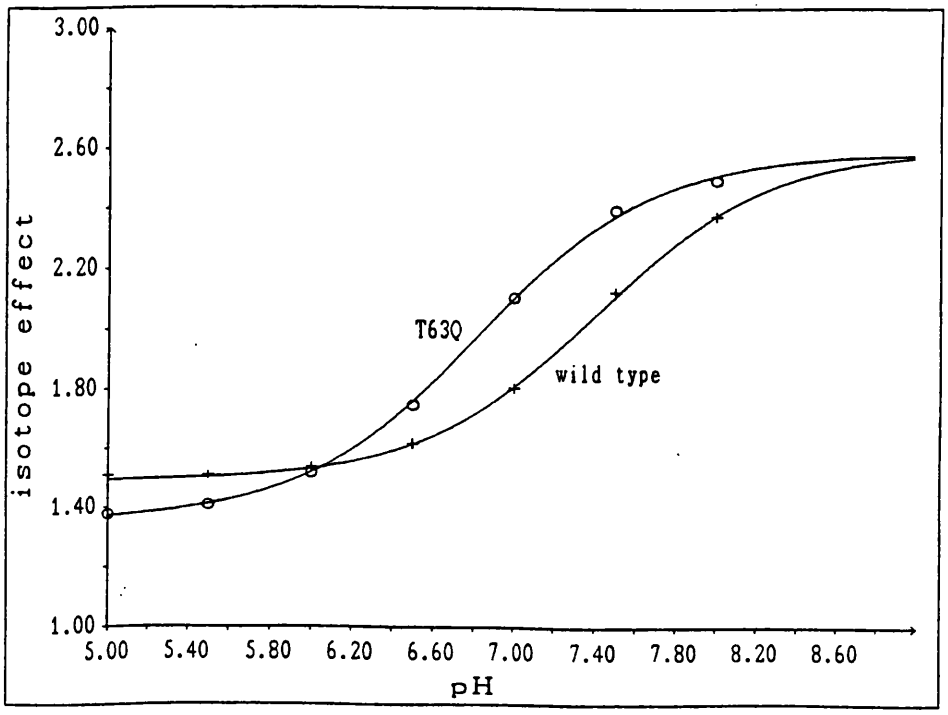

Graph 5.5. Observed association rate as a function of NADPH concentration for wild type DHFR, measured in KMB buffer, pH 6.5

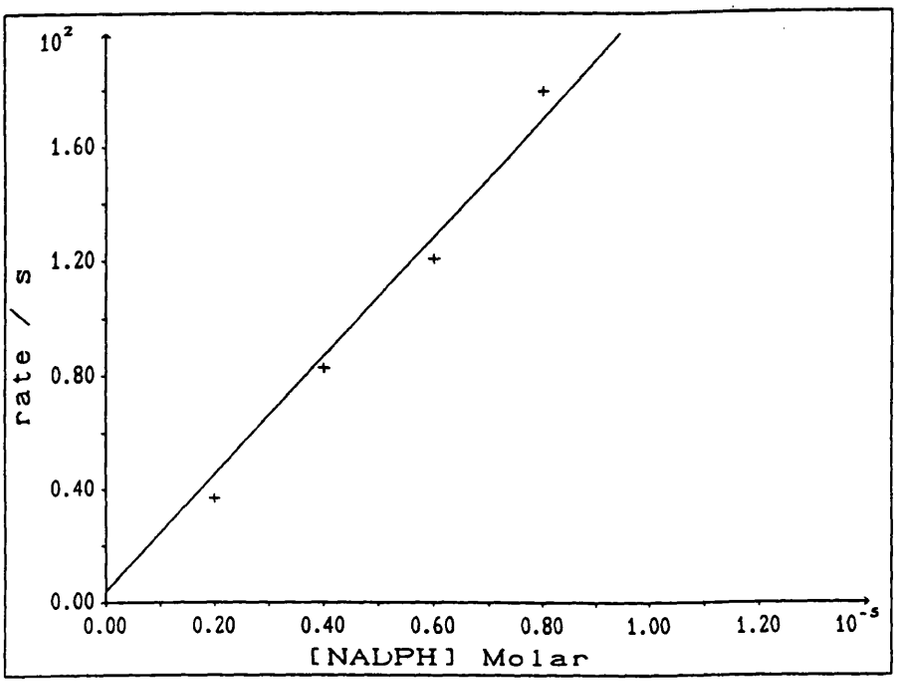

Graph 5.6. Observed association rate as a function of NADPH concentration for T63A DHFR, measured in KMB buffer, pH6.5

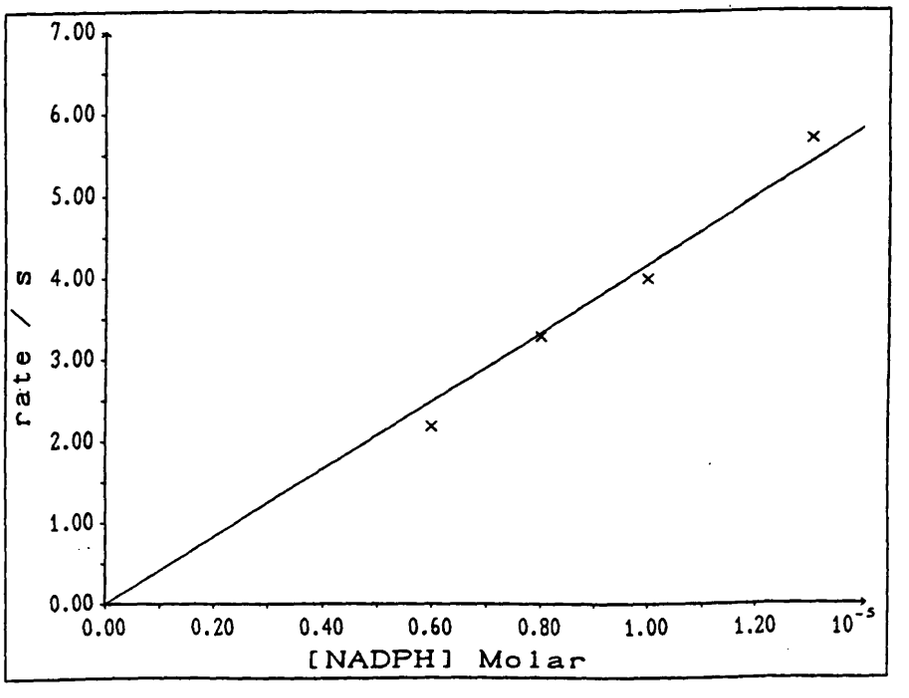

5.4. DISCUSSION

5.4.1 T63Q

The binding constants of NADPH, FH_2, and TMP to the free T63Q mutant and that of $\varepsilon NADP^+$ to the T63Q/MTX complex were very similar to wild type, indicating that any structural changes caused by the mutation were not important to the binding of these ligands. This is particularly interesting in terms of NADPH binding; the mutation was expected to reduce the ability of DHFR to bind NADPH because of the predicted loss of the hydrogen bond between the hydroxyl group of threonine-63 and the 2' phosphate of NADPH. From the nmr results, there was evidence that there was very little structural change in this region of the protein, and the fact that there was no affect on the binding constants is consistent with the nmr data. Therefore, the implication is that either glutamine is forming an hydrogen bond to the 2' phosphate in the same way as threonine, or the hydrogen bond is not important to the binding of NADPH or to the structure of the enzyme in this region. Glutamine of course has the ability to hydrogen bond, but in T63Q it was not expected to fit into the protein in the same way as threonine and thus would be in the wrong orientation to form the hydrogen bond with the 2' phosphate. The lack of effect of such a "non-conservative" mutation on the NADPH binding constant was entirely unexpected, glutamine, not being a conservative mutation and larger than threonine, would be predicted to have some affect on the enzyme, particularly at the site of the mutation.

The binding constants of FH_2 and the inhibitor, TMP, were measured and found to be the same in the T63Q mutant as in the wild type enzyme. The nmr results showed there was a small change in the binding site of MTX and therefore, probably also that of TMP and FH_2, since they bind in the same pocket (although FH_2 binds with a 180° rotation of the pteridine ring). Thus the small structural changes detected appear not to affect the binding of ligands to the substrate binding site of the apoenzyme. A direct comparison of the nmr results with binding constant measurements was not possible for MTX because the binding constant is too tight to be measured ($<10^{-9}$ M^{-1}) and remained high for the T63Q mutant.

The binding of $NADP^+$ and $\varepsilon NADP^+$ to the T63Q apoenzyme was three fold weaker than to the wild type. Therefore the $NADP^+$ binding site has been affected in some way to cause this small change in binding of $NADP^+$, yet the binding of $NADP^+$ to form the ternary complex with MTX is the same as wild type. Thus the positive cooperativity, or the increase in affinity for the second ligand (in this case coenzyme) when the first ligand (MTX) is bound, has been made larger by the mutation. The structural origins of this affect are not certain but some affects were seen in the nmr spectra which may be significant. The

chemical shifts of the proton resonances from the nicotinamide ring of $NADP^+$ were measured and were found to be different from those of wild type. The orientation of the nicotinamide ring when bound to DHFR is known not to be exactly the same in the oxidized and reduced coenzymes (Hyde *et al.*, 1980) and the difference is likely to be part of the reason for the specificity of NADPH over $NADP^+$. The affect of the mutation on the chemical shifts of $NADP^+$ may indicate an adjustment in the binding site, and this may be the reason for the change in binding constant. The alteration of the binding constant probably causes little perturbation to catalysis since at no point in the "preferred" pathway of the kinetic scheme (see the introduction to this chapter), is the oxidised coenzyme bound to the enzyme in a binary complex. The binding constant of $NADP^+$ to the ternary complex is the same as wild type so it is likely that the small affect on binding to form the binary complex will have little repercussion upon catalysis.

For T63Q the K_M of NADPH and k_{cat} were found to be the same as wild type, thus it appears that the mutation had not affected catalysis. However the pH dependence of k_{cat}, and the deuterium isotope effect were both different. Figure 5.2 shows the pH dependence for the hydride transfer step (which has a pK_a of pH 6.5) and the pH independent FH_4 dissociation rate constant for the wild type enzyme. The figure illustrates that the consequence of the change in rate limiting step on going from FH_4 dissociation at low pH, to hydride transfer at high pH, is to affect the pK_a of k_{cat}, producing an apparent pK_a of pH 8.4.

Figure 5.2. Observed rate constants for hydride transfer (—·—·—), FH_4 dissociation (— — —), and k_{cat} (———) as a function of pH (Fierke et al., 1987).

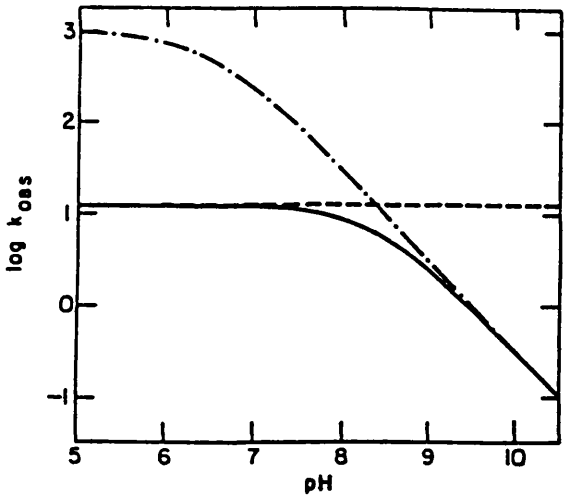

For the T63Q mutant both the apparent pK_a and the pK_a of the isotope effect were 0.5 pH units lower. These effects could arise in one of two ways:

1. the off rate of FH_4 is increased so that it is less rate limiting, i.e. hydride ion transfer becomes more rate limiting, the result being the apparent pK is nearer to the true pK controlling the hydride ion transfer step, or

2. the pK controlling the pH dependent hydride ion transfer step has changed.

Since the rate and the isotope effect at low pH (where product dissociation is the major rate limiting step) were similar in both enzymes, it is most likely that it is the pK of hydride ion transfer that has been altered by the mutation. A difference in the pK_a of hydride ion transfer has been seen in mutants made by Murphy and Benkovic (1989) where the mutants L54G and L54N showed a reduction in pK_a of 0.9 and 0.7 respectively. Interestingly they found another mutant, L54I, had a lower pK_a in the steady state but pre-steady state kinetic analysis showed the cause was an increase in the off rate of FH_4 (which was manifested by a larger k_{cat} than wild type at low pH). The mutants R44L and H45Q have also been shown to have a different pK_a of hydride ion transfer, in these cases an increase in pK_a was seen (Adams *et al.*, 1989). As in the T63Q mutant, these mutations are a large distance away from the Asp26 thought to be the ionising group involved in hydride ion transfer.

The nmr results provide evidence of structural changes around the substrate/inhibitor binding site. This change in structure must be related to the difference in apparent pK between T63Q and wild type enzyme. It is known that folate binds to the enzyme in a different orientation from MTX (Oefner *et al.*, 1988, Bystroff *et al.*, 1990, see the Introduction chapter), with the pteridine ring "turned over" by about 180° compared to MTX, and an additional small 7° "twist" in orientation. The structural differences mean the nmr results, which use bound MTX rather than substrate, can only provide a pointer to what the structural differences there may be in the substrate complex. The change in apparent pK of the reaction also indicates that there is a structural change at this region of the protein. The otherwise markedly similar kinetic and binding results suggest that the changes are specific to a small number of residues (since the binding of substrate is not affected). It is notable that the pK of the reaction can be changed without affecting the binding constant of FH_2, perhaps implying that the residue causing the change in pK is not involved in binding the substrate. This is a similar result to that found for the *E. coli* enzyme where the mutants R44L and H45Q have also been shown to have a different pK_a of hydride ion transfer but no difference in binding of substrate (Adams *et al.*, 1989). The residue important to the protonation of the substrate has been demonstrated to be Asp26 (Howell *et al.*, 1986, see the introduction to this thesis). The role of this residue is to date

unknown, although all the possible mechanisms which have been proposed involve this residue (Gready, 1985, Bystroff *et al.*, 1990, Howell *et al.*, 1986, Stone and Morrison, 1984). If this Asp26 is involved in the protonation of FH_2, it may be the pK_a of this residue that has been altered by the mutation, particularly since it is the only ionisable group nearby. From crystallographic studies, Asp26 forms one of the hydrogen bonds in a complex network between the protein, water molecules and substrate. Any change in structure around this region is highly likely to change either the pattern of hydrogen bonds or at least the hydrogen bond distances and thus is likely to change the pK of the reaction.

The T63Q mutation was designed to alter the specificity of coenzyme binding by increasing the ability of NADH to bind whilst reducing the ability of NADPH to bind. It was not possible to measure the binding constant of NADH to wild type or T63Q because it was too weak (at the concentrations of NADH required it strongly absorbed the excitation light and the fluorescence change could not be accurately measured), therefore the specificity for NADPH over NADH could not be measured. The K_M for NADH was measured and, within experimental error, found to be the same at 150μM ±10μM for the wild type and 181μM ±30μM for the mutant enzyme. Therefore, assuming that the K_M for NADH is limited by its ability to bind to the enzyme, the binding of NADH to the mutant and wild type enzymes are probably the same.

5.4.2 T63A

The binding constant of the substrate FH_2, and the inhibitor TMP, to T63A was the same as for wild type and T63Q, so the mutation has not perturbed this region of the protein sufficiently to alter ligand binding; this is consistent with the nmr studies which gave no indication of structural changes at this binding site.

In contrast to the results with T63Q, in the T63A mutant the binding constant of NADPH was reduced by a factor of 600. This result is in accord with the predicted results of the mutation. The change in free energy of NADPH binding is 3.8 kcal/mol, the contribution equivalent to an hydrogen bond with a charged group (Fersht, 1987). On first inspection this suggests that the reduced affinity for NADPH could easily be explained by the loss of the hydrogen bond, which is what the mutation was designed to investigate. However, other results showed that the explanation is not so simple.

Two rate constants contribute to the magnitude of the binding constant; the rate of association (k_{on}) and the rate of dissociation (k_{off}) of NADPH. k_{on} of NADPH was measured and found to be 50 times slower, and k_{off} was calculated from this to be 12 times

faster, than the wild type enzyme. Therefore, in the T63A mutant, the rate of association of NADPH is no longer diffusion limited. The fact that k_{on} is slower suggests some conformation affect of the mutation which causes steric hindrance and slows the rate of coenzyme binding. It is known that the wild type enzyme is in equilibrium between two or more conformations, only one of which binds NADPH (Dunn *et al.*, 1978, Andrews *et al.*, 1986) which effectively lowers the enzyme concentration. It may be that the mutation "distorts" the apoenzyme and that this distortion can be overcome by NADPH binding, which is consistent with the NMR results. Since the association rate of NADPH is slowed down, the 3.8 kcal/mol difference in free energy of NADPH binding to the mutant enzyme compared to the wild type enzyme therefore can not simply represent the loss of an hydrogen bond. In order to understand the origin of the effect on k_{on} some structural evidence is required. However, good nmr spectra of the apoenzyme are very difficult to obtain because the enzyme is in an equilibrium of an unidentified number of conformations with the consequence of very broad lines. It is therefore difficult to assign the resonances to protons in the protein and to date very little nmr work has been performed on the apoenzyme.

The simplest explanation for the 12 fold increase in the dissociation of NADPH is because of the loss of the hydrogen bond. The nmr results of the ternary NADPH/MTX complex showed there was a difference in coenzyme binding at the region of the adenine ring and 2' phosphate moieties of the coenzyme. The deduction was that the adenine moiety of the coenzyme was not binding as closely to residues in the mutant as to the wild type enzyme. The protein structure alterations that cause these differences could not be determined but were thought to be small. It may be that it is the loss of the hydrogen bond that is not enabling the NADPH to bind as closely to the protein and so causing the small structural changes and making the dissociation rate approximately 12 fold faster.

The K_M for NADPH of the T63A mutant is almost 1000 fold higher than that of wild type, i.e. the affinity of the enzyme for NADPH is very much reduced in the T63A mutant. As discussed in the introduction to this chapter, the K_M provides an indication of the affinity of NADPH to the enzyme/FH_4 complex rather than to the apoenzyme because the dissociation constant of the former is almost 90 times greater than the latter. In the mutant T63A the K_M is still significantly (100 fold) lower than the binding constant of NADPH to the apoenzyme and thus still represents the binding in the ternary complex. The results suggest that the binding of NADPH to the E/FH_4 complex is greatly reduced and by a similar order of magnitude as NADPH binding to the apoenzyme (1000 fold *cf.* 600 fold), as found by direct measurement. Thus the conformational affect which causes the change of NADPH binding to the apoenzyme, discussed above, probably persists when NADPH binds to the binary enzyme.FH_4 complex. There is a puzzle in that the nmr analysis revealed that there were very few structural changes at the substrate binding pocket in the

T63A/MTX complex, thus it appears that small local changes, which were not detected by nmr, are the cause. However, the structure of the E.FH_4 complex is not known but must be different from the wild type E.MTX and E.FH_2 because the binding of NADPH to E.FH_4 is reduced by 90 fold compared to the binding of NADPH to the E.FH_2 complex. Therefore the structural alterations of the E.MTX complex cannot provide conclusive evidence for the reasons behind the much reduced binding of NADPH to the E.FH_4 complex. Studies on the binding of folinic acid (5-formyl-5,6,7,8,-tetrahydrofolate) to the enzyme (Birdsall *et al.*, 1981a) have shown that the binding of this "product analogue" is significantly reduced upon coenzyme binding, 3 fold when complexed with $NADP^+$ and 600 fold with NADPH. Although the structural basis for this "negative cooperativity" is not fully understood there is evidence, obtained by nmr studies, to implicate folinic acid in equilibrium between two conformational states, and structural changes at the adenine moiety of the coenzyme. Similar effects then are seen for the mutant enzyme where structural changes at the adenine binding site and conformational equilibria affects are also implicated in the reduced binding of coenzyme.

k_{cat} of T63A was found to be the same as wild type and T63Q. Therefore, although the binding of NADPH had been dramatically altered, apparently the rate of catalysis had not. The difference is that T63A requires high concentrations of NADPH for saturation in order to provide the same rate as wild type. The variation of rate with pH and the isotope effect could not be measured for T63A because the concentrations required to saturate the enzyme were too high. Therefore, in the absence of a complete kinetic analysis, the contributions of the dissociation of the product and the hydride ion transfer step to the rate limiting step could not be established.

Neither of the T63Q and T63A mutants behaved as predicted when they were designed. It may not be too surprising that T63Q does not behave as predicted since the idea was rather ambitious, however it has provided some very interesting results. T63A on the other hand was a conservative mutation and its behaviour was expected to be reasonably predictable. In fact the mutation did give the predicted results but the reasons for the effects were not those expected. If a reasonably comprehensive study of this mutation had not been performed then the results would have been completely misinterpreted.

Changing the Thr63 side chain has, in both cases, caused unusual structural effects on the enzyme and these have made it impossible to define quantitatively the contribution the hydrogen bond between Thr63 and the 2' phosphate makes to the specificity of NADPH binding. These experiments highlight the care required in interpreting kinetic analyses without any structural knowledge. In practice it is rarely possible to study the structure of the protein, but from these studies it is clear that in this case, interpretation of the effects of

a mutation by steady state kinetic determinations are highly likely to be wrong, even if more than one mutation is made at the same site to try and "even out" the errors. However, it is probable that a complete kinetic analysis, using transient kinetics, is more likely to yield a realistic interpretation of the effects of the mutation.

6. GENERAL CONCLUSIONS

The T63Q mutant was successfully expressed and purified. The equilibrium binding constants of substrates and inhibitors binding to binary and ternary enzyme complexes were the same as wild type except the binding of the oxidised coenzyme to the mutant apoenzyme, which was reduced three fold; however, this has no effect on steady state turnover. The k_{cat} and K_M for NADPH were unaffected by the mutation, but the apparent pK_a of catalysis and the pK_a of the isotope effect were both reduced by 0.5 pH units. It was deduced from these results that the pK_a of the residue involved in hydride ion transfer had been changed by 0.5 pH units. Asp26 is the only ionisable residue at the substrate binding site and generally accepted to be involved in catalysis and it is probably this residue which has an altered pK_a.

Structure analysis of complexes of T63Q by nmr revealed no conformational changes at residues near the mutation or to the bound coenzyme; however, there were small structural effects seen at the substrate binding site, at least 15Å away from the mutation. A movement along the backbone of helix-C from arginine-43 at the mutation site to the substrate binding site was hypothesized to cause these affects. This helix movement causes Phe49 to move closer to Leu54 and causes small changes to MTX binding. This conformational change must also be affecting the binding site of the substrate, and is sufficient to change the pK_a of catalysis. From crystallographic studies, Asp26 forms one of the hydrogen bonds in a complex network between the protein, water molecules and substrate. Any change in structure around this region is highly likely to change either the pattern of hydrogen bonds or at least the hydrogen bond distances and thus is likely to change the pK_a of the reaction.

The mutant T63A was successfully constructed; however, expression of this mutant was only detected when the temperature was at 30^oC rather than the usual 40^oC. This was found to be caused by the much weaker binding of NADPH; DHFR is much more stable when complexed with coenzyme or substrate. The binding of NADPH to the apoenzyme was reduced by six hundred fold, the rate of association reduced by fifty fold and the rate of dissociation increased by twelve fold. The K_M of NADPH was increased by 1000 fold, indicating that the binding of NADPH to the enzyme/FH_4 ternary complex was also much reduced compared to the wild type enzyme complex. Since the rate of association of NADPH had been altered, these affects cannot simply be due to the loss of the hydrogen bond between threonine and the protein, but must also be caused by some conformational change in the protein. k_{cat} and the binding constants of folate substrates and inhibitors were the same as wild type. The results are the opposite to those obtained for the T63Q mutant in that

the binding of coenzyme is affected rather than the binding of substrate, despite the mutation being made at the same residue.

Structure analysis of the T63A mutant enzyme by nmr revealed that the adenine and the 2' phosphate moieties of NADPH are affected by the mutation when the enzyme is in ternary complex with NADPH and MTX, the adenine ring being further away from residues in the protein. Protons in residues around the mutation that have been assigned in the nmr spectrum were not significantly affected by the mutation except for chemical shift differences (i.e. no differences were found in the intensity of their NOESY cross peaks and so their relative positions must be the same as wild type). This implies that the effects of the mutation are on residues which have not been assigned, at least in the case of the binary MTX and ternary MTX/NADPH complexes of the enzyme (as was found for T63Q). However, the effect of the mutation on the coenzyme binding constants suggest there may be more conformational effects on the apoenzyme and the enzyme/FH_4 complexes since the rate of association of the coenzyme was considerably affected.

Neither of the T63Q and T63A mutants behaved as predicted when they were designed. It should not be too surprising that T63Q does not behave as predicted since the idea of changing coenzyme specificity was rather ambitious; however, it has provided some very interesting results. T63A on the other hand was a conservative mutation and in fact it did give the predicted results (i.e. the binding of coenzyme was considerably reduced), but the reasons for the effects were not those expected. If a reasonably comprehensive study of this mutation had not been performed, the results may have been completely misinterpreted.

Changing the Thr63 side chain in both cases caused unusual structural effects on the enzyme and these have made it impossible to define quantitatively the contribution which the hydrogen bond between Thr63 and the 2' phosphate makes to the specificity of NADPH binding. The dissociation rate of the coenzyme was increased in T63A (where this hydrogen bond is lost) indicating that this hydrogen bond probably does contribute to the binding of coenzyme. The Thr63 side chain also appears important in maintaining the precise structure of the protein and this would not have been noticed without the structural analysis.

These experiments highlight the care required in interpreting steady state kinetic and binding data without any structural knowledge or in the absence of a comprehensive kinetic analysis. The nmr experiments in this thesis were essential for the interpretation of the kinetic data for the T63Q mutant whereas the steady state kinetic and binding data for the T63A mutant could not have been correctly

interpreted without the determination of the individual rate constants involved. Therefore, for the correct interpretation of the effects of a mutation, it is apparent from these studies that it is essential to carry out as complete an analysis as possible, even if more than one mutation is made at the same site to try and "even out" the errors.

In this thesis nmr has been proved to be extremely useful in the analysis of mutant enzymes whereas in practice it is unfortunately rarely possible to study the structure of the protein for various practical reasons. However, it is probable that a complete kinetic analysis using transient kinetics, is more likely than steady state kinetics, to yield a realistic interpretation of the effects of the mutation where structural information cannot be obtained.

APPENDIX

A.1. STRAIN LIST

JM101	Δ(*lac-proAB*), *sup*E, *thi*-1, (F', *tra*Δ*36*, *pro*A$^+$B$^+$, *lac*I^q, *lac*ZΔM15)
WK6	Δ(*lac-proAB*), *galE*, *strA*/F' *lac*I^q, *lac*ZΔM15, *proA*$^+$*B*$^+$
WK6λ	WK6 + λcI
WK6 *mutS*	WK6 + *mutS215*::Tn10 (tet^R)
BMH71-18	F', *supE*, *thi*-1, Δ(*lac-pro*AB) *lac*I^q *lac*ZΔM15
BMH71-18 *mutS*	BMH71-18 + *mutS215*::Tn10 (tet^R)
W71-18	*strA* and as BMH71-18 except *supE*

A.2. GROWTH AND MAINTENANCE OF STRAINS

Unless stated otherwise all cultures were grown in Luria broth (L-broth) in a shaking incubator at 37°C. Overnight cultures were grown by picking one colony from a plate and transferring it to 5ml L-broth.

Strains were stored on agar plates containing the appropriate antibiotic at 4°C for short term storage. Strains were also stored in glycerol by transferring 1ml of an overnight culture into 4ml of 20% glycerol and stored at -20 and -80°C.

For storage of BMH71-18, JM101, and WK6, minimal plates were always used to maintain selection for the *pro* marker of the F'-episome.

Buffers:

L-broth	Tryptone		10g/l
	Yeast extract		5g/l
	Sucrose		10g/l
Agar plates	L-broth + 1.5% agar		
Minimal plates	A)	Na_2HPO_4	7g/400ml
		KH_2PO_4	3g/400ml
		NH_4Cl	1g/400ml
		autoclave	

B) Agar 15g/600ml
autoclave

mix A) and B) and add the following sterile solutions:

Glucose (20%)	25ml
$CaCl_2$ (100mM)	1ml
$MgSO_4$ (1M)	1ml
$FeCl_3$ (0.1M)	5ml
Thiamine (1mg/ml)	5ml

(Glucose and thiamine are filter sterilised)

Antibiotic concentrations used in selective media:

Ampicillin (sodium salt)	100µg/ml
Chloramphenicol	40µg/ml
Tetracycline	12.5µg/ml
Streptomycin	25µg/ml

A.3. PREPARATION OF PHASMID ssDNA:

A fresh overnight culture of a pMa/c carrying strain was used to inoculate LB-media supplemented with the appropriate antibiotic. This was allowed to grow until the OD_{650} reached 0.1. The culture was infected with M13K07 (Russel *et al.*, 1986) to give a m.o.i. (multiplicity of infection, see below) of approximately 20. The infected bacteria were incubated for a further 4-5 hours and the cells were then spun down at 6000 r.p.m.. The supernatant containing the phasmid ssDNA was kept at 4°C.

The m.o.i. is the ratio of M13K07 to bacteria. The concentration of phage can be found by plating serial dilutions of the phage on a male *E. coli* strain such as JM109.

A.4. PHOSPHORYLATION USING dATP AND RADIOLABELLED dATP

For phosphorylating 100 pmoles DNA:

2µl of 10x kinase buffer, 1µl of 10mM ATP (^{32}P labelled ATP for making the hybridisation probe), 4 units polynucleotide kinase (PNK), and the oligonucleotide, were mixed and water was added to make a total volume of 20µl. This was incubated at 37 C for 45 minutes then at 65°C for 10 minutes to stop the reaction.

To check the purity of the oligonucleotide, the DNA was phosphorylated with ^{32}P ATP, run on a 20% acrylamide gel and autoradiographed for detection of bands.

To use labelled oligonucleotide for hybridisation screening of mutants the excess labelled ATP was removed using a spun column.

Buffers:

10x Kinase Buffer	Spermidine	5mM
	Dithiothreitol (DTT)	200mM
	$MgCl_2$	100mM
	Tris-HCl	700mM, pH 9.0

A.5. SPUN COLUMN

G-50 sephadex was soaked overnight in TE buffer. A plug of glass wool was placed at the bottom of a 1ml syringe and the syringe was almost filled with the G-50 and placed in a test tube. The G-50 was washed with TE buffer by adding 100µl TE onto the top of the gel and spinning in a centrifuge for a sufficient length of time to get the same volume washed off (this was repeated). To purify the hybridisation probe, 100µl of the kinased DNA was loaded onto the gel and spun as before. The syringe was put into a fresh test tube and washed with a further 100µl buffer and this fraction containing the oligonucleotide was retained. The column was washed again with buffer and the two fractions were pooled if the second fraction contained a large amount of DNA (checked using a Geiger counter or by Cherenkov counting). The labelled ATP remained in the column.

Buffers:

TE Buffer	Tris-HCl	0.1M, pH 7.4
	EDTA	0.01M

A.6. PLASMID PREPARATION (Replicative form or RF prep)

A.6.1. Large Scale (1 litre):

An overnight culture of cells containing the plasmid were spun down at 6000 r.p.m. for 10 minutes and resuspended in Tris-sucrose buffer to a final volume of 10ml.

For gentle lysis the cell walls were removed to form spheroplasts. For this 2ml of lysozyme solution (5mg/ml in Tris-sucrose) were added to the cell suspension and left at

0°C for 5 minutes. 4ml of 0.25M EDTA pH8.2 were added and the solution was again left on ice for 5 minutes with occasional agitation.

The spheroplasts were lysed by adding an equal volume of 10% Triton-EDTA solution dropwise with slow agitation. This gave a viscous solution of lysed cells. The cell debris and chromosomal DNA was removed by spinning at 20000 r.p.m. for 30 minutes and the supernatant was carefully transferred to a clean bottle.

The plasmid DNA was precipitated by adding a half volume of PEG 6000 solution and dry NaCl to a final concentration of 1.5M. This was mixed well and left at room temperature for 15 minutes. The plasmid DNA was then spun down at 6000 r.p.m. for 15 minutes.

The pellet was resuspended in 5ml TE buffer with gentle mixing. This was spun to remove any precipitate not resuspended.

A cesium chloride density gradient was prepared by making the volume up to exactly 10ml with TE buffer. 10.3g CsCl was added and dissolved followed by addition of 300µl ethidium bromide (10mg/ml). The solution was transferred to a centrifuge tube and carefully balanced. To balance two tubes of cesium chloride solution a tube was made lighter by using liquid paraffin in place of some of the solution (the darkly stained protein band was removed entailing no loss of the plasmid). The tube was sealed leaving no air bubbles and spun at 36000 r.p.m. for 60 hours at 18°C.

The tubes were examined under ultraviolet light and the band of covalently closed circular DNA was removed using a 1ml syringe and a 19 gauge needle (see figure A.1).

The ethidium bromide was removed by several extractions with CsCl saturated n-butanol. Finally the DNA was dialysed against three changes of 2 litre volumes of DNA buffer.

To check plasmid purity, the OD_{260}, OD_{230} and OD_{280} were measured and the ratios of OD_{260}/OD_{280} and OD_{280}/OD_{230} calculated. The DNA was deemed pure if the ratios were greater than 1.7. The concentration was determined using the equation:

$$[RF] = OD_{260} \times 50\ \mu g/ml$$

Figure A.1. Removal of Plasmid Bands From a Cesium Chloride Density Gradient.

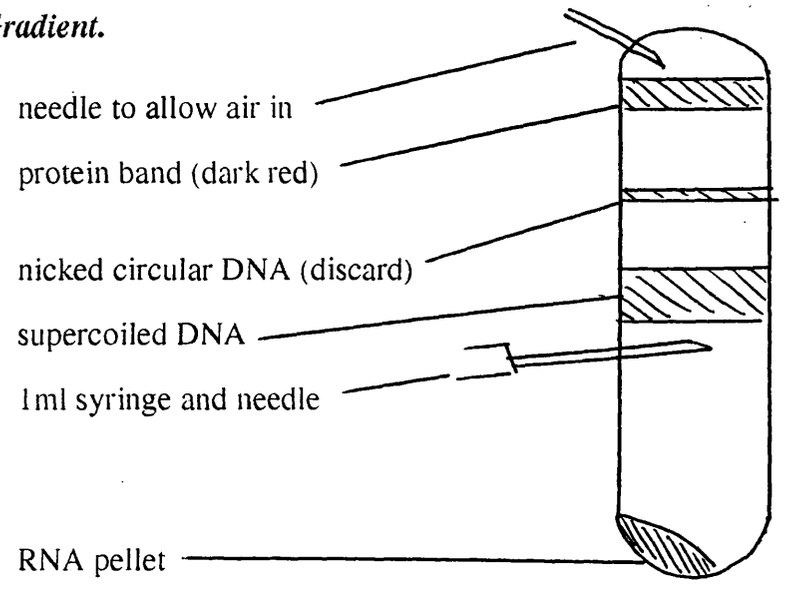

Buffers:

Tris-sucrose buffer	Tris-HCl	0.05M, pH7.4
	sucrose	25%(w/v)
DNA buffer	Tris-HCl	0.01M, pH7.4
	NaCl	0.01M
	EDTA	0.001M
Triton-EDTA	Tris-HCl	0.05M, pH 7.4
	EDTA	0.06M
	Triton-X100	10% (v/v)

A.6.2. Plasmid miniprep:

(Kraft *et al.*, 1988)

1.5ml of an overnight culture were spun down in a microfuge, the supernatant was removed and another 1.5ml was added and spun. As much supernatant was removed as possible. The cells were resuspended in 100µl ice cold glucose buffer. After 5 minutes at room temperature the cells were lysed by addition of 200µl freshly prepared solution of 0.2M NaOH, 1% SDS, mixed by inversion and left for 5 minutes on ice.

The chromosomal DNA was removed by precipitation. 100µl of potassium acetate buffer was added, mixed briefly by vortexing and left on ice for 5 minutes. The tubes were spun at 4°C for 5 minutes, the supernatant transferred to a fresh tube, respun and transferred to another tube to ensure no contamination with precipitate.

To remove the RNA, RNase A was added to a final concentration of 50µg/ml and incubated at 37°C for 30 minutes.

The plasmids were cleaned and concentrated by the following procedure. An equal volume of phenol/chloroform was added, vortexed hard for 5 minutes and spun for 2 minutes. The top aqueous phase was transferred to a fresh tube. 2.5 volumes of ice cold 70% ethanol was added, mixed by inversion and incubated at -70°C for 10 minutes. The plasmid precipitate was spun down, washed in 70% ethanol and dried under vacuum. The pellets were resuspended in 20µl TE buffer. 3.2µl were used for restriction digests to check their purity.

To the remaining 16.8µl, 3.2µl NaCl was added, mixed, and 20µl of 13% polyethylene glycol (PEG) was added, mixed well and incubated on ice for at least 30 minutes. The samples were centrifuged at 4°C for 10 minutes and the supernatant was carefully removed to leave a barely visible "flake-like" pellet of DNA. The pellet was washed with ice cold 70% ethanol and dried under vacuum.

For sequencing, the pellet was redissolved in 22µl TE buffer, 2µl of which was run on a gel to check the DNA yield.

Buffers:

Glucose Buffer	Glucose	50mM
	EDTA	10mM
	Tris-HCl	25mM, pH8.0
Potassium Acetate Buffer	Glacial acetic acid	5M
	Potassium acetate	3M
Phenol/Chloroform	1:1 mixture saturated with TE buffer, pH 8.0	

A.7. ANNEALING , EXTENSION, AND LIGATION

For annealing, the ratio of primer to gapped duplex DNA (gdDNA) was 10:1. 100ng gdDNA was mixed in an Eppendorf tube with 4pmoles of phosphorylated

oligonucleotide primer and made up to 10µl with water. The mixture was heated to 65°C for 5 minutes and allowed to cool to room temperature on a bench.

For extension and ligation, 24µl water and 4µl of 10x Fill-in buffer were added and mixed, followed by the addition of 1µl T4-DNA ligase (5 units/µl) and 1µl Klenow DNA polymerase, large fragment (1 unit/µl; diluted in 50mM potassium-phosphate buffer pH7.2, 50% glycerol). The mixture was incubated at room temperature for 45 minutes. This was stored on ice until required for transformation.

Buffers:

10 x Fill-in Buffer	KCl	625mM
	Tris-HCl	275mM, pH7.5
	$MgCl_2$	150mM
	DTT	20mM
	ATP	0.5mM
	dNTP's	0.25mM each

A.8. TO MAKE COMPETENT CELLS

To transform cells with plasmid DNA the cells must first be made competent by the following procedure. Throughout, the cells were maintained below 5°C.

50ml of L-broth were inoculated with 0.5ml fresh overnight culture and grown for 2.5 hours at 37°C. The culture was cooled on ice and harvested by centrifugation (6000 r.p.m. for 10 minutes) and resuspended in approximately 20ml ice-cold sterile $CaCl_2$ (0.1M). The cells were again harvested at 4°C resuspended in 2.5 ml $CaCl_2$ as before. The cells were left on ice for 60 minutes or stored at 4°C

A.9. TRANSFORMATION OF COMPETENT CELLS

60µl of ice cold 0.1M $CaCl_2$ were added to the plasmid DNA followed by 200µl of competent cells and kept on ice for at least 45 minutes. After a brief vortex the cells were heated to 45°C for 5 minutes. 1ml L-broth was added and the solution was incubated whilst shaking for 30 minutes, for the cells to replicate the transformed DNA.

For pMa/c mutagenesis the cells were mixed with 600µl L-broth and infected with M13K07 (5µl of 10^{12}pfu/ml) to encourage phage production. The cells were incubated with agitation at 37°C. After 30, 60 and 90 minutes 300µl were removed, the cells spun down and 200µl of supernatant (containing phage) were transferred to a fresh tube. The

tubes were stored on ice. Fresh overnight culture of host bacteria (100µl) was added, incubated for 20 minutes and streaked out on plates containing the appropriate antibiotic and grown overnight at 30°C.

For M13 mutagenesis, after the cells were transformed they were diluted 10, 100, 1000, 10000 times. 200µl of each dilution were put into a tube to which were added to 3ml soft agar (0.8%) followed by 200µl late log phase host bacteria. These were mixed by rolling the bottle in the palms and then poured onto agar plates. They were incubated overnight at 37°C for plaques to form.

The cells or plaques were then picked into storage media in microtitre wells using sterile toothpicks. The microtitre trays were incubated at 37°C with gentle agitation. The cultures were then transferred from the wells onto agar plates using a metal comb with 48 prongs and the plates were incubated overnight.

Buffers:

		g/l
Storage media	Tryptone	10
	Yeast Extract	5
	NaCl	5
	KH_2PO_4	1.8
	K_2HPO_4	6.3
	Na citrate	0.45
	$(NH_4)_2SO_4$	0.9
	$MgSO_4.7H_2O$	0.09
	Glycerol	44 (35ml)

A.10. COLONY HYBRIDISATION AND MUTANT SELECTION

A.10.1 Immobilisation and Lysis

Bacteria were transferred to nitrocellulose filters by setting a filter on the surface of the plate, leaving until it was completely wetted and then the filter was peeled off. The cells were lysed and the DNA denatured by setting the filters down (face up) onto 2ml puddles of the following solutions;

1. Denaturing solution	0.5M NaOH 1.5M NaCl	7-10 minutes
2. Neutralising solution	1M Tris-HCl, pH7.5	2 minutes

3. Repeat 2

4. Wash solution	0.5M Tris-HCl pH 7.5 1.5M NaCl	4 minutes

The filters were air dried on blotting paper for approximately 15 minutes.

The filters were then rinsed in approximately 100ml of the following solutions in 500ml beakers;

1. 20% Ethanol
2. 50% Ethanol
3. 80% Ethanol

The filters were blotted and baked in an oven at 80°C for 2 hours.

A.10.2 Prehybridisation

The filters were placed two to a bag, back to back, with 5ml prehybridisation solution;

1x Denhardt's
5X SSC pH7.2
0.5% SDS

The bags were sealed and placed in a 37°C water bath overnight.

A.10.3 Hybridisation

The corner of the bag was cut off and ^{32}P labelled oligonucleotide was added. The oligonucleotide solution contained;

6x NET
10x Denhardt's
0.1% SDS
10^6-10^7 c.p.m. [^{32}P]/ml (1 pmol/ml DNA)

The mixture was briefly warmed to 70°C and the hybridisation was allowed to proceed at room temperature for 2-3 hours (or overnight). The bags were opened, the solution removed and the filters were washed for 3 x 2 minutes in cold 6xSSC.

A.10.4. Autoradiography

The filter was air dried, attached to filter paper in a film cassette, covered with cling film and autoradiographed using high sensitivity X-ray film (Kodak XAR-5) and an intensifier screen. The exposure time was dependant upon the concentration of label.

A.10.5. Selective Washes

The filters were removed and washed for 1 minute in 6xSSC at T_d-2°C and autoradiographed. T_d is the dissociation temperature (see the Mutagenesis Protocols, Chapter 2). Strongly hybridising colonies were noted. The procedure was repeated at T_d where only mutants should give a strongly hybridising response.

Buffers

20xSSC	NaCl	3M
	Sodium citrate	0.3M
20xDenhardt's	Bovine Serum Albumin	0.4%
	Ficol 400	0.4%
	Polyvinylpyrolidine (PVP-360)	0.4%
18xNET	NaCl	2.7M
	Tris-HCl, pH 8.3	270mM
	EDTA	18mM

A.11. TEMPLATE (PHAGE) PREPARATION

A.11.1. M13:

5ml L-broth were inoculated with 50µl of phage supernatant or a single plaque picked from a fresh plate. 50µl of an overnight culture of host bacteria (eg JM101) were added and grown at 37°C for 6 hours.

1ml of the culture was spun down and the supernatant transferred to a clean tube. The phage were precipitated by adding 200µl of 2.5M NaCl in 20% PEG 6000, this was mixed and left for 30 minutes at room temperature. The precipitate was spun for 10 minutes and all the supernatant was thoroughly removed.

To clean the DNA of protein, the pellet was resuspended in 100µl of TE buffer. 50µl of redistilled phenol solution (equilibrated with TE buffer) was added, vortexed hard and centrifuged for 2 minutes. The top aqueous layer was transferred to a clean tube. A further 50µl of TE buffer was added to the remaining phenol, vortexed, centrifuged and the aqueous layer combined with the previous tube. The extraction was repeated with chloroform/isoamyl alcohol (24:1).

The DNA was concentrated by ethanol precipitation and resuspended in 50µl TE buffer for sequencing.

A.11.2. pMa/c

The same protocol was used as for M13 but using phage supernatant produced by the method described under section A.3. Preparation of Phasmid ssDNA.

A.12. SEQUENCING

For sequencing, the Pharmacia T7Sequencing Kit and protocols were used.

A.12.1. Annealing Primer to Template

A.12.1.1. Plasmid Sequencing:

To denature the plasmid, 2µl of 2M NaOH, 2mM EDTA was added to 20µl of plasmid solution (2-10µg DNA), mixed and incubated for 5 minutes at room temperature.

The denatured DNA was precipitated by adding 8µl of 1M Tris-HCl, pH <5, followed by 3µl 3M sodium acetate and mixed. 75µl of ice cold, 100% ethanol was then added and the DNA was precipitated on dry ice. The precipitate was spun down and the pellets were rinsed in 70% ethanol and dried under vacuum.

To the dried DNA, 10ng of primer and 2µl of Sequenase Annealing Buffer were added and made up to 14µl with distiled deionised water. These samples were mixed and incubated at 37°C for 30 minutes to allow annealing to occur. The tubes were then left at room temperature for at least 10 minutes.

A.12.1.2. Single Stranded Template Sequencing:

To 10µl template DNA (1.5-2µg), 2µl (10ng) of primer and 2µl Sequenase Annealing buffer were added and mixed. The solution was incubated at 60°C for 10 minutes and then left at room temperature for at least 10 minutes.

A.12.2. Sequencing Reactions

T7 DNA polymerase was diluted using cold Sequenase Enzyme Dilution Buffer to a concentration of 1.5units/µl. 2µl of this dilution was used for each set of four sequencing reactions.

Four wells of a small microtitre tray were labelled A, C, G, or T. 2µl of the appropriate Sequenase Mix-short solutions was pipetted into each well for sequencing up to 500 bases.

A.12.2.1. Labelling Reactions:

3µl Sequenase Labelling Mix, 1µl (10µCi) [γ^{32}P]dATP and 2µl diluted T7 DNA polymerase were added to the tube containing the annealed template and primer . The solutions were mixed briefly, centrifuged and incubated at room temperature for 5 minutes. Meanwhile the microtitre trays were floated in a water bath at 37°C to pre-warm the solutions. The termination reactions were then carried out immediately.

A.12.2.2. Termination Reactions:

4.5µl of the labelling solution were added to each of the four sequencing mixes using a fresh pipette tip for each addition, and incubated at 37°C for 5 minutes. 5µl of Sequenase Stop solution was added to each well. 3µl from each well were transferred to a fresh microtitre tray and heated to 75-80°C in a water bath for 2 minutes. 1.5-2µl were immediately loaded onto a sequencing gel. The remaining material was stored in a -20°C freezer or used for a second loading on the gel (after heating) following a period of electrophoresis.

A.12.3. Sequencing Gel Electrophoresis

Glass plates were thoroughly cleaned, rinsed with ethanol and dried. One plate was siliconised (in a fume cupboard) by pipetting 1ml non-binding silane onto one side of the clean plate and spread over the plate with a tissue. The plate was thoroughly rinsed with distiled water. The plates were assembled with the silicanized side facing inwards, 0.2mm spacers between each side of the plates with an extra 2.5cm piece of spacer at the bottom of each side to make a wedge gel 0.4mm thick at the bottom. The plates were taped together and clamped with bulldog clips.

For the gel, 21g of urea were dissolved in a solution of 10ml 40% Acrylamide, 5ml TBE buffer, 16ml water, and 100µl 16% fresh ammonium persulphate. When the urea was dissolved, 100µl TEMED was added, the solution was swirled to mix and immediately poured between the gel plates taking care not to introduce air bubbles. A sharkstooth comb was inserted with the flat edge into the gel. The gel was left to set for at least an hour by resting one end of the plates on a pipette to keep them just off the horizontal.

After slashing the tape along the bottom the plates were clamped onto the buffer assembly unit. TBE buffer was poured into each tank at the top and bottom of the plates, the comb was removed from the gel and unpolymerised acrylamide was rinsed from the surface of the gel by squirting in buffer with a pipette. The comb was replaced so the sharksteeth just touched the gel surface.

The gel was pre-run at 2000Volts (ca. 30mA) for 30 minutes. The current was switched off, the wells rinsed again and the denatured sequencing reactions were loaded in sets of four, cleaning the Gilson tip in buffer between each application. The loaded gel was run at 2000Volts until the dye reached the bottom of the gel.

A.12.4. Autoradiography:

The power was switched off and the plates removed from the assembly. The plates were carefully separated so the gel remained attached to the unsilicanized plate. The plate and gel were submerged in 10% acetic acid, 40% methanol for approximately 15 minutes then transferred to filter paper by drying most of the liquid off the gel and carefully overlaying with the paper. The gel-paper was placed on a sheet of filter paper, covered with cling film and dried on a vacuum gel dryer for 30 minutes.

The dry gel-paper was placed in film cassette, covered with X-ray film and autoradiographed (with an intensifying screen if necessary). The film was developed using an automatic developing machine and the sequence was read off the film.

Buffers:

10xTBE	Tris-HCl, pH 8.2	105g/l
	Boric acid	55g/l
	EDTA	9.3g/l
40% Acrylamide	40% Acrylamide	380g/l
	Bis-acrylamide	20g/l
	Stirred with 20g MB-1 resin and filtered	

A.13. RESTRICTION DIGESTION REACTIONS

For each 10µl DNA (1µg DNA) 1 unit of enzyme was added plus 2µl 10xdigestion buffer, and made up to 20µl with water. The digestion was left to proceed at 37°C for 1 hour followed by heating to 65°C to stop the reaction.

Buffers:

10x EcoR1 buffer	Tris-HCl, pH 7.5	500mM,
	$MgCl_2$	100mM
	NaCl	1M
	Dithioerythretol (DTE)	10mM

10x HINDIII buffer	Tris-HCl, pH 8.0	100mM
	$MgCl_2$	50mM
	NaCl	1M
	2-mercaptoethanol	10mM
10x BglII buffer	Tris-HCl, pH 7.5	100mM
	$MgCl_2$	100mM
	NaCl	500mM
	DTE	10mM

A.14. AGAROSE GELS

1% agarose gels were usually used for analysis of restriction digests, plasmid and template preps.

The gel was prepared by suspending 1g agarose in 100ml TAE buffer and heating in a microwave oven to melt the agarose. The agarose was allowed to cool slightly and then poured into a gel chamber that had been sealed at both ends with tape. Air bubbles were flamed or pricked out with a hot loop. A comb was inserted and the gel allowed to set. When set. the tape was removed and the gel was submerged in TAE buffer in a buffer chamber and the was comb removed.

To 10µl of DNA (or restriction digest mixture) and 1µl of agarose dye mix was added and mixed. The mixture was pipetted into a well in the gel and run at 200 volts until the two dyes were separated by approximately 2.5cm.

The power was switched off and the gel was submerged in ethidium bromide solution for 15 minutes with agitation. The gel was washed in water for 30 minutes, after which it was viewed under ultraviolet light.

Buffers:

10x TAE buffer	Tris-HCl, pH8.0	48.4g
	Acetic acid	11.42ml
	EDTA (0.5M)	20ml
	made to 1 litre	

A.15. ELECTROELUTION OF DNA FROM AGAROSE

The band of DNA required was cut out of the gel and placed in dialysis tubing with AEB buffer. The tubing was sealed and placed in an electrophoresis tank in the same

buffer. The current was switched on and run at 100 Volts for 3 hours and then was reversed for 2 minutes. The tubing was removed from the tank and the buffer containing the DNA transferred to a clean Eppendorf tube. The DNA was ethanol precipitated, washed in 70% ethanol and dried. The ethidium bromide was then removed on a NAC's column.

A.16. NAC's COLUMN FOR DNA PURIFICATION

The resin in the column was hydrated by washing three times with 2M NaCl in TE buffer using a 1ml gilson to force the liquid through. The resin was then equilibrated with loading buffer in a similar fashion.

The DNA (suspended in the loading buffer) was added to the top of the column and allowed to flow through by gravity. The column was washed with 3-5ml of loading buffer again using gravity flow.

The DNA was eluted by gravity with 3 additions of 200µl elution buffer.

Buffers:

For double stranded DNA of <1000base pairs;

Loading buffer	NaCl 0.2M in TE buffer
Elution buffer	NaCl 1M in TE buffer

For double stranded DNA of >1000base pairs;

loading buffer	NaCl 0.5M in TE buffer
Elution buffer	NaCl 2M in TE buffer

REFERENCES

Adams, J., Johnson, K., Matthews, R., Benkovic, S.J., Biochemistry 28 6611-6618 (1989).

Andrews, J., Clore, G.M., Davies, R.W., Gronenborn, A.M., Gronenborn, B., Kalderon, D., Papadopoulos, P.C., Schafer, S., Sims, P.F.S., Stancombe, R., Gene 35 217-222 (1985).

Andrews, J., Fierke, C.A., Birdsall, B., Ostler, G., Feeney, J., Roberts, G.C.K., & Benkovic, S.J. Biochemistry 28 5743-5750 (1989).

Appleman, J.R., Howell, E.E., Kraut, J., Kuhl, M., Blakely, R.L., J. Biol. Chem. 263 9187-9198 (1988).

Baccanari, D.P., Daluge, S., King, R.W., Biochemistry 21 5068-5075 (1982).

Baccanari, D.P., Joyner, S.S., Biochemistry 20 1710-1716 (1981)

Baker, D.J., Beddall, C.R., Champness, J.N., Goodford, P.J., Norrington, F.E.A., Smith, D.R., Stammers, D.K., FEBS Lett. 126 49-52 (1981).

Barbehenn, E.K., Kaufmann, B.T., Biochem. Biophys. Res. Commun. 85 402 (1978)

Bax, A., Davies, D.G., J. Mag. Res. 65 355-357 (1985).

Benkovic, S.J., in Chemistry and Biology of Pteridines Walter de Gruyter, New York. (Cooper, B.A., Whitehead, V.M., eds) 13-28 (1986).

Benkovic, S.J., Fierke, C.A., Naylor, A.M., Science 239 1105-1110 (1988).

Bennett, C.D., Nature (London) 248 67 (1974).

Bennett, C.D., Rodkey, J.A., Sondey, J.M., Hirschmann, R., Biochemistry 17 1328-1377 (1978).

Birdsall, B., Andrews, J., Ostler, G., Tendler, S.J.B., Feeney, J., Roberts, G.C.K., Davies, R.W., Cheung, H.T.A., Biochemistry 28 1353-1362 (1989a).

Birdsall, B., Arnold, J.R.P., Jiminez Barbero, J., Frenkiel, T.A., Bauer, C.J., Tendler, S.J.B., Carr, M.D., Thomas, J.A., Roberts, G.C.K., Feeney, J., Eur. J. Biochem. 191 659-668 (1990)

Birdsall, B., Bevan, A.W., Pascual, C., Roberts, G.C.K., Feeney, J., Gronenborn, A., Clore, G.M. Biochemistry 23 4733-4742 (1984).

Birdsall, B., Burgen, A.S.V., Hyde, E.I., Roberts, G.C.K., Feeney, J., Biochemistry 20 7186-7195 (1981a).

Birdsall, B., Burgen, A.S.V., Roberts, G.C.K., Biochemistry 19 3723-3731 (1980a).

Birdsall, B., Burgen, A.S.V., Roberts, G.C.K., Biochemistry 19 3732-3737 (1980b).

Birdsall, B., Burgen, A.S.V., Rodrigues de Miranda, J., Roberts, G.C.K., Biochemistry 17 2102-2110 (1978).

Birdsall, B., DeGraw, J., Feeney, J., Hammond, S.J., Searle, M.S., Roberts, G.C.K., Colwell, W.T., Crase, J., FEBS Lett. 217 106-110 (1987).

Birdsall, B., Feeney, J., Tendler, S.J.B., Hammond, S.J., Roberts, G.C.K., Biochemistry 28 2297-2305 (1989b).

Birdsall, B., Griffiths, D.V., Roberts, G.C.K., Feeney, J., Burgen, A.S.V. Proc. R. Soc. London Ser. B196 251-265 (1977a).

Birdsall, B., Gronenborn, A., Clore, G.M., Roberts, G.C.K., Feeney, J. Burgen, A.S.V., Biochem. Biophys. Res. Commun. 101 1139-1144 (1981b).

Birdsall, B., Gronenborn, A., Hyde, E.I., Clore, G.M., Roberts, G.C.K., Feeney, J., Burgen, A.S.V. Biochemistry 21 5831-5838 (1982).

Birdsall, B., King, R.W., Wheeler, M.R., Lewis Jr, C.A., Goode, R.B., Dunlap, R.B., Roberts, G.C.K., Analytical Biochemistry 132 353-361 (1983).

Birdsall, B., Roberts, G.C.K., Feeney, J., and Burgen, A.S.V., FEBS Lett., 80 313-316 (1977b).

Birdsall, B., Tendler, S.B., Arnold, J.R.P., Feeney, J., Griffin, R.J., Carr, M.D., Thomas, J.A., Roberts, G.C.K., Stevens, F.G., Biochemistry 29 9660-9667 (1990).

Bitar, K.G., Blankenship, D.T., Walsh, K.A., Dunlap, R.B., Reddy, A.V., Freisheim, J.H., FEBS Lett. 80 119-122 (1977).

Blakely, R.L., The Biochemistry of Folic Acid and Related Pteridines. North-Holland, Amsterdam. (1969)

Blakely, R.L., in Folates and Pterins, Vol 1. John Wiley and Sons, New York (Blakely, R.L., Benkovic, S.J., eds.) 191-253 (1984).

Bolin, J.T., Filman, D.J., Matthews, D.A., Hamlin, R.C., Kraut, J., J. Biol. Chem. 257 13650-13662 (1982).

Bystroff, C., Oatley, S.J., Kraut, J., Biochemistry 29 3263-3277 (1990).

Campbell, I.D., Sheard, B., Tibtech. 5 302-306 (1987).

Cayley, P.J., Dunn, S.M.J., King, R.W., Biochemistry 20 874-879 (1980).

Champness, J.N., Stammers, D.K., Beddell, C.R., FEBS Lett. 199 61-67 (1986).

Charlton, P.A., Young, D.W., Birdsall, B., Feeney, J., and Roberts, G.C.K. J. Chem. Soc. Chem. Commun., 922-924 (1979).

Chen, J.-T., Mayer, R.J., Fierke, C.A., Benkovic, S.J., J. Cell. Biochem. 29 73-82 (1985).

Chen, J.-T., Taira, K., Tu, C.-P.D., Benkovic, S.J., Biochemistry 26 4093-4100 (1987).

Cheung, H.T.A., Searle, M.S., Feeney, J., Birdsall, B., Roberts, G.C.K., Kompis, I., Hammond, S.J., Biochemistry 25 1925-1931 (1986).

Cleland, W.W., Bioorganic Chemistry 15 283-302 (1987).

Clore, G.M., Gronenborn, A., Crit. Rev. Biochem. Mol. Biol. 24 479-564 (1989)

Clore, G.M., Gronenborn, A., Birdsall, B., Feeney, J., and Roberts, G.C.K. Biochem. J. 217 659-666 (1984).

Cocco, L., Groff, J.P., Temple, C., jr., Montgomery, J.A., London, R.E., Matwiyoff, N.A., Blakely, R.L., Biochemistry 20 3972-3978 (1981a).

Cocco, L., Roth, B., Temple, C.Jr., Montgomery, J.A., London, R.E., Blakely, R.L., Arch. Biochem. Biophys. 226 567-577 (1983).

Cocco, L., Temple, C., jr., Montgomery, J.A., London, R.E., Blakely, R.L., Biochem. Biophys. Res. Comm. 100 413-419 (1981b).

Dann, J.G., Ostler, G., Bjur, R.A., King, R.W., Scudder, P., Turner, P.C., Roberts, G.C.K., Burgen, A.S.V., Hardings, N.G.L., Biochem. J. 157 559-571 (1976).

Dawson, R.M.C., Elliott, D.C., Elliott, W.H., Jones, K.M., Data for Biochemical Research, 3rd Edition, Oxford University Press, U.K. (1986).

Dente, L., Cesareni, G., Cortese, R., Nucl. Acids Res. 11 1645-1655 (1983).

D'Souza, L., Freisheim, J.H., Biochemistry 11 3770-3774 (1972).

Duffy, T., Beckman, S., Peterson, S., Vitols, K., Huennekens, F., J. Biol. Chem. 262 7028-7033 (1987).

Dunn, S.M.J., Batchelor, J.G., King, R.W., Biochemistry 17 2356-2364 (1978).

Erickson, J.S., Mathews, C.K., J. Biol. Chem. 247 5661-5667 (1972).

Erickson, J.S., Mathews, C.K., Biochemistry 12 372-380 (1973).

Fawcett, C.P., Giotti, C.P., et.al., Biochem. Biophys. Acta., 54 210 (1961).

Feeney, J., Birdsall, B., Akiboye, J., Tendler, S.J.B., Barbero, J.J., Ostler, G., Arnold, J.R.P., Roberts, G.C.K., Kuhn, A., Roth, K., FEBS Lett. 248 57-61 (1989)

Feeney, J., Birdsall, B., Albrand, J.P., Roberts, G.C.K., Burgen, A.S.V., Charlton, P.A., Young, D.W., Biochemistry 20 1837-1842 (1981).

Feeney, J., Birdsall, B., Roberts, G.C.K., Burgen, A.S.V., Nature 257 564-566 (1975).

Feeney, J., Birdsall, B., Roberts, G.C.K., Burgen, A.S.V., Biochemistry 22 628-633 (1983).

Feeney, J., Roberts, G.C.K., Birdsall, B., Griffiths, D.V., King, R.W., Scudder, P., Burgen, A.S.V., Proc. Roy. Soc. Lond. B196 267-290 (1977).

Fersht, A.R., TIBS. 12 301-304 (1987).

Fierke, C.A., Benkovic, S.J., Biochemistry 28 478-486 (1989).

Fierke, C.A., Johnson, K.A., Benkovic, S.J., Biochemistry 26 4085-4092 (1987).

Filman, D.J., Bolin, J.T., Matthews, D.A., Kraut, J., J. Biol. Chem. 257 13663-13672 (1982).

Fontecilla-Camps, J.C., Bugg, C.E., Temple, C., Jr., Rose, J.D., Montgomery, J.A., Kisliuk, R.L., J. Am. Chem. Soc. 101 6114-5115 (1979).

Freisheim, J.H., Bitar, K.G., Reddy, A.V., Blankenship, D.T., J. Biol. Chem. 253 6437-6444 (1978).

Freisheim, J.H., Matthews, D.A., in Folate Antagonists as Therapeutic Agents (Sirotnak, F.M., Burchill, J.J., Ensminger, W.B., Montgomery, J.A., Eds.) Vol 1. pp 69-131, Academic Press Inc. London. (1984).

Gleisner, J.M., Peterson, D.L., Blakely, R.L., Proc. Natl. Acad. Sci. U.S.A., 71 3001-3005 (1974).

Gleisner, J.M., Peterson, D.L., Blakely, R.L., J. Biol. Chem. 250 4937-4944 (1975).

Gorenstein, D. G., in Methods in Enzymology, Vol 177, 295-316. (Oppenheimer, N. J., James, T.L., Eds.) Academic Press Inc. London. (1989).

Gready, J.E., in Advances in Pharmacology and Chemotherapy (Garattini, S., Goldin, A., Hawking, F, Kopin, I. J., Eds.) 37-102, Academic Press, New York. (1980)

Gready, J.E., Biochemistry 24 4761-4766 (1985)

Greenfield, N.J., Williams, M.N., Poe, M., Hoogsteen, K., Biochemistry 11 4706-4711 (1972).

Gronenborn, A., Birdsall, B., Hyde, E.I., Roberts, G.C.K., Feeney, J., Burgen, A.S.V., Nature 290 273-274 (1981b).

Gronenborn, A., Birdsall, B., Roberts, G.C.K., Feeney, J., Burgen, A.S.V., Mol. Pharmacol. 20 145-153 (1981a).

Gupta, S.V., Greenfield, N.J., Poe, M., Makulu, D.R., Williams, M.N., Moronson, B.A., Bertino, J.R., Biochemistry 16 3037-3079 (1977).

Hammond, S.J., Birdsall, B., Searle, M.S., Roberts, G.C.K., Feeney, J., J. Mol. Biol. 188 81-97 (1986).

Hood, K., Roberts, G.C.K., Biochem. J. 171 357-366 (1978).

Howell, E.E., Villafranca, J.E., Warren, M.S., Oatley, S.J., Kraut, J., Science 231 1123-1128 (1986).

Howell, E.E., Warren, M.S., Booth, C.L.J., Villafranca, J.E., Kraut, J., Biochemistry 26 8591-8598 (1987).

Huang, S., Delcamp, T.J., Tan, X., Smith, P.L., Prendergast, N.J., Freisham, J.H., Biochemistry 28 471-478 (1989).

Huennekins, F.M., Scrimgeour, K.G., in Pteridine Chemistry (Pfleiderer, W., Taylor, E.C., eds.) 355-376. Pergammon, Oxford. (1964).

Hyde, E.I., Birdsall, B., Roberts, G.C.K., Feeney, J., Burgen, A.S.V., Biochemistry 19 3738-3746 (1980a).

Hyde, E.I., Birdsall, B., Roberts, G.C.K., Feeney, J., Burgen, A.S.V., Biochemistry 19 3746-3754 (1980b).

Jimenez, M.A., Arnold, J.R.P., Andrews, J., Thomas, J.A., Roberts, G.C.K., Birdsall, B., Feeney, J., Prot. Eng. 2 627-631 (1989).

Kimber, B.J., Griffiths, D.V., Birdsall, B., King, R.W., Scudder, P., Feeney, J., Roberts, G.C.K., Burgen, A.S.V. Biochemistry 16 3492-3500 (1977).

Kraft, R., Tardiff, J., Krauter, K.S., Leinwand, L.A., BioTechniques 6 (6), 544-547 (1988).

Kramer, W., Drutsa, V., Jansen, H.-W., Kramer, B., Pflugfelder, M., Fritz, H.-J., Nucl. Acids Res. 12 (24), 9441-9456 (1984).

Kumar, A.A., Blankenship, D.T., Kaufman, B.T., Freisheim, Biochemistry 19 667-678 (1980).

Kuyper, L.F., Roth, B., Baccanari, DP., Ferone, R., Beddell, C.R., Champness, J.N., Stammers, D.K., Dann, J.G., Norrington, F.E., Baker, D.J., Goodford, P.J., J. Med. Chem. 28 303-311 (1985).

Lai, P.-H., Pan, Y.-C.E., Gleisner, J.M., Peterson, D.L., Williams, K.R., Blakely, R.L., Biochemistry 21 3284-3294 (1982).

Leatherbarrow, R.J., Enzfitter, Elsevier Science Publishers BV, Amsterdam, (1987).

London, R.E., Groff, J.P., Blakely, R.L., Biochem. Biophys. Res. Commun. 86 779-786 (1979).

London, R.E., Howell, E.E., Warren, M.S., Kraut, J., Blakely, R.L., Biochemistry 25 7229-7235 (1986).

Lund, H., in Chemistry and Biology of Pteridines (Pfleiderer, W., ed.) 645-670 , de Gruyter, Berlin (1976).

Masters, J.N., Attardi, G., Gene 21 59-63 (1983).

Masui, Y., Coleman, J., Inouye, M., Experimental Manipulation of Gene Expression, Academic Press Inc. USA. (1981).

Matthews, D.A., Alden, R.A., Bolin, J.T., Filman, D.J., Freer, S.T., Hamlin, R., Hol, W.G.J., Kisliuk, R.L., Pastore, E.J., Plante, L.T., Xuong, N., Kraut, J., J. Biol. Chem. 253 6946-6954 (1978).

Matthews, D.A., Alden, R.A., Bolin, J.T., Freer, S.T., Hamlin, R., Xuong, N., Kraut, J., Poe, M., Williams, M., Hoogsteen, K., Science 197 452-455 (1977).

Matthews, D.A., Alden, R.A., Freer, S.T., Xuong, N., Kraut, J., J. Biol. Chem. 254 4144-4151 (1979).

Matthews, D.A., Bolin, J.T., Burridge, J.M., Filman, D.J., Volz, K.W., Kaufman, B.T., Beddall, C.R., Champness, J.N., Stammers, D.K., Kraut, J., J. Biol. Chem. 260 (1) 381-391 (1985a)

Matthews, D.A., Bolin, J.T., Burridge, J.M., Filman, D.J., Volz, K.W., Kraut, J., J. Biol. Chem. 260 (1) 392-399 (1985b).

Mayer, R.J., Chen, J.-T., Taira, K., Fierke, C.A., Benkovic, S.J., Proc. Natl. Acad. Sci. USA 83 7718-7720 (1986).

Morrison, J.F., Stone, S.R., Biochemistry 27 5499-5506 (1988).

Murphy, D.J., Benkovic, S.J., Biochemistry 28 3025-3031 (1989).

Neuhaus, D., Williamson, M.P., The Nuclear Overhauser Effect in Structural and Conformational Analysis. VCH Publishers (UK) Ltd. (1989).

Oefner, C., D'Arcy, A., Winkler, K.K., Eur. J. Biochem. 174 377-385 (1988)

Orr, G.A., Blanchard, J.S., Anal. Biochem. 142 232-234 (1984).

Pastore, E.J., Kistiuk, R.L., Plante, L.T., Wright, J.M., Kaplan, N.O., Proc. Natl. Acad. Sci. U.S.A. 71 3849-3853 (1974).

Penner, M.H., Frieden, C., J. Biol. Chem. 260 5366-5369 (1985).

Penner, M.H., Frieden, C., J. Biol. Chem. 260 15908-15914 (1987).

Peterson, D.L., Gleisner, J.M., Blakely, R.L., Biochemistry 14 5261-5267 (1975).

Poe, M., Greenfield, N.J., Hirshfield, J.M., Hoogsteen, K., Cancer. Biochem. Biophys. 1 7-11 (1974).

Poe, M., Williams, M.N., Greenfield, N.J., Hoogsteen, K., Biochem. Biophys. Res. Commun. 67 240-247 (1975).

Prendergast, N.J., Appleman, J.R., Delcamp, T.J., Blakely, R.L., Freisheim, J.H., Biochemistry 28 4645-4650 (1989).

Prendergast, N.J., Delcamp, T.J., Smith, P.L., Freisheim, J.H., Biochemistry 27 3664-3671 (1988).

Raccah, B., Applebaum, S.W., Tahori, A.S., Insect Biochem. 3 367 (1973).

Roberts, G.C.K., in Chemistry and Biology of Pteridines. Walter de Gruyter, New York. (Curtius, H.-Ch., Ghisla, S., Blau, N., eds) (1989).

Roberts, G.C.K., Feeney, J., Burgen, A.S.V., Yuferov, V., Dann, J.G., and Bjur, R.A. Biochemistry 13 5351-5357 (1974).

Roth, B., Strelitz, J.Z., J. Org. Chem. 34 821-836 (1969).

Russel, M., Kidd, S., Kelly, M.R., Gene 45 333-338 (1986).

Schweitzer, B.I., Dicker, A.P., Bertino, J.R., FASEB J. 4 2441-2452 (1990).

Searle, M.S., Forster, M.J., Birdsall, B., Roberts, G.C.K., Feeney, J., Cheund, H.T.A., Kompis, I., Geddes, A.J., Proc. Natl. Acad. Sci. USA 85, 3787-3791 (1988).

Searle, M.S., Hammond, S.J., Birdsall, B., Roberts, G.C.K., Feeney, J., King, R.W., Griffiths, D.V., FEBS Letts. 194 165-170 (1986).

Seeger, D.R., Cosulich, D.B., Smith, J.M., Hultquist, M.E., J.Am.Chem.Soc 71 1753-1758 (1949).

Shaw, W.V., Biochem. J., 246 1-17 (1987).

Singh, U.C., Proc. Natl. Acad. Sci. 85 4280-4284 (1988).

Stammers, D.K., Champness, J.N., Beddell, C.R., Dann, J.G., Eliopoulos, E., Geddes, A.J., Ogg, D., North, A.C.T., Febbs. Letts. 218 (1), 178-184 (1987).

States, D.J., Haberkorn, R.A., Ruben, D.J., J. Magn. Reson., 48 286- (1982).

Stone, S.R., Morrison, J.F., Biochemistry 21 3753-3765 (1982).

Stone, S.R., Morrison, J.F., Biochim. Biophy. Acta. 745 247- (1983).

Stone, S.R., Morrison, J.F., Biochemistry 23 2753-2758 (1984).

Stone, S.R., Morrison, J.F., Biochemistry 27 5493-5499 (1988).

Taira, K., Benkovic, S.J., J. Med. Chem. 31 129-137 (1988).

Taira, K., Fierke, C.A., Chen, J.-T., Johnson, K.A., Benkovic, S.J., TIBS 12 275-278 (1987).

Thillet, J., Adams, J.A., Benkovic, S.J., Biochemistry 29 5195-5202 (1990).

Tsay, J.-T., Appleman, J.R., Beard, W.A., Prendergast, N.J., Delcamp, T.J., Freisheim, J.H., Blakely, R.L., Biochemistry 29 6428-6436 (1990).

Verkade, J.G., Quin, L.D., Phosphorous-31 NMR Spectroscopy in Stereochemical Analysis. VCH Publishers, Inc. Florida. (1987).

Villafranca, J.E., Howel, E.E., Voet, D.H., Strobel, M.S., Ogden, R.C., Abelson, J.N., Kraut, J., Science 222 782-788 (1983).

Volz, K.W., Matthews, D.A., Alden, R.A., Freer, S.T., Hansch, C., Kaufman, B.T., Kraut, J., J. Biol. Chem. 257 (5) 2528-2536 (1982).

Wider, G., Macura, S., Kumar, A., Ernst, R.R., Wüthrich, K., J. Magn. Reson. 56 207-234 (1984).

Wuthrich, K., In Methods in Enzymology Vol 177 (Oppenheimer, N.J., and James, T.L., Eds) pp125-131, Academic Press, USA. (1989).